# Regulation of cell fate decisions in the developing forebrain by DLX transcription factors

by

Mikaela Nevin

A thesis submitted in partial fulfillment of the requirements for the degree of

Master of Science

Medical Sciences- Medical Genetics

University of Alberta

# Abstract

Introduction

The *Dlx1/Dlx2* double knockout (DKO) mouse exhibits major defects in forebrain development including a block in differentiation and migration of GABAergic interneurons from the subpallium to the cortex. In addition, the *Dlx1/Dlx2* DKO mouse generates more oligodendrocyte progenitor cells (OPC) during forebrain development, and this occurs at the expense of interneuron generation. This phenotype suggests a role for DLX genes in mediating the neuronal-glial cell fate switch in the developing forebrain. Furthermore, expression of many oligodendroglial lineage genes is increased and occurs earlier in the DKO forebrain. As such, we hypothesized that DLX2 actively represses acquisition of oligodendroglial cell fate in a subset of forebrain neural progenitor cells by direct transcriptional repression of multiple genes required for oligodendroglial development. Here, I aimed to determine whether DLX2 represses expression of the oligodendroglial lineage genes *Myt1* and *Plp1* during forebrain development. In order to further characterise this gene regulatory network, I also investigated regulation of *Plp1* by MYT1. I also investigated whether DLX2 may play a role in regulating progenitor cell fate in the pediatric brain tumour Diffuse Intrinsic Pontine Glioma (DIPG).

Methods

Chromatin immunoprecipitation with a polyclonal DLX2 antibody was performed on E13.5 mouse forebrain chromatin to determine whether DLX2 occupied candidate promoter regulatory regions of the *Myt1* and *Plp1* promoters, and with an MYT1 antibody on E14.5 and E18.5 forebrain to determine if MYT1 occupied candidate regulatory regions of the *Plp1* promoter. Electrophoretic mobility shift assays were carried out to determine whether ChIP-positive

candidate regions were directly bound by DLX2 *in vitro*. Luciferase reporter assays were used to determine whether DLX2 binding to candidate regulatory regions affected reporter gene transcriptional output *in vitro.* Quantitative polymerase chain reaction was used to compare *Myt1* and *Plp1* transcript levels in DKO and WT E13.5 forebrain, and immunofluorescence was used to compare PLP1 protein expression in DKO and WT E13.5 forebrain. To examine the effect of DLX2 expression on DIPG differentiation status and phenotype, a patient-derived DIPG cell line (SF8628) was transfected with a DLX2 expression plasmid and expression levels of DLX2 target and oligodendroglial genes were assessed with qPCR.

Results

The promoter-proximal regions of *Myt1* and *Plp1* were found to contain multiple candidate homeodomain binding sites, and DLX2 occupied both promoters *in vivo*. Electrophoretic mobility shift assays showed that recombinant DLX2 directly bound multiple regulatory regions of the *Plp1,* but not the *Myt1* promoter, *in vitro.* Reporter assays showed that co-expression of DLX2 and *Plp1* regulatory regions may affect reporter transcription *in vitro*. Although *Plp1* and *Myt1* transcripts were not significantly increased in the DKO forebrain, PLP protein was expressed earlier and in an expanded domain in DKO forebrain. MYT1 may occupy the *Plp1* promoter *in vivo*. SF8628 cells did not show a transcriptional response to DLX2 overexpression.

Conclusions

DLX2 may negatively regulate *Plp1* during forebrain development supporting our hypothesis that DLX2 promotes the acquisition of GABAergic interneuron cell fates and actively represses oligodendroglial differentiation in neuronal progenitor subsets.

**Preface**

This thesis is an original work by Mikaela Nevin. Chapter 1 contains excerpts from material that has been submitted for publication.

All animal experiments received ethics approval from the University's Animal Care and Use Committees (ACUC); protocol number AUP 0001115.

ChIP-PCR for the *Plp1* promoter, EMSA experiments investigating DLX2 binding to *Plp1* promoter regions, luciferase gene reporter experiments for *Plp1*, and qPCR examining *Plp1* and *Myt1* expression in DKO vs WT mouse were all performed together with Janine Gallego. *Plp1* promoter analysis (Figure 5.1) and IF for PLP1 expression (Figures 5.7 and 5.8) were performed by Janine Gallego.

All data and figures presented in Chapter 7 involving the mouse DIPG cell line were generated by Ms. Xiaohua Song.

**Acknowledgements**

This thesis would not have been possible without the contributions of many people. Although I could never thank every individual person who has helped me over the past few years, I would like to highlight the most important ones.

First and foremost, I would like to thank my supervisor, Dr. David Eisenstat for giving me the opportunity to come to Edmonton. Not all supervisors would take a chance on a student without research experience, but I am truly grateful that you did and have learned so much.

I would also like to thank my committee members, Dr. Anastassia Voronova and Dr. Roseline Godbout for all of their guidance and advice.

I would like to thank all members of the Eisenstat lab. I couldn't have asked for a better group of people to work with. I would like to extend a special acknowledgement to Janine Gallego. Any undergraduate students I work with in the future will have some very big shoes to fill.

I would like to thank Dr. Sarah Hughes, Dr. Rachel Wevrick, and Dr. Mike Walter for all of their guidance for students in the Department of Medical Genetics.

A big thanks to Heather and Shari for everything they do for the Medical Genetics students.

I would also like to thank Nichole, Shelley, Stacey, and Joanne from HSLAS for all they do in taking care of our mice and making our animal work possible.

I would like to thank my friends and all of the students in the Department of Medical Genetics for being such a wonderful and supportive group of people.

I would like to thank my family members. Although having such an academic family creates a lot of pressure, it also means that you are never without someone who can relate and give you advice. Your support over the past few years has been invaluable.

Finally, I would like to thank Yuliyan. I think that a long-distance relationship is a little bit like grad school, in the sense that everyone warns you about how tough it will be at times, but it is difficult to understand what that means until you experience it for yourself. Thank you for your unwavering support, patience, and encouragement over the past several years. I can't wait to start our "real" life together in Toronto.

**List of Figures**

**List of tables**

**List of abbreviations**

Ab, antibody

AEP, anterior entopeduncular area

ANR, anterior neural ridge

bHLH, basic helix loop helix

BMP, bone morphogenic protein

Bp, base pair

BSA, bovine serum albumin

cDNA, complementary DNA

CH, cortical hem

ChIP, chromatin immunoprecipitation

CNP, cyclic nucleotide phosphodiesterase

CNS, central nervous system

dATP, deoxyadenosine triphosphate

dGTP, deoxyguanosine triphosphate

DIPG, diffuse intrinsic pontine glioma

DKO, double knockout

dLGE, dorsal lateral ganglionic eminence

DMEM, Dulbecco's Modified Eagle Medium

DNA, Deoxyribonucleic acid

dNTP, deoxyribonucleoside triphosphate

DP, dorsal pallium

E, embryonic day

EDTA, Ethylenediaminetetraacetic acid

EMSA, electrophoretic mobility shift assay

FBS, fetal bovine serum

FGF, fibroblast growth factor

GABA, Gamma aminobuytric acid

Gapdh, glyceraldehyde 3-phosphate dehydrogenase

gDNA, genomic DNA

GE, ganglionic eminence

GFP, green fluorescent protein

HBSS, Hank's Balanced Salt Solution

HCl, hydrochloric acid

HDAC, histone deacetylase

IF, immunofluorescence

ISH, *in situ* hybridization

LB, lysogeny broth

LP, lateral pallium

LV, lateral ventricle

MBP, myelin basic protein

MGE, medial ganglionic eminence

miRNA, microRNA

MOG, myelin oligodendrocyte glycoprotein

MP, medial pallium

MTT, Methylthiazolyldiphenyl-tetrazolium bromide

Myrf, myelin regulatory factor

MZ, mantle zone

NCX, neocortex

NFAT, nuclear factor of activated T-cells

OCT, optimal cutting temperature

OPC, oligodendrocyte progenitor cell

PBS, phosphate-buffered saline

PCR, polymerase chain reaction

PCX, paleocortex

PDGFRA, platelet derived growth factor receptor alpha

PIC, protease inhibitor cocktail

PLP, proteolipid protein

pMN, motor neuron progenitor domain

PMSF, phenylmethylsulfonyl fluoride

PRC2, polycomb repressive complex 2

qPCR, quantitative PCR

R, region

rDLX2, recombinant DLX2

RGC, radial glial cell

RNA, ribonucleic acid

RPM, revolutions per minute

SDS, sodium dodecyl sulfate

Shh, sonic hedgehog

SVZ, subventricular zone

TEMED, tetramethylethylenediamine

TF, transcription factor

tRNA, transfer RNA

vLGE, ventral lateral ganglionic eminence

VP, ventral pallium

VZ, ventricular zone

WNT, wingless-related integration site

WT, wild-type

# Chapter 1: Introduction

## 1.1 Embryonic origin and anatomy of the forebrain

The forebrain, or prosencephalon, is the most anterior part of the brain, and comprises the telencephalon, diencephalon (thalamus, and hypothalamus), as well as the neural retina and optic nerve. (Rubenstein, Shimamura et al. 1998). It is an ectodermal derivative that arises from the anterior neural plate (Weinstein and Hemmati-Brivanlou 1999). Its development begins at the time of gastrulation, when the neural plate is induced in the ectoderm dorsal to the notochord by the overlying dorsal mesoderm. The neural plate next folds to form the neural tube. Rudimentary anterioposterior patterning of the central nervous system (CNS) now begins with patterning of the neural tube by morphogen signaling originating from specific organising structures, such as Sonic Hedgehog (Shh) from the floor plate and bone morphogenic proteins (BMPs) and Wnts from the roof plate. (Rowitch and Kriegstein 2010). The rough pattern established at this stage will continue to be refined as development proceeds.

The anterior end of the neural tube becomes divided into three primary vesicles, which will develop into the brain. The forebrain forms from the most anterior vesicle, also known as the prosencephalon. The middle vesicle forms the mesencephalon, or midbrain, and the most posterior vesicle, the rhombencephalon, will form the hindbrain. The primary vesicles become further subdivided as development continues, with the prosenecephalon forming the telencephalon and the diencephalon. (Anderson, Marin et al. 2001, Wigle and Eisenstat 2008). Figure 1.1 shows the major subdivisions of the early neural tube.

*Figure 1.1 Early patterning of the neural tube.* Before neurulation, the anterior end of the neural tube becomes subdivided into t

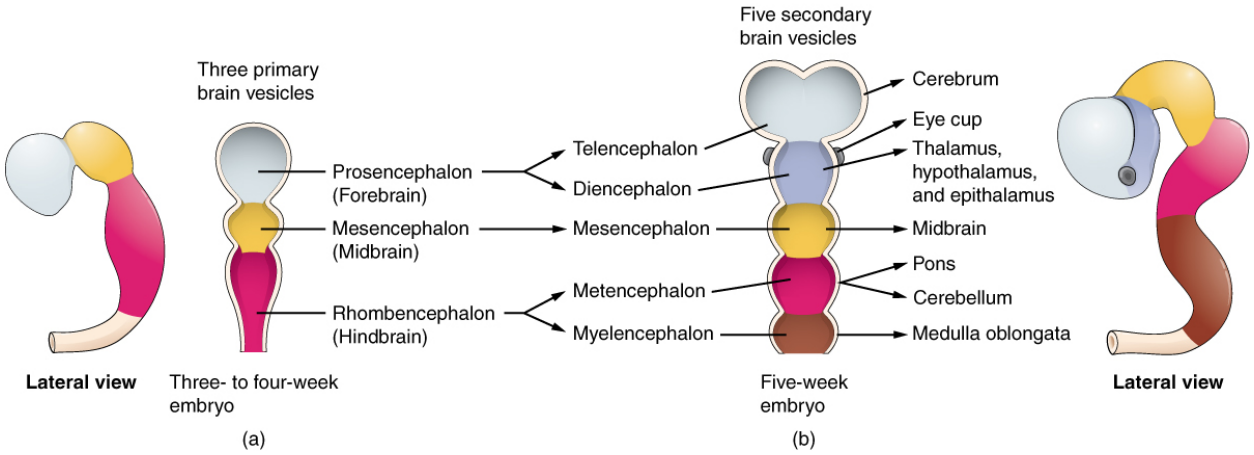


he three primary brain vesicles: the prosencephalon, which will develop into the forebrain; the mesencephalon, which forms the midbrain; and the rhombencephalon, which forms the hindbrain. As development proceeds, the primary vesicles differentiate further into five secondary vesicles. The prosencephalon develops into the telencephalon and the diencephalon. The telencephalon will comprise the cerebrum, while the diencephalon gives rise to the thalamus and hypothalamus, as well as the retina. The mesencephalon remains as a single vesicle and develops into the midbrain. The rhombencephalon is divided into the metencephalon, which will form the pons and cerebellum, and the myelencephalon, which forms the medulla oblongata.

*Figure adapted from OpenStax, Anatomy & Physiology. OpenStax CNX. January 30, 2020. Download for free http://cnx.org/contents/14fb4ad7-39a1-4eee-ab6e-3ef2482e3e22@8.24 .*

## 1.2 Embryonic development of the telencephalon

### 1.2.1 Induction of the telencephalon

Early patterning of the anterior neural plate, including induction of the telencephalon, occurs under the control of signaling from an organizer known as the anterior neural ridge (ANR), which is the region located at the junction between the anterior neural tissue and the non-neural ectoderm (Shimamura and Rubenstein 1997). Specifically, establishment of telencephalic identity involves repression of Wnt signaling via expression of Wnt antagonists, and expression of fibroblast growth factors (Fgfs), especially Fgf8, from the ANR (Shimamura and Rubenstein 1997, Wilson and Houart 2004).

### 1.2.2 Specification, regionalisation, and patterning

Generation of all of the cell types of the mature CNS involves a complex series of patterning events in which graded expression of morphogens and other cell-extrinsic factors partition the neuroepithelium into distinct progenitor domains by activating or repressing the expression of various transcription factors, which impart positional identity for neural progenitor cells by acting on downstream target genes to restrict their lineage potential. In this manner, the initially undifferentiated neuroepithelium becomes progressively more finely patterned into molecularly distinct regions that will give rise to different neuronal subtypes of the nervous system as well as glial cells. Figure 1.2 shows the expression domains of the major transcription factors involved in subdividing the telencephalon.

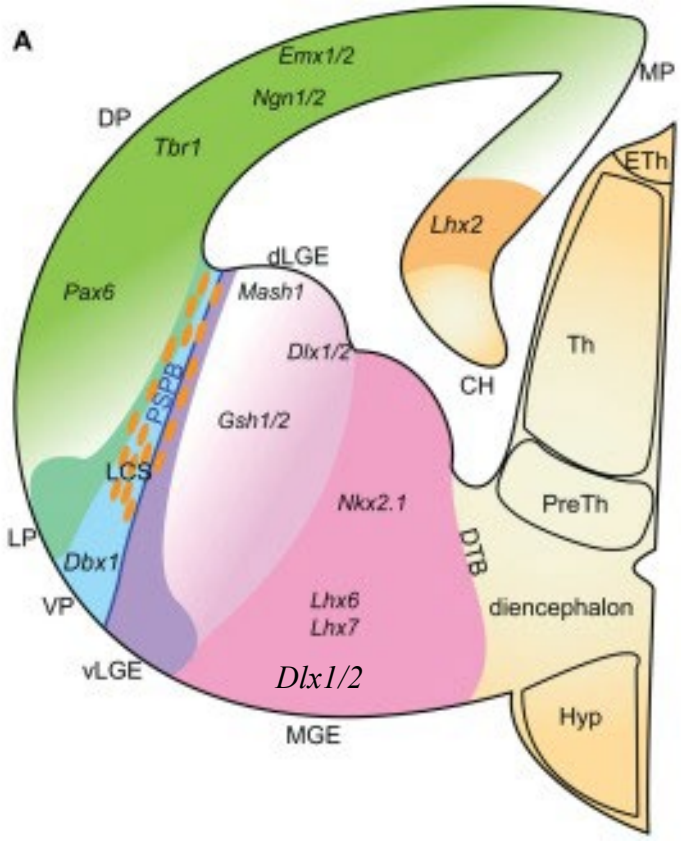


*Figure 1.2 Gene expression boundaries involved in subdivision of the developing telencephalon.* Green: The dorsal pallium (which primarily becomes the neocortex) is marked by expression of *Pax6*, *Tbr1, Emx1* and *Emx2, Ngn1*, and *Ngn2*. Light purple: The lateral ganglionic eminence (LGE) is marked by expression of *Mash1*, *Gsh1/2*, and *Dlx1/2.* Pink: The MGE is marked by expression of *Dlx1/2*, *Nkx2.1, Lhx6,* and *Lhx7*.

DP: Dorsal pallium; MP: Medial pallium; CH: Cortical hem; dLGE: dorsal lateral ganglionic eminence; MGE: Medial ganglionic eminence; vLGE: Ventral lateral ganglionic eminence; LP: Lateral pallium; VP: Ventral pallium. Modified from Grant et al Front. Neurosci. 2012. No permissions required.

Specification of the telencephalic anlagen from the anterior neural plate first involves expression of the forebrain-specific forkhead box transcription factor *Foxg1* (Hebert and Fishell 2008). *Foxg1* expression is induced by FGF8 (Kumamoto and Hanashima 2017) at approximately E8.5 in the mouse, when the telencephalon still consists of a single layer of undifferentiated neuroepithelial cells. (Hebert and Fishell 2008). Once *Foxg1* expression is initiated, it immediately becomes compartmentalised into several molecularly distinct regions. Dorsally, these consist of the anterior and lateral dorsal telencephalon, which will primarily become the neocortex, and the posterior and medial dorsal telencephalon, which will give rise to the hippocampus, cortical hem, and choroid plexus. Meanwhile, the ventral telencephalon is subdivided into the medial, lateral, and caudal ganglionic eminences (GE). The ganglionic eminences are transitory embryonic structures in the ventral telencephalon that guide axonal and neuronal migration and give rise to the projection neurons of the basal ganglia and the amygdala (Hebert and Fishell 2008, Lindtner, Catta-Preta et al. 2019). They also generate the majority of interneurons for the cortex, hippocampus, and olfactory bulb.

Dorsal-ventral patterning of the telencephalon involves the ventralizing morphogen Sonic hedgehog (Shh) secreted from the ventral midline, as well as the dorsalizing influence of the transcription factor *Gli3*. Demarcation of the boundary between the dorsal and ventral telencephalon requires the paired-box transcription factor PAX6. Establishment and maintenance of ventral telencephalic identity also requires expression of *Foxg1* and FGF signaling (which is induced by FOXG1).

### 1.2.3 Forebrain neurogenesis

Initially, the neural tube consists of a single layer of pseudostratified neuroepithelium (Götz and Huttner 2005). Prior to the onset of neurogenesis, around E8-E9, neuroepithelial cells divide symmetrically, giving rise to the ventricular zone (VZ), a proliferative compartment directly adjacent to the neural tube lumen that is populated with neuroepithelial cells. The neuroepithelium becomes further subdivided into the subventricular zone (SVZ), an additional proliferative zone, and the mantle zone (MZ), which contains differentiated neurons. With the onset of neurogenesis, neuroepithelial cells transition into radial glial cells (RGC), which divide to produce all the neuronal subtypes of the CNS. Production of neurons can occur directly via asymmetric division of RGC (generating one neuron and one RGC) or via production of intermediate progenitor cells from RGC (Götz and Huttner 2005, Paridaen and Huttner 2014). Neurons are born in the VZ and, in some cases, the SVZ, and migrate out to the MZ. After the initial period of neurogenesis, RGC also generate glial cells.

In the dorsal telencephalon, cortical development begins with the formation of the cortical preplate, a thin layer of cells just underneath the pial surface. The neurons that will form cortical layer VI then migrate to the preplate, which they split into the subplate and the marginal zone. As the neurons that will form each cortical layer are born, they migrate radially past the subplate and layers of earlier-born neurons, and stop just underneath the marginal zone (Gilmore and Herrup 1997). The six layers of the neocortex are thus built in an "inside-out" manner, in which excitatory cortical neurons are stratified according to their birthdate, with the youngest neurons in layer II and the oldest neurons in layer VI. Layer I consists of neurons derived from the

marginal zone, and the subplate neurons become the deep neurons of layer VI. (Gilmore and Herrup 1997). The laminar organisation of the cortex is shown in Figure 1.3.

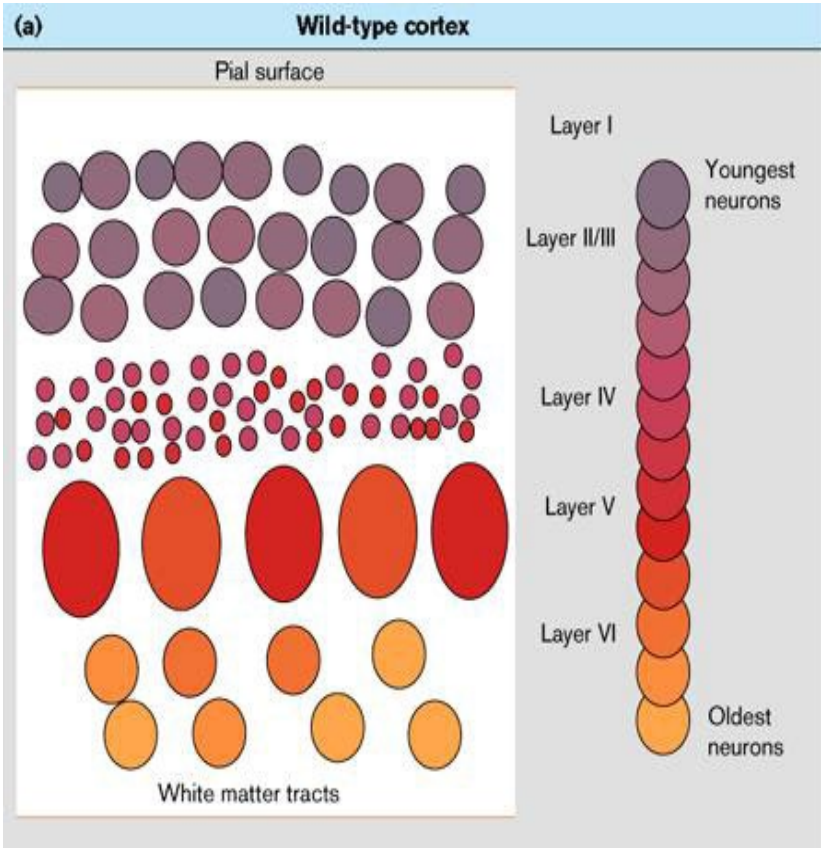


*Figure 1.3 Laminar arrangement of the cerebral cortex.* The projection neurons of each cortical layer are generated in a fixed temporal order in the ventricular zone (not shown). After birth they migrate radially past the earlier-born neurons to reach their correct layer. The end result is that cortical neurons are arranged with the oldest neurons (those of layer VI) in the deepest layer and the youngest neurons (those of layer I) in the outermost layer closest to the pial surface. Modified from Gilmore and Herrup. Curr Biol. 1997. License number 4821001214873.

In addition to excitatory projection neurons, the cortex also contains GABAergic inhibitory interneurons, which play important roles in modulating cortical neural circuit activity (Tremblay, Lee et al. 2016). In contrast to excitatory neurons, nearly all cortical interneurons are generated in the ganglionic eminences (Wonders and Anderson 2006, Lim, Mi et al. 2018). Following birth in the GE, interneurons migrate tangentially to the cortex and other telencephalic regions, where they differentiate and become integrated into neural circuits (Anderson, Eisenstat et al. 1997, Anderson, Marin et al. 2001, Wonders and Anderson 2006, Lim, Mi et al. 2018).

### 1.2.4 Forebrain gliogenesis

Following the initial period of neurogenesis in the CNS, production of glial cells (astrocytes and oligodendrocytes) begins. The progenitor domains that first generated neurons now switch to generating glial progenitors and glial cells. In the forebrain, the dorsal pallium, which first generates excitatory pyramidal cortical neurons, also gives rise to astrocytes, whereas the ventral telencephalon produces oligodendrocytes. Later in development, some oligodendrocytes also arise from the cortex (Rowitch and Kriegstein 2010). RGC lineage progression from neurogenic to gliogenic output appears to be regulated in a deterministic manner (Gao, Postiglione et al. 2014, Beattie and Hippenmeyer 2017). Clonal lineage analysis of RGCs indicates that, in the mammalian neocortex, about one in six RGCs go on to generate glial cells following the completion of neurogenesis (Gao, Postiglione et al. 2014).

It was previously thought that there might be a common CNS glial progenitor that could generate both astrocytes and oligodendrocytes (Rowitch 2004). This is not the case as astrocytes and

oligodendrocytes have been shown to be generated from largely mutually exclusive regions of the developing CNS (Rowitch 2004). Furthermore, *Olig1/2* null neural precursor cells have been shown to be able to generate only astrocytes, although, as will be discussed shortly, no OPCs are specified in the absence of *Olig* gene function (Lu, Sun et al. 2002, Zhou and Anderson 2002). This indicates that the mechanisms involved in generating these two types of glial cell are distinct. During development, most oligodendrocytes arise instead from discrete progenitor domains that sequentially generate particular neuronal subtypes, followed by oligodendrocyte progenitor cells (OPC). In the ventral spinal cord, the pMN domain generates motor neurons and oligodendrocytes. In the ventral telencephalon, the medial ganglionic eminence (MGE) gives rise to both GABAergic interneurons and OPCs (He, Ingraham et al. 2001, Petryniak, Potter et al. 2007).

### 1.2.5 Neuron-glial switch

After the initial period of neurogenesis, progenitor domains switch from generating neurons to generating glia (astrocytes and oligodendrocytes). Downregulation of the proneural basic helix-loop helix (bHLH) transcription factors Neurogenin-1 (*Ngn1*) and Neurogenin-2 (*Ngn2*) is a major regulator of the switch from neuronal to glial cell production (Rowitch and Kriegstein 2010). In the pMN domain, which generates motor neurons followed by OPCs, *Ngn2* is expressed in some of the *Olig2* expressing cells, and becomes downregulated prior to OPC production (Lee, Lee et al. 2005), and it has been shown in embryonic chick ventral spinal cord that downregulation of *Ngn1* and *Ngn2* is required for induction of OPCs by *Olig2* (Kessaris,

Pringle et al. 2001, Zhou, Choi et al. 2001). BMP signaling can also have either neurogenic or gliogenic effects, depending on the level of *Ngn1* in the cell (Miller and Gauthier 2007).

Delta-Notch pathway activity is also implicated in regulation of the switch from neurogenesis to gliogenesis. In the pMN domain, continued Delta-Notch activity seems to be required until the onset of OPC production in order to maintain sufficient numbers of glial-competent neural progenitors (Rowitch 2004, Rowitch and Kriegstein 2010) and in Notch mutants, the pMN domain produces only motor neurons (Itoh, Kim et al. 2003), whereas when a constitutively active form of the Notch1 receptor is expressed, the pMN domain produces excess OPCs. (Itoh, Kim et al. 2003). It has also been shown that oligodendrocytes do not form in the absence of Notch signaling (Park and Appel 2003, Yang, Tomita et al. 2006). The timing of OPC generation is unchanged with constitutive Notch pathway activity, indicating Notch activity might be permissive rather than instructive for OPC generation (Park and Appel 2003). In contrast, Notch signaling has been shown to instructively regulate the onset of astrogenesis in the forebrain (Rowitch and Kriegstein 2010) both via inhibition of neurogenic bHLH factors such as *Mash1/Ascl1*, and by promoting activity of the JAK-STAT pathway. Activated STAT transcription factors (STAT3) collaborate with the BMP pathway and the transcriptional coactivator p300/CBP to activate the promoters of multiple genes required for astrocyte development such as *Gfap* and *S100b* (Miller and Gauthier 2007, Rowitch and Kriegstein 2010). Finally, gliogenesis also requires expression of glial-specific genes such as *Sox9* (Rowitch and Kriegstein 2010).

In the forebrain, the DLX transcription factors have been implicated in regulating interneuron versus OPC cell fate decisions in the MGE. Their role in this process forms the focus of the current study and will be discussed further in Section 1.6.

## 1.3 Oligodendroglial lineage development

Oligodendrocytes are the last major neural cell type to be generated during CNS development (Goldman and Kuypers 2015). Their development begins with the specification of oligodendrocyte progenitor cells (OPCs) from distinct domains in the spinal cord and forebrain. SHH signaling is required for establishing oligodendrogenic domains and in early stages of oligodendroglial lineage development, primarily because it activates expression of *Olig2*. *Olig2* is a bHLH transcription factor that, together with a related member *Olig1,* form a distinct subclass of bHLH transcription factors that were first identified based on their expression in both myelinating oligodendrocytes and OPCs (Lu, Yuk et al. 2000, Zhou, Wang et al. 2000, Meijer, Kane et al. 2012). *Olig2* has multiple and stage-specific roles in oligodendroglial development. At early stages, it functions as an anti-neurogenic transcription factor, sustaining proliferation of neural progenitors that will go on to generate OPCs following the initial period of motor neuron generation from the pMN domain (Lee, Lee et al. 2005). Hence, OLIG2 sustains replication of glial competent progenitors. Later, it has a neurogenic function, and promotes OPC specification, cell cycle exit, and differentiation in the spinal cord (Lu, Sun et al. 2002). *Olig2* is necessary for OPC specification in most parts of the CNS, although partial compensation by *Olig1* occurs in some regions (Zhou and Anderson 2002). No oligodendrocytes can be detected in the brain of *Olig1/Olig2* double knockout (DKO) mice, and these mice also fail to generate OPCs in the

spinal cord (Rowitch and Kriegstein 2010) indicating the importance of the Olig TFs for OPC specification (Meijer, Kane et al. 2012) . However, as mentioned, *Olig2* expression alone is not sufficient for OPC generation unless the neurogenic transcription factors *Ngn1* and *Ngn2* are also downregulated (Kessaris, Pringle et al. 2001, Zhou, Choi et al. 2001)

Following specification, OPCs proliferate, disperse throughout the CNS, and differentiate postnatally into myelinating oligodendrocytes. In the mouse, the earliest site of OPC production is the spinal cord, and it takes place in three spatiotemporally distinct waves. The first wave takes place at E12.5 in the spinal cord pMN domain, in the ventral neural tube. A second wave takes place at E15.5 in the dorsal neural tube, and a third wave occurs at birth (Rowitch and Kriegstein 2010, Goldman and Kuypers 2015). In the forebrain, as in the spinal cord, there are three distinct waves of OPC generation after the initial period of neurogenesis, progressing from ventral to dorsal regions. The first wave of OPC production occurs at about E12.5 in the MGE. These OPCs are marked by expression of *Nkx2.1*, and they migrate out from the MGE and colonize the dorsal forebrain (Kessaris, Fogarty et al. 2006). A second wave of OPC generation at E15.5 occurs primarily from the LGE, under the control of *Gsx2*. The final wave of OPC generation occurs around the time of birth (P0) in a dorsal domain adjacent to the corpus callosum (dorsal SVZ); these OPCs are marked by *Emx1* expression (Kessaris, Fogarty et al. 2006). In both spinal cord and forebrain, postnatally-generated OPCs normally seem to outcompete earlier-born ones (Kessaris, Fogarty et al. 2006, Goldman and Kuypers 2015).

### 1.3.1 Transcriptional control of OL development

Oligodendrocyte lineage progression is characterized by sequential expression of various transcription factors, cell surface markers, and genes involved in synthesis of myelin components (Figure 1.4) (Goldman and Kuypers 2015, Elbaz and Popko 2019). At each stage, transcriptional feedback loops involving stage-specific TFs regulate the decision to continue proliferating as OPCs or terminally differentiate into myelinating oligodendrocytes (Elbaz and Popko 2019). Some of the major factors involved in oligodendroglial lineage development are summarized in Figure 1.4. OPC fate acquisition is first marked by expression of platelet-derived growth factor alpha receptor (*Pdgfra*) (Noble, Murray et al. 1988, Richardson, Pringle et al. 1988, Hart, Richardson et al. 1989). Prior to onset of *Pdgfra* expression, there is upregulation of glial-specific transcription factors such as *Sox8* and *Sox9*, as well as downregulation of various neuroepithelial transcripts (Goldman and Kuypers 2015). Although *Pdgfra* expression is considered to mark commitment to OPC fate, recent single-cell RNA sequencing of *Pdgfra*-positive OPCs indicates that at E13.5 in the forebrain some *Pdgfra*-expressing progenitors have a transcriptional profile that is distinct from that of postnatal OPCs, and which suggests they could have the potential to give rise to cells of other lineages (Marques, van Bruggen et al. 2018). However, the majority of E13.5 *Pdgfra*-expressing cells do appear to give rise to OPCs (Marques, van Bruggen et al. 2018). Besides *Olig2* and *Pdgfra*, newly generated OPCs are also characterised by expression of *Nkx6.1, Nkx6.2,* and *Nkx2.2* (Elbaz and Popko 2019).

Control of oligodendrocyte differentiation is complex and involves a number of transcription factors, but the core transcription factors that regulate oligodendroglial differentiation and the onset of myelination are OLIG2, NKX2.2, SOX10, ZFP24, and MYRF (Elbaz and Popko 2019). In addition, other TFs and their posttranslational modifications, miRNAs, metabolic signaling, and other signaling pathways such as the Raf-MAPK-ERK1/2 pathway are also involved in terminal differentiation (Elbaz and Popko 2019).

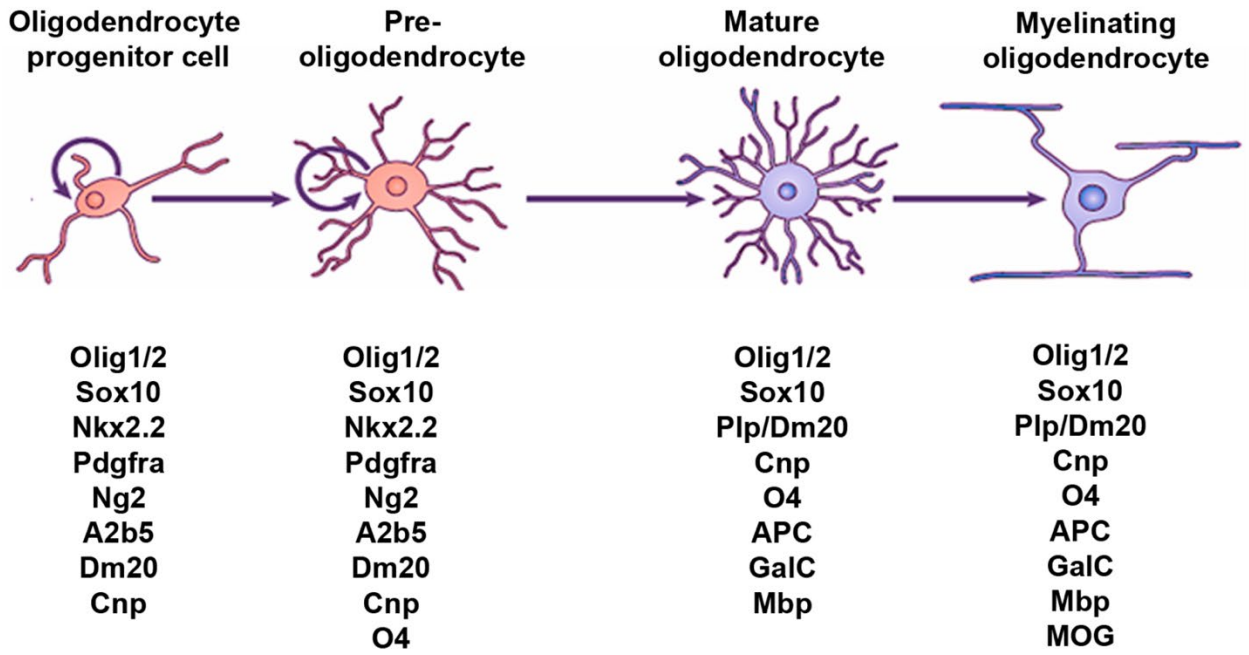


*Figure 1.4 Stage-specific transcription factors and surface antigens involved in oligodendroglial lineage development.* Early stages of lineage progression are characterised by expression of *Pdgfra* and *Olig2. Olig1/2* and *Sox10* are expressed throughout the developmental process. Myelin component expression begins later. Figure from Traiffort et al J. Dev. Biol. 2016. No permission required.

OLIG2 and NKX2.2 are particularly important in the control of oligodendrocyte differentiation, and they must be co-expressed for differentiation to occur (Elbaz and Popko 2019). Terminal differentiation also requires the transcription factor SOX10 (Küspert, Hammer et al. 2011). SOX10 promotes differentiation via interaction with a number of other pathways. Firstly, OLIG2 and NKX2.2 normally cross-repress each other in the developing ventral neural tube, and terminal differentiation of oligodendrocytes requires this interaction to be relieved. OLIG2 directly activates expression of *Sox10*, which collaborates with nuclear factor of activated T cell (NFAT) proteins to relieve inhibition of OLIG2 expression by NKX2.2, and *vice versa* (Weider, Starost et al. 2018, Elbaz and Popko 2019).

SOX10 also promotes differentiation through direct activation of multiple genes encoding myelin components (Li, Lu et al. 2007) and indirect interaction with three other major partners: Myelin regulatory factor (MYRF), Chromodomain Helicase DNA-binding protein 7 (CHD7), and transcription factor 7 like 2 (TCF7L2) (Elbaz and Popko 2019). These interactions lead to activation of multiple genes required for oligodendrocyte differentiation and myelin production. Crucially, SOX10 both directly (Hornig, Fröb et al. 2013) and indirectly (Lopez-Anido, Sun et al. 2015) activates the promoter of myelin regulatory factor (*Myrf*) which is a key regulator of oligodendrocyte maturation and myelination. MYRF is required for expression of myelin genes both during development (Emery, Agalliu et al. 2009) and for continued maintenance of myelin sheaths in the adult CNS (Koenning, Jackson et al. 2012). It directly induces expression of a number of genes encoding myelin components, including myelin basic protein *(Mbp),* proteolipid protein 1 *(Plp1),* myelin-associated glycoprotein *(Mag),* myelin oligodendrocyte protein *(Mog)* and cyclic nucleotide phosphodiesterase *(Cnp)* (Emery, Agalliu et al. 2009).

SOX10 also induces expression of the transcription factor ZFP24 (Lopez-Anido, Sun et al. 2015), which acts to further increase expression of SOX10 and MYRF (Elbaz, Aaker et al. 2018). Finally, ongoing expression of MYRF and of its target myelin components requires continued transcription of *Olig2* and *Sox10* (Goldman and Kuypers 2015).

## 1.4 DLX transcription factors

The *Distal-less* (*Dlx)* genes are the vertebrate homologues of the *Drosophila melanogaster distal-less* (*Dll*) gene. They encode homeodomain containing transcription factors that bind DNA through their 60 amino acid homeodomain. Like other homeodomain transcription factors, they recognize consensus sequences containing ATTA/TAAT motifs (Bürglin and Affolter 2016), and can act as transcriptional repressors or activators (Lindtner, Catta-Preta et al. 2019).

The mouse genome has six *Dlx* members: *Dlx1, Dlx2, Dlx3, Dlx4, Dlx5,* and *Dlx6*. The genes are organised into convergently transcribed bigenic clusters, and each *Dlx* gene pair is linked to a *Hox* gene cluster. (Panganiban and Rubenstein 2002). The intergenic region between each gene pair spans approximately 10 kb in the case of the *Dlx1* and *Dlx2* gene pair (McGuinness, Porteus et al. 1996) and contains common *cis*-regulatory elements. Figure 1.5 shows the structure of the *Dlx* genes. During development, the *Dlx* genes are primarily expressed in the branchial arches, forebrain, and limbs (Qiu, Bulfone et al. 1997, Panganiban and Rubenstein 2002).

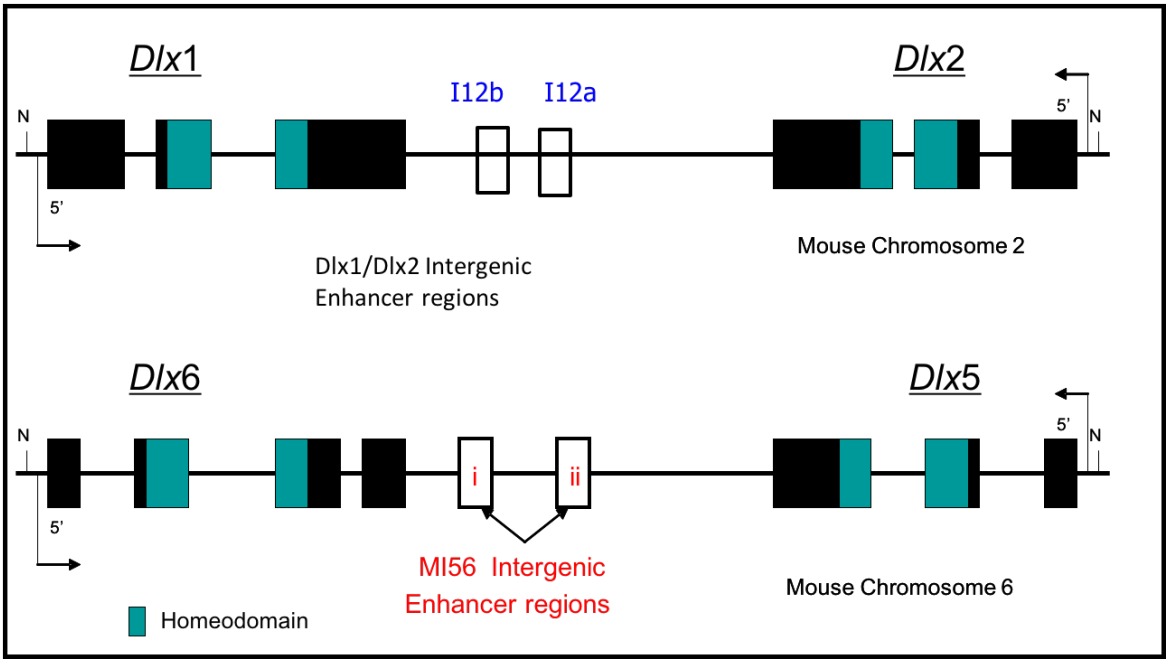


*Figure 1.5 Structure of the Dlx1/Dlx2 and Dlx5/6 loci.* The *Dlx* gene pairs share a common structure, exemplified in the above figure. They are arranged in bigenic clusters with the two *Dlx* members facing each other and transcribed convergently. The homeodomain (light turquoise) is split between exons 2 and 3. The intergenic regions contain shared regulatory elements: I12b and I12a are intergenic enhancers involved in regulation of *Dlx1/2* expression, and MI56i and MI56ii are involved in regulation of *Dlx5/6* expression. *Dlx1/2* are located on mouse chromosome 2, and *Dlx5/6* are located on mouse chromosome 6. Modified from Q.P. Zhou et al. NAR. 2004. License number 4821011214613.

### 1.4.1 Role of *Dlx* genes in forebrain development

Four of the *Dlx* genes are expressed in the developing forebrain: *Dlx1, Dlx2, Dlx5,* and *Dlx6*. *Dlx* gene expression pattern defines different stages of subpallial differentiation. *Dlx1* and *Dlx2* are expressed primarily in less differentiated cells in the VZ and SVZ; *Dlx5* and *Dlx6* expression is most prominent in the MZ which contains more differentiated neurons.
(Liu, Ghattas et al. 1997, Panganiban and Rubenstein 2002)

In the mouse, *Dlx* gene expression begins at E9.5 in GE progenitors (Lindtner, Catta-Preta et al. 2019). *Dlx2* is expressed first, followed by *Dlx1*, *Dlx5,* and *Dlx6* (Anderson, Qiu et al. 1997, Liu, Ghattas et al. 1997). The spatial expression pattern of the *Dlx* genes during forebrain development is shown in Figure 1.6.

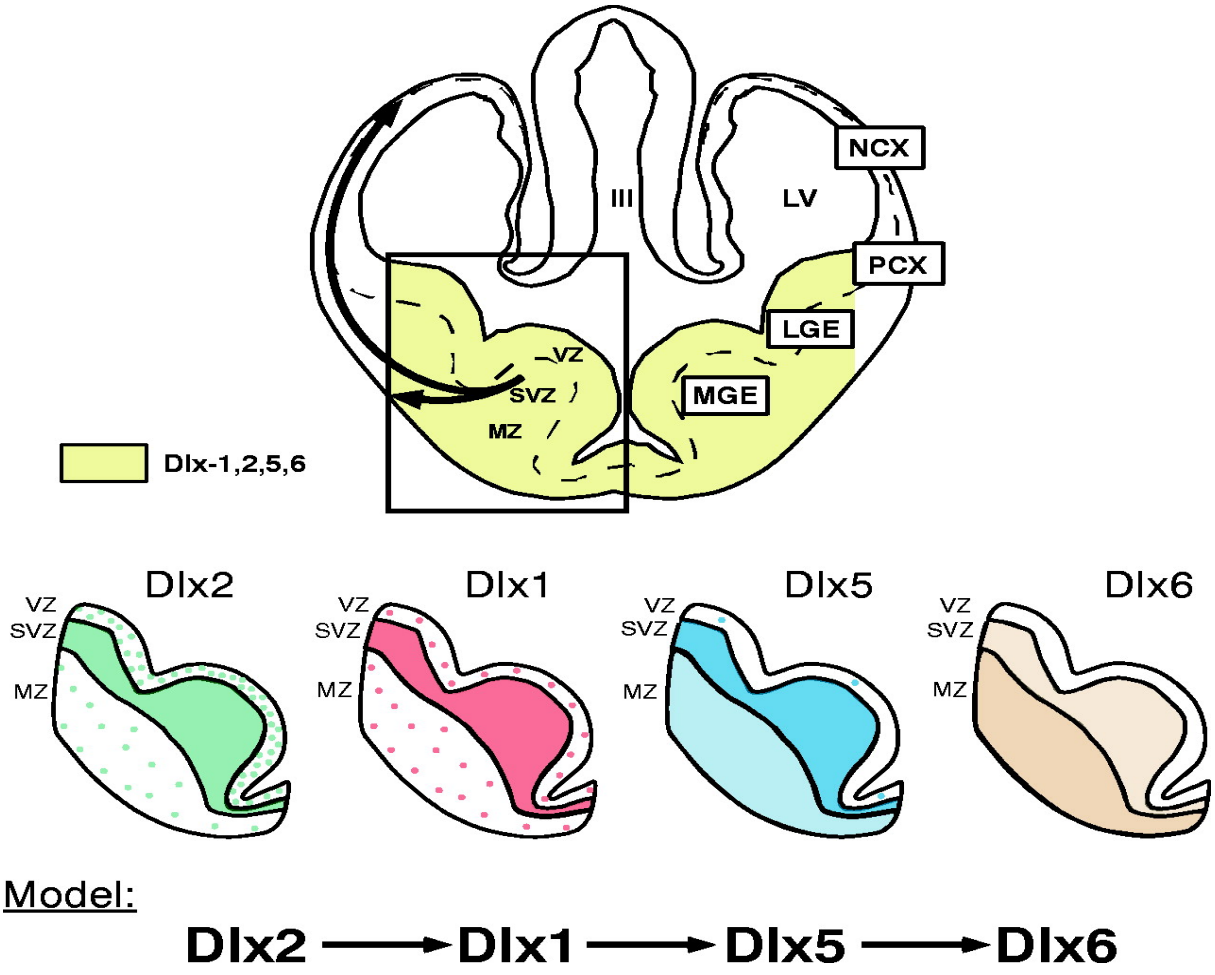


*Figure 1.6 Spatial and temporal expression pattern of Dlx genes during murine forebrain development.*

**Top:** Schematic of a coronal cross-section through an E12.5 mouse telencephalon. The yellow area indicates the expression domain of all four *Dlx* genes expressed in the developing forebrain. The arrow indicates the direction of migration of interneurons from the subpallium to the cortex. **Middle:** Expression patterns of *Dlx* gene family members within the germinal zones of the subpallium. *Dlx2* is primarily expressed in relatively undifferentiated cells in the ventricular zone (VZ) (green dots) as well as in the subventricular zone (SVZ) (solid green) and is only seen in a

few scattered cells in the mantle zone (MZ). *Dlx1* expression pattern largely overlaps with that of *Dlx2* (solid pink and pink dots) though it is somewhat less expressed in the VZ. *Dlx5* is predominantly expressed in the SVZ and the MZ (dark and light blue). *Dlx6* expression largely overlaps with *Dlx5*, but with higher expression in the mantle zone (dark and light beige). **Bottom**: Model for temporal expression pattern of *Dlx* genes during forebrain development. *Dlx2* is expressed in the earliest progenitors.

NCX: neocortex, PCX: palliocortex, LGE: lateral ganglionic eminence, MGE: medial ganglionic eminence, VZ ventricular zone, SVZ: subventricular zone, MZ: marginal zone, LV: lateral ventricle, III: third ventricle.

Adapted from Panganiban & Rubenstein. Dev. 2002. Order license number 1032367-1.

Understanding of the developmental function of the *Dlx* genes has been aided by the generation of single and double homozygous mutants for each individual gene and bigenic pair. Phenotypic analysis has been limited to the embryonic and immediate perinatal period since both single and double *Dlx* knockouts are lethal at P0. All heterozygotes are phenotypically normal. Homozygous single mutants for *Dlx1* and *Dlx2* show no or few defects in forebrain development, indicating that these genes function mostly redundantly in this tissue. This is probably explained by the overlap in their expression pattern. In contrast, the *Dlx1/2* double knockout (DKO) mouse shows major defects in forebrain development.

First, in the DKO telencephalon there is a loss of tangential migration of most interneurons from the MGE to the cortex and the LGE to the olfactory bulb (Anderson, Qiu et al. 1997, Bulfone, Wang et al. 1998, Le, Du et al. 2007). This defect in tangential migration is time-dependent. Accordingly, at birth these mice have a severe reduction in the number of GABA-expressing interneurons in the cortex, hippocampus, and olfactory bulb (Marín and Rubenstein 2001). The DKO GEs contain ectopic accumulations of GABA-positive cells that resemble partially-differentiated interneurons in the SVZ, which likely represent interneurons that have failed to migrate to the cortex (Anderson, Qiu et al. 1997, Marın, Anderson et al. 2000, Le, Du et al. 2007). The DKO forebrain also has a block in differentiation of late-born (E12.5 and later) striatal neurons.

The loss of tangential migration of interneurons may be the result of de-repression of the class 3 semaphorin co-receptor Neuropilin 2 (*Nrp2*) in the DKO subpallium (Le, Du et al. 2007). We have shown that DLX1 and DLX2 bind and directly repress the *Nrp2* promoter, and we

hypothesize that in the absence of Dlx gene function, late-born interneurons may be unable to migrate out of the GE because they cannot downregulate *Nrp2* to decrease their sensitivity to repulsive Sema3 signalling from cells in the striatum and at the pallial-subpallial boundary (Le, Du et al. 2007).

DLX genes are also involved in regulation of GABA synthesis. The main pathway for GABA synthesis occurs from glutamate via the enzyme glutamate decarboxylase (Gad) (Le, Zhou et al. 2017). There are two glutamate decarboxylase isoforms: *Gad1* (Gad67) and *Gad2* (Gad65). Previous work from our lab indicates that DLX1 and DLX2 bind to and directly activate the promoters of both *Gad1* and *Gad2* (Le, Zhou et al. 2017), thereby promoting GABA synthesis and GABAergic interneuron differentiation.

In addition to their essential roles in the development and tangential migration of GABAergic interneurons, *Dlx1/2* genes negatively regulate oligodendrogenesis in a subset of progenitor cells in the developing MGE. At E12.5 in the germinal zones of the MGE, many progenitor cells show transient co-expression of DLX2 and OLIG2 (Petryniak, Potter et al. 2007), which is essential for oligodendrocyte specification in most parts of the CNS, including the forebrain (Lu, Yuk et al. 2000, Zhou and Anderson 2002, Rowitch 2004, Meijer, Kane et al. 2012).

After this transient period of co-expression, as progenitors differentiate and move from the germinal zones to the mantle zone, DLX2 and OLIG2 expression become mutually exclusive. Petryniak *et al* (2007) hypothesize that this suggests a regulatory interaction between DLX2 and OLIG2 in MGE progenitors, such that their expression eventually becomes restricted to different

cell types (Petryniak, Potter et al. 2007). In the *Dlx1/2* DKO, the number of OLIG2-expressing cells is greatly increased in the SVZ of the MGE and AEP (Petryniak, Potter et al. 2007). These OLIG2-positive cells likely represent OPCs since *in situ* hybridisation for the OPC markers *Pdgfra* and *Sox10* revealed a large increase in *Pdgfra*+ *Sox10*+ cells in the DKO MGE at E12.5, E15.5, and E18.5. *Olig1*+ cells were also greatly increased in the DKO MGE at E15.5 (Petryniak, Potter et al. 2007).

In addition to increased OPC production, the DKO forebrain displays accelerated differentiation of OPCs. Petryniak and colleagues (Petryniak, Potter et al. 2007) examined expression of *Nkx2.2*, *Plp,* and *Mbp*, which are expressed in mature or differentiating OPCs, in DKO and WT telencephalon at E15.5. At E15.5, the DKO forebrain contained many *Nkx2.2*-positive cells, whereas *Nkx2.2* expressing cells were rare in the WT at this time point. Furthermore, at E15.5, *Plp* and *Mbp* were not yet detectable at all in the WT, whereas the DKO forebrain contained numerous *Plp*- and *Mbp*-expressing cells at this time, an increase which persisted through E18.5. This aspect of the DKO phenotype was suggested to result from the increased expression of *Olig1* (Petryniak, Potter et al. 2007), since *Olig1* controls multiple aspects of OPC maturation (Lu, Yuk et al. 2000).

Proliferation was found to be unaltered in the DKO telencephalon, so increased OPC proliferation is not the reason for increased generation of OPCs. Furthermore, the DKO ventral forebrain produces a reduced number of interneurons concomitantly with increased OPC production (Petryniak, Potter et al. 2007). The large increase in OPC production and decrease in neuron production in DKO MGE suggests that the majority of MGE progenitors that initially co-

express DLX2 and OLIG2 will become oligodendrocytes in the absence of active repression of oligodendroglial fate by DLX1/2 (Petryniak, Potter et al. 2007).

This cell fate decision is mediated, at least partially, via direct transcriptional repression of *Olig2* by DLX1/2. As discussed previously, *Olig2* is required for OPC specification in almost all parts of the CNS (Zhou and Anderson 2002) and the increased OPC generation in the DKO was shown to be completely dependent on *Olig2*, as no OPCs can be detected in triple *Dlx1/Dlx2/Olig2*-null mice (Petryniak, Potter et al. 2007). DLX1/2 are sufficient to repress *Olig2* expression in slice electroporation experiments (Petryniak, Potter et al. 2007). Finally, unpublished data from our laboratory indicates that DLX2 directly represses the *Olig2* promoter *in vivo* during forebrain development (Jiang Q, Zagozewski J and Eisenstat DD, unpublished observations).

We hypothesize that regulation of forebrain neuronal-oligodendroglial cell fate decisions by DLX1/2 involves suppression of multiple genes involved in differentiation along the oligodendroglial pathway in those progenitors that will go on to become GABAergic interneurons. This would function as a robust developmental mechanism to ensure production of sufficient GABAergic interneurons. In agreement, unpublished data from our laboratory indicates that in addition to *Olig2*, DLX2 represses the homeodomain transcription factor *Nkx2.2*, which is involved in OPC maturation, but not initial specification (Qi, Cai et al. 2001).

Therefore, we are investigating whether DLX2 negatively regulates the expression of other genes that are involved at multiple stages of oligodendroglial development and maturation.

The aim of the current study was to determine whether DLX2 regulates expression of two such genes during forebrain development: *Myt1* (myelin transcription factor 1) and *Plp1* (proteolipid protein). These genes were initially chosen because together their expression spans a large part of oligodendrocyte development, from early to late stages. Their expression patterns will be discussed in detail in the following sections. Briefly, Myt1 expression characterizes earlier stages of oligodendrocyte development and is downregulated as oligodendrocytes begin to mature and accumulate myelin components (Armstrong, Kim et al. 1995), whereas Plp1 expression was thought to characterize a later, myelinating stage. By investigating these two genes as potential targets, we hoped to gain insight into whether DLX1/2 are acting to repress oligodendroglial fate at multiple points of oligodendrocyte lineage progression.

## 1.5 Myelin transcription factor 1

Myelin transcription factor 1 (MyT1) is a zinc-finger transcription factor that was first identified via a phage display screen for proteins that could interact with *cis*-regulatory regions of the human proteolipid protein promotor (Kim and Hudson 1992). MyT1 belongs to the Cys-Cys-His-Cys (C2HC) subclass of zinc finger transcription factors. In vertebrates, there are two other members of this class: Myt1-like (Myt1l) (Kim, Armstrong et al. 1997) and Myt3 (Matsushita, Kameyama et al. 2014). The defining structural feature of this class of proteins is the presence of two sets of C2HC zinc fingers. The zinc finger domains in Myt1 are organized into one cluster of two and one cluster of four zinc fingers, separated by a serine-rich domain-containing spacer region (Kim and Hudson 1992, Manukyan, Kowalczyk et al. 2018).

During CNS development, the *Myt1* transcript is broadly expressed in the neuroepithelial germinal zones, and becomes downregulated in post-mitotic neurons, although expression does persist in a few mature neurons (Hudson, Romm et al. 2011).

In cultured oligodendrocyte progenitor cells, MyT1 is expressed from the earliest identifiable stages of oligodendroglial differentiation (Armstrong, Kim et al. 1995, Kim, Armstrong et al. 1997) and declines as oligodendrocytes differentiate and accumulate the myelin component proteolipid protein (Armstrong, Kim et al. 1995). MyT1 is not expressed in mature oligodendrocytes (Hudson, Romm et al. 2011).

Matushita *et al* (2014) analysed *Myt1* transcript distribution and expression levels during mouse nervous system development in detail via *in situ* hybridisation. In the future basal ganglia (i.e subpallial region) *Myt1* transcripts were detectable starting at E10.5, and declined to undetectable levels by about E18.5. Expression was seen in postmitotic neurons and some cells in the SVZ and VZ (Matsushita, Kameyama et al. 2014). Expression was also noted in the hippocampus at E14.5-15.5, and was strongly downregulated at E18.5. In the developing cortex, *Myt1* expression was detected starting at E10.5 and continuing through E14.5 (later time points were not assessed in the cortex by ISH), and was expressed in all regions of the cortical germinal zones.

Although expression is not restricted to glial lineages, *Myt1* is the only Myt1 family member to be expressed in the oligodendroglial lineage (Kim, Armstrong et al. 1997, Romm, Nielsen et al. 2005).

The exact function of *Myt1* in the development of the oligodendroglial lineage is not well-studied. *Myt1* knock-in and knockout mice have been generated, and died at birth, apparently due to respiratory failure caused by abnormal innervation of the lungs (Wang, Zhang et al. 2007, Hudson, Romm et al. 2011). These mice did not show any gross defects in neuronal differentiation within the spinal cord or development of the neural precursors that normally express *Myt1* (Hudson, Romm et al. 2011). This study did not assess the effects of *Myt1* loss on oligodendroglial development and myelination, presumably because these processes are only completed postnatally. Understanding of Myt1 family member function has also been complicated by compensatory upregulation of other family members when one is knocked out. For example, it was reported that when *Myt1* was conditionally ablated in the pancreas, *Myt1l* and *Myt3* were both upregulated (Wang, Zhang et al. 2007).

Consistent with its developmental expression pattern, in both neuronal and glial lineages *Myt1* generally seems to play a role in regulating the transition between progenitor proliferation and terminal differentiation (Bellefroid, Bourguignon et al. 1996, Nielsen, Berndt et al. 2004, Vasconcelos, Sessa et al. 2016). A role for *Myt1* in promoting differentiation has been shown for neuronal precursors, possibly via transcriptional repression of Notch pathway effectors, thereby suppressing the proneural gene expression program (Vasconcelos, Sessa et al. 2016). Overexpression of MyT1 has also been demonstrated to promote neuronal differentiation in *Xenopus* (Bellefroid, Bourguignon et al. 1996). *Myt1* also seems to be required for pancreatic islet cell differentiation (Wang, Zhang et al. 2007).

The role of Myt1 in oligodendroglial development has been investigated by overexpressing two of its putative functional domains in different cell types: the four zinc finger DNA binding region, or a central protein-protein interaction domain that is predicted to lack transactivation activity (Nielsen, Berndt et al. 2004). The expression of full-length *Myt1* in an oligodendrocyte cell line (CG4) was shown to activate expression of the myelin gene CNP (Nielsen, Berndt et al. 2004). Yeast and mammalian two-hybrid assays also revealed that Myt1 (and Myt1l) form complexes with the histone deacetylase (HDAC)-associated corepressor protein Sin3B (Romm, Nielsen et al. 2005), and it is suggested that MYT1 and Myt1l recruit Sin3B to neural promoters to promote gene silencing during neural development (Romm, Nielsen et al. 2005).

Regarding regulation of the *Plp1* promoter, it was noted that *Myt1* expression begins substantially before expression of its presumed target *Plp1* (Kim and Hudson 1992), at least *in vitro*. Because of this expression pattern as well as the unique domain structure of this class of protein, Hudson and Kim (1992) speculated that MYT1 binding to the *Plp1* promoter might alter the configuration of the DNA to facilitate promoter activation later on in development.
It has been shown via electrophoretic mobility shift assays that MYT1 fragments containing either the two or four zinc finger cluster can only both bind a *cis*-regulatory element in the *Plp1* promoter (Kim and Hudson 1992). Binding and regulation of the *Plp1* promoter by MYT1 or MYT1 family members has not been demonstrated *in vivo*.

Our lab has previously shown that DLX2 occupies a proximal region of the *Myt1* promoter *in vivo* (Figure 1.7) (Zhang S and Eisenstat D, unpublished data).

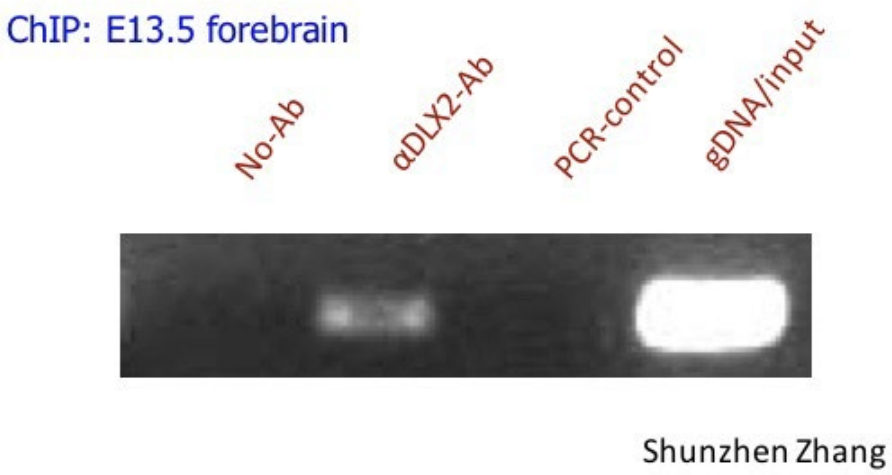


*Figure 1.7 Chromatin immunoprecipitation with a DLX2 antibody demonstrates that DLX2 occupies the Myt1 promoter in E13.5 forebrain.* Courtesy, Shunzhen Zhang.

## 1.6 Proteolipid protein

The second DLX2 target investigated in the current study is the gene *Plp1*. Alternative splicing of the *Plp1* primary transcript generates two products: the myelin proteolipid protein PLP, and an alternative product, DM20 (Ikenaka, Kagawa et al. 1992, Timsit, Bally-Cuif et al. 1992). PLP and DM20 are identical in primary structure, except that the second half of exon 3 (exon 3B), which contains amino acid residues 116-150 in the PLP form, is spliced out of the DM20 transcript (Nave, Lai et al. 1987, LeVine, Wong et al. 1990). Together PLP and DM20 are the

most abundant components of CNS myelin, comprising approximately 50% of its total protein content (Eng, Chao et al. 1968). The ratio of DM20 to PLP protein changes throughout development. Initially, DM20 protein predominates, and as development proceeds and myelination begins, PLP becomes the major isoform (LeVine, Wong et al. 1990) and it remains the most abundant product in mature myelin (Dickinson, Fanarraga et al. 1996). In the rat, the ratio of PLP to DM20 protein approaches that of mature myelin by P16 in the cerebrum and P7 in the hindbrain (LeVine, Wong et al. 1990). The developmental ratios of PLP and DM20 mRNA and of protein are not the same, implying that the PLP/DM20 ratio might be regulated by processes that occur post-transcriptionally and post-splicing (LeVine, Wong et al. 1990). Although the PLP product is most highly expressed at the peak of myelination, which occurs postnatally (Timsit, Bally-Cuif et al. 1992, Snaidero and Simons 2014), expression of the DM20 isoform begins much earlier (LeVine, Wong et al. 1990). *Dm20* transcript expression has been reported as early as E9.5 in mouse (Ikenaka, Kagawa et al. 1992, Timsit, Bally-Cuif et al. 1992). It has also been appreciated for some time that expression of DM-20 is not restricted to the oligodendroglial lineage (Ikenaka, Kagawa et al. 1992, Michalski, Anderson et al. 2011) and that this isoform may play roles that are related to glial differentiation in addition to acting as a myelin structural component (Ikenaka, Kagawa et al. 1992, Timsit, Bally-Cuif et al. 1992). More recently, it has become apparent that this may also be the case for *Plp*. For example, it has been shown using *Cre*-mediated labelling of cells expressing the *Plp1* promoter that the *Plp1* promoter shows widespread activity outside of the oligodendroglial lineage through to postnatal day 28, and only becomes restricted to oligodendrocytes later on (Michalski, Anderson et al. 2011). Studies on transgenic mice with EGFP-labelled *Plp1* knocked in also showed widespread promoter activity at early developmental stages in both neuronal and glial lineages (Harlow, Saul

et al. 2014), and further revealed that the *Plp1* promoter shows a biphasic pattern of expression in the oligodendrocyte lineage (Harlow, Saul et al. 2014). *Plp1* is first expressed early in the neuroepithelium, downregulated following migration of immature progenitors from the germinal zones, and then upregulated again in mature oligodendrocytes as myelination begins (Harlow, Saul et al. 2014). *Plp1* promoter activity also might precede expression of *Olig2* and *Pdgfra* in newly-born OPCs (Harlow, Saul et al. 2014). However, when PLP/DM20 expression was ablated, OPCs formed as normal and onset of myelination was not disrupted (Harlow, Saul et al. 2014), so the role that early expression of PLP and DM20 plays in early development of the oligodendroglial lineage is unclear. The *Plp1* promoter also showed activity in neuronal and astrocytic progenitors, in keeping with previous studies, but they did not produce PLP protein (Harlow, Saul et al. 2014).

Functionally, PLP and DM20 are myelin structural components, but their role in myelin structure is not well-understood. Oligodendrocytes from *Plp1*-null mice still myelinate axons and form compacted myelin sheaths as normal, although the myelin displays some ultrastructural abnormalities (Klugmann, Schwab et al. 1997). PLP also functions in the regulation of oligodendrocyte apoptosis (Somayajulu, Bessert et al. 2018) which is a normal part of oligodendroglial lineage development (Barres, Hart et al. 1992).

## 1.7 H3K27M-mutant diffuse midline glioma (diffuse intrinsic pontine glioma)

H3K27M-mutant diffuse midline glioma (previously known as diffuse intrinsic pontine glioma, or DIPG) is a uniformly lethal pediatric brain tumour that arises in the ventral pons, typically in middle childhood (Monje, Mitra et al. 2011). Approximately 80% of DIPG harbour a heterozygous missense mutation in one of the genes encoding the histone H3 variants H3.3 (encoded by H3F3A) or less commonly H3.1 (encoded by HIST1H3B) (Cordero, Huang et al. 2017) that results in a change of lysine residue 27 to a methionine (H3K27M mutation). H3K27M mutations reprogram the epigenetic landscape in a dominant-negative manner, resulting in widespread transcriptional dysregulation that drives tumorigenesis. The major effect is a global reduction in levels of the repressive epigenetic mark tri-methylated H3K27 (H3k27me3), which is important in silencing of developmental genes and establishment and maintenance of cell identity (Comet, Riising et al. 2016). H3K27me3 is also focally increased at some loci, as are levels of acetylated H3K27, which marks open or active chromatin. The mechanism by which H3K27M mutations exert these effects is unclear but is currently under intense investigation. Suggested mechanisms/contributing factors include interference with the function of the Polycomb repressive complex (PRC2) which deposits the H3K27me3 mark, and alteration of PRC2 chromatin residency dynamics by H3K27M histones (Chan, Fang et al. 2013).

### 1.7.1 Oligodendrocyte progenitor cell of origin of H3K27M-mutant midline glioma

H3K27M (H3.3K27M) tumours arise almost exclusively in CNS midline structures (brainstem and thalamus) during early-middle childhood. This anatomical and temporal specificity suggests a specific developmental origin for these tumours. That is, there is a specific cell type proliferating in midline brain structures at a particular time point that is vulnerable to oncogenic transformation by H3K27M mutations (Monje, Mitra et al. 2011). A better understanding of the developmental origins of these tumours is important because it may help inform the development of novel therapeutic strategies for this highly lethal disease.

Many H3K27M DIPG have an oligodendroglial progenitor cell-like phenotype, with features including amplification of *PDGFRA* and high expression of *OLIG2.* The cell of origin for at least some DIPG has thus been suggested to be an OPC (Monje, Mitra et al. 2011). A recent single-cell RNAseq analysis of six H3K27M DIPGs identified cells with an OPC-like gene expression signature as the predominant cycling population (Filbin, Tirosh et al. 2018). In one study, *DLX2* was identified as one of the most highly downregulated genes in H3K27M-mutant pediatric glioblastomas compared to tumours with an alternate (G34R/V) or no H3.3 mutation (Schwartzentruber, Korshunov et al. 2012). This finding, together with the hypothesized OPC origin of DIPG, suggested to us that there could be a role for DLX2 in driving differentiation in this tumour type.

# Chapter 2: Research aims and hypotheses

## 2.1 Aim 1: Characterise DLX2 transcriptional regulation of *Myt1*

**Hypothesis:** We hypothesize that DLX2 directly represses *Myt1* during forebrain development.

**Specific aims:**

**1. Determine if DLX2 occupies the *Myt1* promoter region in E13.5 GE**

To determine if DLX2 occupies potential regulatory regions in the *Myt1* promoter-proximal region, chromatin immunoprecipitation (ChIP) with a DLX2 antibody will be performed on chromatin obtained from E13.5 wild-type mouse forebrain.

**2. Determine if DLX2 directly binds *Myt1* promoter regions**

Promoter occupancy detected by ChIP assays could be indirect. To determine if DLX2 can directly bind regulatory regions identified in the *Myt1* promoter, electrophoretic mobility shift assays will be performed using recombinant DLX2 and radiolabelled probes corresponding to any regions of the *Myt1* promoter that are found to bind DLX2 in ChIP assays.

**3. Determine if DLX2 binding to *Myt1* promoter regions affects transcriptional output**

Transcription factor binding does not always have functional consequences for promoter activity. To determine if DLX2 binding to regulatory regions affects transcription from the *Myt1* promoter, luciferase reporter assays will be performed. Regions of the *Myt1* promoter that are bound by DLX2 identified by ChIP and validated by EMSA will be cloned into a luciferase reporter vector. Reporter plasmids will be co-transfected into HEK293 cells along with a *Dlx2* expression plasmid, and reporter gene activity will be measured *in vitro*.

**4. Determine if *Myt1* expression is upregulated during forebrain development in the absence of *Dlx1/2* gene function**

If DLX2 is repressing the *Myt1* promoter during forebrain development, then *Myt1* transcripts should be upregulated in the *Dlx1/2* DKO forebrain. To assess this, qPCR will be performed on

RNA extracted from E13.5 DKO forebrain and their WT littermates. E13.5 is chosen as a convenient developmental time point for this experiment because it falls in the middle of the peak period of DLX2 expression in the forebrain. If DLX1/2 repress *Myt1,* then *Myt1* expression should be significantly increased in the DKO forebrain compared to the WT *in vivo*.

## 2.2 Aim 2: Characterise DLX2 transcriptional regulation of *Plp1*

**Hypothesis:** We hypothesize that DLX2 directly represses *Plp1* during forebrain development

**Specific aims:**

**1. Determine if DLX2 occupies the *Plp1* promoter region in E13.5 GE**

To determine if DLX2 occupies potential regulatory regions in the *Plp1* promoter-proximal region, ChIP with a DLX2 antibody will be performed on chromatin from E13.5 WT forebrain.

**2. Determine if DLX2 directly binds *Plp1* promoter regions**

Promoter occupancy detected by ChIP assays could be indirect. To determine if DLX2 can directly bind regulatory regions identified in the *Plp1* promoter, electrophoretic mobility shift assays will be performed using recombinant DLX2 and radiolabelled probes corresponding to any regions of the *Plp1* promoter that are found to bind DLX2 in ChIP assays.

**3. Determine if DLX2 binding to *Plp1* regulatory regions affects transcriptional output**

Transcription factor binding does not always have functional consequences for promoter activity. To determine if DLX2 binding to regulatory regions affects transcription from the *Plp1* promoter, luciferase reporter assays will be performed. Regions of the *Plp1* promoter that are bound by DLX2 identified by ChIP and validate by EMSA will be cloned into a luciferase reporter vector. Reporter plasmids will be co-transfected into HEK293 cells along with a *Dlx2* expression plasmid, and reporter gene activity will be measured *in vitro*.

**4. Determine if *Plp1* expression is upregulated during forebrain development in the absence of *Dlx1/2* gene function**

If DLX2 is repressing the *Plp1* promoter during forebrain development, then *Plp1* transcripts should be upregulated in the *Dlx1/2* DKO forebrain. To assess this, qPCR will be performed on RNA extracted from E13.5 DKO forebrain and their WT littermates. E13.5 is chosen as a convenient developmental time point for this experiment because it falls in the middle of the peak period of DLX2 expression in the forebrain. If DLX1/2 repress *Plp1,* then *Plp1* expression should be significantly increased in the DKO forebrain compared to the WT. To examine PLP protein expression, immunofluorescence (IF) will be performed with a PLP antibody on DKO and WT E13.5 and E18.5 forebrain to determine if PLP protein expression is increased and/or expanded in the DKO forebrain *in vivo*.

## 2.3 Aim 3: Characterization of MYT1 transcriptional regulation of *Plp1*expression

**Hypothesis:** We hypothesize that MYT1 activates the *Plp1* promoter during forebrain development

**Specific aim 1: Determine if MYT1 occupies the *Plp1* promoter region during forebrain development, before the onset of *Plp1* expression**

If, as hypothesized in earlier studies of MYT1 function (Kim and Hudson 1992), MYT1 functions to physically enable the *Plp1* promoter to be activated later on in oligodendroglial development, then MYT1 should be localized to the *Plp1* promoter early in development, before myelination begins. To assess this, ChIP will be performed with a MYT1 antibody on forebrain chromatin at pre-myelinating time points, followed by PCR with primers designed to amplify regions of the *Plp1* promoter containing putative MYT1 binding sites.

## 2.4 Aim 4: Assess the effect of DLX2 overexpression of DIPG differentiation and the cancer cell phenotype.

**Hypothesis:** Because of the proposed OPC origin of DIPG, we hypothesize that DLX2 overexpression in DIPG cell lines will result in a more differentiated, less invasive, and less proliferative phenotype.

**Specific Aim 1: Assess whether DIPG cells are competent to respond to DLX2 transcriptional regulation.**

Not all DIPG tumour cell lines may be competent to respond to DLX expression. To assess this, patient-derived DIPG cell lines will be transiently transfected with a *Dlx2* expression construct and expression levels of known DLX target genes (*Gad1, Gad2*) and genes involved in oligodendroglial lineage development (*Nkx2.2*, *Olig2, Myt1*) will be measured with qPCR. If the cells are competent to respond, *Dlx2* overexpression should result in upregulation of *Gad* genes and downregulation of oligodendroglial genes.

**Specific Aim 2: Determine whether DLX2 overexpression results in a less invasive and less proliferative phenotype**

If cells are found to be responsive to DLX2 regulation, we will assess whether DLX2 has functional consequences on the cancer cell phenotype by performing *in vitro* proliferation, migration, invasion, and soft colony formation assays on DLX2-transfected cells.

# Chapter 3: Materials and Methods

## 3.1 Animals and tissue collection

Tissue for ChIP experiments was dissected from timed-pregnant CD1 mice obtained from the Charles River Laboratory. For interrogation of DLX2 occupancy of *Myt1* and *Plp1* promoters, E13.5 tissue was used as this falls within the peak period of DLX2 expression in the developing brain. For MYT1 ChIP experiments, tissue from E14.5 and E18.5 forebrain was used. These time points were chosen based upon E18.5 as the time when we first detected PLP1 protein expression in the wild-type brain. I also chose to investigate the earlier time point of E14.5 because it has been hypothesized that regulation of the *Plp1* promoter by MYT1 occurs substantially before the onset of PLP1 expression (Kim and Hudson 1992). Therefore, I reasoned that although *Plp1* expression is not detectable in the WT at E14.5, its promoter might still be occupied by regulatory factors including MYT1 at that time point.

For investigation into differential gene expression in the absence of *Dlx* gene function, we used *Dlx1/Dlx2* double knockout transgenic mice (provided by Dr. John Rubenstein (UCSF, CA, USA). Generation of the DKO mouse is described in detail in (Qiu, Bulfone et al. 1997). Briefly, *Dlx1/2* gene knockout was accomplished with the use of a targeting vector that removed all of exons 2 and 3 of both *Dlx1* and *Dlx2,* the entire intergenic region, and part of exon 1 of *Dlx2* (See Figure 1.5 for *Dlx* gene structure).

Embryonic age was determined by the day of appearance of the vaginal plug (designated E0.5). Dams were sacrificed by cervical dislocation at the appropriate time point of pregnancy and the embryos were euthanized by decapitation, then dissected.

All animal experiments were approved by the University of Alberta animal care user committee under the animal use protocol 00001115 (Transcription factors and mouse development).

### 3.2 Tissue preparation and cryopreservation

Whole mouse E13.5 and E18.5 heads were collected and placed in freshly-made 4% paraformaldehyde (PFA) either for 3 hours or overnight with rotation at 4°C for fixation. Following fixation, tissue was washed with cold phosphate-buffered saline (PBS) and passed through a series of 10%, 20%, and 30% sucrose solutions for subsequent cryoprotection. Tissue was then embedded in Optimal Cutting Temperature Compound (OCT; VWR, catalog number 95057-838) and the embedded tissue blocks were stored wrapped in foil at -80°C until sectioning. Sectioning of tissue was done on a Leica CM1900 cryostat at a thickness of 12 μm and sections were placed on Superfrost Plus slides (Fisher Scientific). Slides were stored at -80°C in sealed boxes for later use in immunofluorescence experiments.

### 3.3 Tissue immunofluorescence

Sections were blocked for 1-2 hours in blocking buffer consisting of 0.1% bovine serum albumin (BSA, Fisher Scientific, catalog #: BP1600-100), 0.2% Triton-X 100 (Biorad, catalog #: 1610407), 5% serum in PBS at room temperature (RT). Sections were then incubated overnight at 4°C with the primary antibody diluted in blocking buffer. The following day, primary antibody was removed and slides underwent 3 5-minute washes with 0.05% Triton-X in 1X PBS, followed by incubation in the dark with the secondary antibody (diluted in blocking buffer) for 2

hours at room temperature. Slides were washed again as described above, then coverslips were mounted using VECTASHIELD Antifade Mounting Medium with DAPI (Vector Labs, catalog number H-1200) and sealed with nail polish. Slides were imaged using an Eclipse TE2000U (Nikon) and NIS Elements software.

## 3.4 Chromatin immunoprecipitation

Ganglionic eminences were dissected from E13.5 embryos from timed-pregnant wild-type CD1 mice. As an additional negative control for DLX2 ChIP, E13.5 hindbrain tissues were also collected since hindbrain does not express any *Dlx* family members.

*Fixation*

Tissue was rinsed twice with ice-cold PBS, then dissociated into a single-cell suspension by pipetting up and down several times followed by passage through a cell strainer **(**Corning, catalog number #352235**)**. Cells were crosslinked in 1% freshly-prepared PFA, 1X Protease Inhibitor Cocktail (PIC; Roche, catalog number 11836153001), and 1 mM phenylmethylsulfonyl fluoride (PMSF) for 90 minutes at room temperature, then collected by centrifugation at 2000 RPM for 5 minutes, 4°C. PFA supernatant was removed and cells were washed twice with ice-cold 1X PBS.

*Lysis and chromatin shearing*

Following fixation, cells were resuspended in lysis buffer (1% SDS, 10mM Tris-HCL (pH 8.1), 10mM EDTA, 1X PIC, 0.5 mM PMSF) for chromatin shearing. Shearing was conducted using a 60 Sonic Dismembrator probe sonicator (Fisher) set at 40% output. To avoid overheating, sonication was done in intervals of 15 seconds sonication, 30 seconds rest, with the samples on ice. 25-35 cycles of sonication were carried out to obtain fragments of an average size of

between 300 and 500 bp. Fragment size was determined by running 3-5 µL chromatin on a 1% agarose gel. Sheared chromatin was centrifuged at 14000x*g* for 20 minutes at 4°C in order to pellet cell debris. Chromatin was aliquoted and snap-frozen in liquid nitrogen, then stored at -80°C for use in ChIP.

*Preclearing and Immunoprecipitation*

Two sets of Pierce UltraLink Protein A/G beads (Thermo Fisher Scientific, catalog number #53132) (60 µL per sample) were washed twice in 1 mL dilution buffer (0.01% SDS, 1.1% Triton X-100, 1.2 mM EDTA, 16.7 mM Tris-HCL pH 8.1, 167 mM NaCL, 1X protease inhibitor cocktail (PIC, Roche, catalog number 04693159001). Then, for preclearing, a 50% slurry of beads was prepared in dilution buffer and 1X PIC. 60 µL of beads was added to each sample tube and samples were rotated at 4°C for 1 hour. Samples were centrifuged and transferred to new tubes, and the beads were discarded. BSA and yeast tRNA (Invitrogen, catalog number #AM7119) were added to each sample at a final concentration of 50 µg/mL. Antibody-designated samples received 1.5 µl (1.5 µg) of anti-DLX2 antibody (for amounts used in MYT1 ChIP, see below.)

At the same time, a 50% slurry of beads was prepared with the addition of 500 µg/ml each BSA and yeast tRNA for use in the immunoprecipitation. Samples and beads were incubated separately overnight at 4°C with rotation. The next morning, 60 µl of beads was added to each sample tube and incubated for 24 hours at 4°C with rotation. Then, beads were pelleted by centrifugation and the supernatant (containing unbound chromatin) was removed. The beads were washed with a series of washes to remove non-specifically bound chromatin and proteins. Low salt buffer (0.1% SDS, 1% Triton X-100, 2 mM EDTA, 20 mM Tris-HCL pH 8.1, 150 mM

NaCl) for 5 minutes, high salt buffer (0.1% SDS, 1% Triton X-100, 2 mM EDTA, 20 mM Tris-HCL pH 8.1, 500 mM NaCl) for 30 minutes; LiCl buffer (0.25M LiCl 1% deoxycholate, 1mM EDTA, 10mM Tris-HCl, 1% NP-40); followed by two 5 minute washes with 1X TE (pH 8.0). All washes were carried out at 4°C with rotation.

After washing, bound chromatin-antibody complexes were eluted from the beads by adding elution buffer (1% SDS, 0.1 M $NaHCO_3$) pre-warmed to 65°C and incubating for 15 minutes with agitation. This step was repeated twice, with eluted chromatin being collected by centrifugation and transferred to fresh tubes.

25 µL of 5M NaCl was added to the eluted chromatin samples and they were incubated overnight at 65°C to reverse the crosslinking. RNAse A was also added to degrade any RNA that would interfere with column-based purification of chromatin later. The next morning, 20 µL of 1M Tris-HCL (pH 6.5), 10 µL of 0.5 M EDTA (pH 8.0) and 2 µL Proteinase K were added and samples were incubated for 2 hours at 55°C to degrade proteins. Chromatin was then purified using a QIAQuick PCR purification kit (Qiagen, catalog number #28104) and ChIP-PCR and qPCR was carried out using primers designed to amplify putative *Myt1* and *Plp1* regulatory regions.

ChIP-positive regions were verified by gel extraction and sequencing (TAGC, University of Alberta).

*MYT1 ChIP*

For MYT1 ChIP, some modifications were made to the protocol described above, based on the protocol described for MyT1 ChIP by Islam *et al* 2015. IP buffer (50 mM HEPES (pH 7.4), 20 mM NaCl, 1 mM EDTA, 0.1% Triton X-100, 1X PIC) was used in place of dilution buffer. I

used a ratio of 10 μg chromatin to 1 μg antibody as reported in the paper. For E14.5, 25 μg of chromatin was used in the IP (and 2.5 μg antibody). For E18, 36 μg of chromatin was used in the IP (and 3.6 μg antibody) due to differences in chromatin yield from an E14.5 litter versus an E18.5 litter. Rather than use no antibody as a control, negative control sample tubes were incubated with an equivalent amount of nonspecific rabbit IgG (Abcam, Ab37415). A negative control tissue was not used for MyT1 ChIP. Chromatin preparation and all steps until bead washing were performed as described above. For E14.5 samples, beads were washed using the buffers described above for DLX2 ChIP, except each wash was carried out for 10 minutes at 4°C with rotation.

For E18.5 samples, after immunoprecipitation, beads were washed as follows: 2 washes in IP buffer; 2 washes in MyT1 wash buffer (100 mM Tris-HCL pH 8.0, 500 mM LiCl, 1% NP-40, 1% sodium deoxycholate, 1X PIC); 1 wash in MyT1 high salt wash buffer (100 mM Tris-HCL pH 8.0, 500 mM LiCl, 1% NP-40, 1% sodium deoxycholate, 150 mM NaCl, 1X PIC). All washes were carried out for 10 minutes with rotation at 4°C. For all samples, elution, de-crosslinking, and purification were performed as described for DLX2 ChIP.

*DLX2 and MYT1 ChIP-qPCR*

For ChIP-qPCR (quantitative ChIP assays), ChIP was performed as described above except that instead of no antibody, control samples of forebrain chromatin were prepared that received equivalent amounts of species-matched IgG. Hindbrain chromatin was not used as a control for ChIP-qPCR. The qPCR data were normalized using the fold-enrichment method. For each tested region (primer pair), the DLX2 or MYT1 ChIP signals were first normalized to the IgG ChIP

signals by subtracting the average IgG sample Ct value from the average DLX2 or MYT1 sample Ct. This normalized Ct value was then used to calculate fold-enrichment using the ddCT method (Livak and Schmittgen 2001), to obtain the fold-enrichment of that region over the background (IgG) signal.

For both MYT1 and DLX2, ChIP-qPCR was performed in only one biological replicate; therefore, no statistical analysis was performed.

### 3.5 Molecular cloning

ChIP-positive regulatory regions were modified by addition of appropriate restriction sites to allow cloning into the pGL3 Basic vector's multiple cloning site. Briefly, primers were designed to amplify each region that would result in the addition of appropriate restriction sites to the 5' and 3' end of each region (Table 3.6). Regions were amplified using Phusion Polymerase (NEB, catalog number #M0530S) using wild-type CD1 mouse genomic DNA as the template. PCR products were purified using a QIAquick PCR purification kit (Qiagen) and digested using the appropriate restriction enzyme, 6 μL of appropriate buffer, 6 μL of 10X BSA in a total reaction volume of 60 μL at 37°C for two hours. Empty pGL3 vector was digested at the same time using the same enzymes. Digested vector was run on a 1% agarose gel, and the gel band corresponding to the vector was purified using an illustra GFX PCR DNA and Gel Extraction Purification kit (GE Healthcare, catalog number 28903466). Digested inserts were purified using a QIAquick PCR purification kit (Qiagen). Ligation was then performed using T4 DNA ligase (New England Biolabs, catalog number M0202S) at a molar ratio of 1:3.

DH5α competent *E. coli* cells (Invitrogen, catalog number #18265017) were transformed by incubating 3 μL of ligation mixture with 30 μL of competent cells on ice for 30 minutes,

followed by a 45 second 42°C heat shock. Then LB media was added and cells were incubated for 2 hours at 37°C with rotation at 225 RPM. 100-200 μL of cells were spread onto LB agar plates containing 50 mg/ml of carbenicillin, and the plates were incubated at 37°C overnight. The following morning, single colonies were picked and used to inoculate selective overnight cultures (50 mg/ml carbenicillin), and plasmid DNA was isolated using a QIAprep Spin Miniprep kit (Qiagen). Successful insertion of the desired region in the correct orientation was verified by Sanger sequencing at TAGC (University of Alberta). A diagnostic digest was also performed and run on an agarose gel to verify presence of a correctly-sized insert.

### 3.6 Electrophoretic mobility shift assays

Complementary single-stranded oligonucleotides corresponding to ChIP-positive promoter regions were ordered from Integrated DNA Technologies (Iowa). Some regions were split into multiple subregions containing only some of all the candidate homeodomain binding sites contained within the entire region. Forward and complementary oligonucleotides (oligos) were made up to a final concentration of 10 pmol each in annealing buffer, then placed in a 100°C heat block which was switched off and slowly allowed to cool to room temperature. Annealed oligonucleotides were 5' labelled using T4 Polynucleotide Kinase (Invitrogen, catalog number #EK0031) and [γ-32P]-dATP (Perkin Elmer). The labelling reaction was terminated with 1 μL 0.5 M EDTA (pH 8.0 and 20 μL 1x TE (pH 8.0), and labelled probes were purified using GE Healthcare illustra MicroSpin G-25 columns (GE Life Sciences, catalog number 27356501). Radioactivity of probes was measured on an LS 6500 Multi-Purpose Scintillation Counter (Beckman Coulter) and all probes were diluted in 1X TE to approximately 80,000 counts per million (CPM)/μL for use in EMSA. Binding reactions for EMSA were prepared by incubating

175-200 ng recombinant DLX2 protein, Poly(DI-dC) (Thermo Fisher Scientific, catalog #: 20148E), and 5X binding buffer (Promega, catalog#: E3581) for thirty minutes at room temperature. At this time the supershift sample also received 500 ng of anti-DLX2 antibody. After thirty minutes labelled probe (80,000 CPM or higher) was added; at this time the cold competition sample received 10 µl of unlabelled probe. Binding reactions were then incubated for another thirty minutes at room temperature before being run on a 4% polyacrylamide gel at 300V for approximately one hour in 0.5X TBE running buffer. Gels were dried using a gel dryer and HydraTech vacuum pump (Biorad) for 1-1.5 hours at 80°C. Gel was exposed to BioMax XAR film (Carestream) overnight at -80°C.

### 3.7 Quantitative polymerase chain reaction

Quantitative reverse transcription PCR (qRT-PCR) was performed on WT and *Dlx1/2* DKO mouse E13.5 forebrain to determine if loss of *Dlx* gene function affects expression of *Myt1* and *Plp1 in vivo.* Ganglionic eminences were dissected from each pup and snap-frozen in liquid nitrogen, then stored at -80°C until pups were genotyped. Following genotyping, tissue from DKO and WT pups was aggregated to produce one WT and one DKO RNA pool per litter. RNA extraction was performed with TRIzol (Invitrogen, catalog number #15596018) according to the manufacturer's instructions. cDNA synthesis was carried out using Invitrogen Superscript III Reverse Transcriptase (Invitrogen, catalog number #18080044) according to the manufacturer's instructions. Briefly, 500 ng-1 µg RNA template was combined with 1 µL oligoDT(18-20)(50 µM) primer (Invitrogen, catalog number #18418012), 1 µL 10 mM dNTP mix, and ultrapure water to a final volume of 13 µL. This was heated to 65°C for 5 minutes, then incubated on ice for 1 minute. Then, 4 µL 5X First-Strand buffer (Invitrogen, catalog number #18080044), 1 µL

0.1m DTT (Invitrogen, catalog number #18080044 ), 1 μL RNAseOUT (Invitrogen, catalog number #10777019), and 1 μL Superscript III Reverse Transcriptase (Invitrogen, catalog number #18080044) were added to each reaction. Reactions were then incubated at 55°C for 60 minutes, then at 70°C for 15 minutes. cDNA was diluted 2-fold in nuclease-free water for use in qPCR. For RNA extraction protocol used for SF8628 cells, see section 3.9.

qPCR was performed on a Roche LightCycler 96 Instrument. Primers used for gene expression analysis were validated before use in qPCR using a six-point 10 fold dilution series of WT cDNA to confirm their acceptable amplification efficiency across this range and that they only gave a single major product (melting peak). Primers used for ChIP PCR and qPCR were validated using a six-point four or five fold dilution series of genomic DNA or purified sheared forebrain chromatin as the template. Fold-change for gene expression was calculated using the ddCT method (Livak and Schmittgen 2001). For ChIP-qPCR, fold enrichment relative to the IgG samples was calculated. Statistical significance was calculated using Student's unpaired t-test. $p < 0.05$ was used as the cut-off for the determination of statistical significance in all cases.

### 3.8 Luciferase reporter assays

HEK293 cells were maintained in Dulbecco's Modified Eagle Medium (DMEM; Gibco, catalog number #12320032) supplemented with 10% fetal bovine serum (FBS; Gibco, catalog number #12483020) and 1% penicillin/streptomycin (Gibco, catalog number #15140122) until they reached 90% confluence. 24 hours before transfection, cells were trypsinized (0.25% Trypsin-EDTA, Gibco, catalog number #25200056) and seeded at a density of 15,000 cells/well in 12-well plates. Cell counting was performed using a Countess II FL Automated Cell Counter

(Invitrogen). At this time cells were switched to antibiotic-free media (DMEM + 10% FBS) for transfection. Cells were incubated for 24 hours at 37°C, 5% CO2, to reach 70% confluence. The next day, cells were transfected. The following table shows the four different transfection conditions and plasmids used. 0.5 μg of each plasmid per well was used, except for the renilla plasmid (6.67 ng per well).

| 1. Empty vectors | 2. DLX2 alone | 3. Regulatory element alone | 4. DLX2 + regulatory element |
|---|---|---|---|
| Empty pGL3 + Empty pcDNA3 + Renilla | Empty pGL3 + pcDNA3-DLX2 + Renilla | pGL3-region + empty pcDNA3 + Renilla | pGL3-region + pcDNA3-DLX2 + Renilla |

Each transfection was performed in three technical replicates (3 wells of the plate transfected for each condition). Plasmids for each condition were first mixed in 300 μl of Opti-MEM (Gibco, catalog number #31985070) pre-warmed to 37°C. Separately, Lipofectamine 2000 (Invitrogen, catalog number #11668027) and Opti-MEM were mixed at a ratio of 1 μL Lipofectamine in 10 μL Opti-MEM. Mixtures were incubated separately at room temperature for 5 minutes. Lipofectamine and Opti-MEM mixture was then added to each tube of plasmids. Tubes were briefly vortexed to mix, then incubated at room temperature for five minutes. 200 μL of final plasmid and Lipofectamine mixture was added dropwise to each well of the plate. The following morning, media was replaced with fresh DMEM/10% FBS/1% pen-strep. Cells were incubated for 48 hours post-transfection at 37°C, 5% $CO_2$. Then, media was removed and cells were washed on ice twice with ice-cold HBSS. 200 μL of 1X reporter lysis buffer, prepared from 5X reporter lysis buffer (Promega, catalog number #E4030) in 1X PBS, was added to each well.

Plates were incubated at -80C for 15 minutes, then allowed to thaw to room temperature, scraped, and the lysate for each well collected in a separate 1.5 mL Eppendorf tube. Samples were briefly vortexed, then either read immediately or stored at -80°C until ready for use. Luciferase and renilla activity were measured using a SpextraMax L Microplate reader (Molecular Devices). Experiments were performed in three biological and technical replicates. Statistical significance of fold-change in normalised luciferase activity was calculated using Student's unpaired t-test. $p < 0.05$ was used as the cut-off for the determination of statistical significance in all cases.

### 3.9 DXL2 overexpression in SF8628 human DIPG cells

Cells were maintained in Dulbecco's Modified Eagle Medium (DMEM; Gibco, catalog number #12320032) supplemented with 10% fetal bovine serum (FBS; Gibco, catalog number #12483020) and 1% penicillin/streptomycin (Gibco, catalog number #15140122). 24 hours before transfection, $1x10^5$ cells were seeded in 12-well plates in DMEM supplemented with 10% FBS. Cells were transfected using Lipofectamine 2000 with a Lipofectamine: plasmid ratio of 1:3. As the plasmids contain a GFP tag, successful transfection was confirmed by visual inspection of the cells using an Eclipse TE2000U (Nikon). For gene expression analysis, RNA was harvested from transfected cells using TRIzol (Qiagen) following the manufacturer's instructions for cultured cells.

### 3.10 Migration and invasion assays in mouse DIPG cells

**Media:**

a. Starvation media: Mouse NeuroCult Medium (STEMCELL Technologies, catalog #05700), 1% penicillin-streptomycin (Gibco, catalog number #15140122)

b. 1X growing media: Mouse NeuroCult Medium (STEMCELL Technologies, catalog #05700), 10% NeuroCult Proliferation Supplement (STEMCELL Technologies, catalog number 05701), 1% penicillin-streptomycin (Gibco, catalog number #15140122), human basic FGF 20 ng/mL, human EGF 10 ng/mL, heparin 2 μg/mL

c. 2X growing media: Mouse NeuroCult Medium (STEMCELL Technologies, catalog #05700), 20% NeuroCult Proliferation Supplement (STEMCELL Technologies, catalog number 05701), 1% penicillin-streptomycin (Gibco, catalog number #15140122), human basic FGF 20 ng/mL, human EGF 10 ng/mL, heparin 2 μg/mL

**Migration assay:**

Murine DIPG cells (mDIPG cells) stably overexpressing DLX2-GFP or GFP were maintained in 1X growing media until the night before the experiment, when they were switched to starvation media.

Chambers were prepared on the day of the experiment. The base membranes of 12-well Transwell chambers (VWR, catalog number #10769-212) were hydrated by adding 1 mL of starvation media to each well. 200 μL of starvation media was added to the upper chamber of each well. Plates were then incubated at 37°C for 30 minutes to 1 hour. Cells were washed twice with sterile 1X PBS and disassociated by treatment with Accutase (STEMCELL Technologies, catalog number #07920) for ten minutes. Accutase was inactivated by the addition of an

equivalent volume of media, and cells were dissociated by gently pipetting up and down. Cells were centrifuged to pellet and washed twice with media to remove remaining Accutase, then resuspended in starvation media to yield a suspension with a concentration of 1.6 x $10^6$ cells/mL. Cell counting was performed using a hemocytometer. The hydrated Transwell inserts were inserted into 12-well plates containing 1 mL of 2X growing media per well. 6 x $10^5$ cells were then added to the upper chamber for the 24-hour migration assay, and 1.6 x $10^5$ cells for the 48-hour migration assay. Cells were incubated for 24 or 48 hours at 37°C, 5% $CO_2$. Then, the insert was removed and gently washed in Dulbecco's Phosphate Buffered Saline. Debris and cells remaining on the upper side of the membrane were gently removed with a cotton swab. The cells on the lower side of the membrane were fixed for 20 minutes using 4% polyoxymethylene, then stained for 20 minutes with 1% cresyl violet in 2% ethanol. Cells on the lower side of the membrane were counted via brightfield microscopy on an Eclipse TE2000U (Nikon) and NIS Elements software. The average of multiple randomly selected fields was used to obtain an average number of cells that had migrated through the membrane.

**Invasion assay:**

Cells were maintained as described for the migration assay and changed to starvation media the night before the experiment. On the day of the experiment, 24-well Matrigel invasion chamber plates (Corning, catalog number #354480) were prepared by adding 1 mL starvation media into the wells. 200 μL of starvation media was placed into the upper chamber of each well. Plates were incubated at 37°C for 30 minutes to 1 hour. 24-well plates were then prepared by the addition of 1 mL 2X growing media to each well and the hydrated chambers were placed into the plate. Cells were dissociated, prepared, and placed into the invasion chambers as described for

the migration assay, and allowed to migrate for 24 to 48 hours. Fixation, staining, and counting was performed as described for the migration assay.

### 3.11 Soft agar colony formation assay in mouse DIPG cells

A 5% (weight/volume) 10X stock of Bacto-Agar (Difco, catalog number #158783) was prepared by boiling the agar in distilled water to dissolve, followed by autoclaving. To prepare the soft agar dishes, this stock was melted by boiling, then cooled to 45°C. For each dish, 1 mL of agar was then added to a prewarmed 37°C mixture of 7.9 mL 1X growing media and 1 mL 2X growing media (see migration assay) and 100 μL of 100X penicillin-streptomycin. 7 mL of this mixture was plated onto 60-mm dishes and allowed to solidify at room temperature, then stored at 37°C until the addition of the top agar layer containing the cells. The rest of the agar mixture was reserved for the preparation of the top layer. mDIPG cells were dissociated using Accutase and dilutions of $4 \times 10^5$, $2 \times 10^6$, and $5 \times 10^6$ cells were prepared in 1X growth medium. Cell suspensions were warmed to 37°C and 2 mL of the medium/agarose mixture was added to the suspensions for a final concentration of 0.33% (weight/volume) agar. 1.5 mL of this mixture was quickly overlaid onto the prepared bottom layer of agar in the dishes. Cells were then incubated at 37°C, 10% $CO_2$ and fed weekly by dropwise addition of 0.5 mL growth medium per dish. After two or three weeks, colonies were stained with cresyl violet and scored by counting with brightfield microscopy on an Eclipse TE2000U (Nikon) and NIS Elements software.

### 3.12 MTT assay in mouse DIPG cells

Cells were plated into flat-bottomed 96-well plates at a density of $3 \times 10^5$ cells/well for 1 day, $1.5 \times 10^5$ cells/well for 2 days, $5 \times 10^4$ cells/well for 5 days, and $2.5 \times 10^4$ cells/well for 7 days. Cells

were grown for the indicated time, then 10 μL of 5 mg/mL Methylthiazolyldiphenyl-tetrazolium bromide (MTT) (Sigma-Aldrich, catalog number M-2128) in PBS was added to each well and plates were incubated at 37°C for 30 minutes to 1 hour. 50 μL of freshly-prepared 0.04N HCL in isopropanol was added to each well. Absorbance was then measured at 560 or 570 nM using a SpextraMax L Microplate reader.

## 3.12 Tables

**Table 3.1.** Primers used in DLX2 ChIP-PCR and ChIP qPCR

| **Region** | **Forward Primer Sequence (5'-3')** | **Reverse Primer Sequence (5'-3')** |
|---|---|---|
| *Myt1* region 1 | 5-GCACAAGCACATGCACATAGAA-3 | 5-CACCGTTCGTAAGGACTTGTCAG-3 |
| *Myt1* region 2 | 5-TCTGGAACAAGGGATCAAGG-3 | 5-CCACCCAGGGTATGAGCAG-3 |
| *Myt1* region 3 | 5-GGTTTAGTTAATACTCATCCCTTC-3 | 5-GCCCAGTTCAGCTAATTTATTTC-3 |
| *Myt1* region 4 | TCTGAGGTCAATTACACCCTATTC | GCTACCCTTGACGCCACATC |
| *Myt1* region 5 | GCAGACCAATTTGCTTAGAGG | CACTCACTTCTGCTCCAGTTTC |
| *Myt1* region 6 | CAGGCTAGCTGACTTGTGGA | AGAGTCTCTCTGCCCTGACC |

| | | |
|---|---|---|
| *Myt1* region 7 | GCTAGCAGAGACATTGTGTGG | CAGCTGTTAACCCAGCTTTATTC |
| *Myt1* region 8 | TCAGAGTTAGGGTTGAACTGTCTT | CCTTCCCACTTCAAGATTCC |
| *Myt1* region 9 | CCCTTGTATCCCAATTTCTCA | CTGGTTGAAGTGACAGGAAGG |
| *Myt1* region 10 | TGCCTTTGTTTACAGTCCTACC | CACCTGGGATCATAGGGTTT |
| *Myt1* region 11 | GTCCACTGCTTGCTCGTTT | AAGCCCAATCTGGTCACTTC |
| *Myt1* region 12 | GGCCTGTTGTGTCCAAGTTC | TTGAACAGTGAAGGAGGAGATG |
| *Myt1* region 13 | GTGACAGCCCAATTCTAGCC | CCACAACCAGCCAATCAAA |
| | | |
| *Plp1* region 1 | TACTGAGGGCTGCCTGAGAT | CCGAGGGGGAATGTCTATTT |

| | | |
|---|---|---|
| *Plp1* region 2 | CAGGCTAGGTGTACCATTCCA | GCTTTGCCCACTCCAGAAA |
| *Plp1* region 3 | TTCTTGTGGCCAGGGATG | CTGCTGGGATGCTTCTTAGGT |
| *Plp1* region 4 | CCATCCTCCCCTTTGCTATT | TGGTTGTCAATAGTCACCTAACTC |
| *Plp1* region 5 | TCTGGATGAGCCCGAGAAC | CAGGGCATTGAGAAGTCCAG |
| *Plp1* region 6 | AAGAAGGATGCAGAGGGACTG | CCCAGTAAACTCCCAGACACAA |
| *Plp1* region 7 | GGAGGGACAAGAGAAAGAGAACAG | CTCAGCCATTCTCAGCAGCA |
| *Plp1* region 8 | AGCTGCTTGCCAGTTTGTGA | AGCCAGACGTGCAATGAGAG |
| *Plp1* region 9 | GAGTTAGGTGACTATTGACAACCAG | AAAACTTGGCTGGCTTTGC |

**Table 3.2.** Primers used in MYT1 ChIP-PCR

| **Gene Region** | **Forward Primer (5' to 3')** | **Reverse Primer (5' to 3')** |
|---|---|---|
| *Plp1* region 1 | ACAGTCCCAGAGATGCTGCT | TATTGACAGCCCTGGAGGAG |

| | | |
|---|---|---|
| *Plp1* region 2 | TTTCCTTAGAGCCATTCAGCA | TGACGTCTGTGAAGGAACCA |
| *Hes1* | GGGAAAGAAAGTTTGGGAAGT | GTTATCAGCACCAGCTCCAG |
| *Olig1* | GTGAACAGTCCCCCTTCTGT | GCTGCCAAACCTTCAGTCTA |

**Table 3.3.** Oligonucleotide probes used for electrophoretic mobility shift assays

| **Oligo name** | **Oligo sequence (5'-3')** |
|---|---|
| Myt1 R1 F | GTGGAAGGTAATGTCAGTGGGGAT |
| Myt1 R1 Comp | ACCTTCCATTACAGTCACCCCTA |
| Myt1 R2 F | GTATGGCTAGTAATTGGGGACT |
| Myt1 R2 Comp | CATACCGATCATTAACCCCTGA |
| Myt1 R10 F | TGCCATTATCTCTCTGTGACTAATAGGCAC |
| Myt1 R10 Comp | CGGTAATAGAGAGACACTGATTATCCGTG |
| Myt1 R11 F | CACCCTTATTATAGACACTAC |
| Myt1 R11 Comp | GTGGGAATAATATCTGTGATG |
| Myt1 R12.1 F | AAGTTCATTATTCAAAAGGGCCTC |
| Myt1 R12.1 Comp | TTCAAGTAATAAGTTTTCCCGGAG |

| | |
|---|---|
| Myt1 R12.2 F | ACATAGGGTAATGTAGAGGACTC |
| Myt1 R12.2 Comp | TGTATCCCATTACATCTCCTGAG |
| Plp1 R1.12 F | TGAGATCCATATAATTACCAACCACAGC |
| Plp1 R1.12 Comp | GCTGTGGTTGGTAATTATATGGATCTCA |
| Plp1 R1.3 F | AACGGCTTCCCTTAATCTCCAAATTCCC |
| Plp1 R1.3 Comp | GGGAATTTGGAGATTAAGGGAAGCCGTT |
| Plp1 R2.1 F | TGACTTCATATTTTAATCATATACAAAG |
| Plp1 R2.1 Comp | CTTTGTATATGATTAAAATATGAAGTCA |
| Plp1 R2.2 F | AGGAGAGAAAATAATAGAACAAACCTCC |
| Plp1 R2.2 Comp | GGAGGTTTGTTCTATTATTTTCTCTCCT |
| Plp1 R2.34 F | ATGTAGTTGTAATAATTATCAACATTTG |
| Plp1 R2.34 Comp | CAAATGTTGATAATTATTACAACTACAT |
| Plp1 R2.56 F | ATTTGGCTCATTATTTCATTAAATCTTG |
| Plp1 R2.56 Comp | CAAGATTTAATGAAATAATGAGCCAAAT |
| Plp1 R2.7 F | AATCTTGTTATTACATTTTTCTGGAGTG |
| Plp1 R2.7 Comp | CACTCCAGAAAAATGTAATAACAAGATT |
| Plp1 R6.1 F | GGAGGGTGTGACATAATCGCCTGGCTGA |
| Plp1 R6.1 Comp | TCAGCCAGGCGATTATGTCACACCCTCC |
| Plp1 R6.2 F | CCTTTCCTAGCCATTAGCAGAAGAGCAT |
| Plp1 R6.2 Comp | ATGCTCTTCTGCTAATGGCTAGGAAAGG |
| Plp1 R8.1 F | GCCAGTTTGTGATAATGTCTTGTCTCAG |
| Plp1 R8.1 Comp | CTGAGACAAGACATTATCACAAACTGGC |

**Table 3.4.** qPCR primers used for gene expression studies

| **Primer name** | **Primer sequence (5' to 3')** |
|---|---|
| Myt1-F | ATACCTCTGTCCAGAAGGCG |
| Myt1-R | TGTCATCATCAGAGCGAACC |
| Plp1-F | GTTCCAGAGGCCAACATCAAGCTC |
| Plp1-R | AGCCATACAACAGTCAGGGCATAG |
| Gapdh-F | CATCACTGCCACCCAGAAGACTG |
| Gapdh-R | ATGCCAGTGAGCTTCCCGTTCAG |
| hDlx2-F | GCACATGGGTTCCTACCAGT |
| hDlx2-R | TCCTTCTCAGGCTCGTTGTT |
| hGad1-F | AGGCAATCCTCCAAGAACC |
| hGad1-R | TGAAAGTCCAGCACCTTGG |
| hGad2-F | CGCATGGTCATCTCAAAC |
| hGad2-R | AGTGGAACAGCTTGGTGAGC |
| hOlig2-F | GCTGCGTCTCAAGATCAACA |
| hOlig2-R | CACCAGTCGCTTCATCTCCT |
| hNkx2.2-F | CGCGTGCTTTCAAAGAAGACA |
| hNkx2.2-R | CACTTGGTCAATTCGTGGCG |
| hMyt1-F | TTCAGACCAGCGAAACCTCACC |

| | |
|---|---|
| hMyt1-R | TGTGGCTTCGTGCTGAGGTTCT |

**Table 3.5.** List of primers used for genotyping of *Dlx1/2* DKO mice

| **Primer name** | **Primer sequence (5' to 3')** |
|---|---|
| Dp4-F | TCCGAATAGTGAACGGGAAGCCAAAG |
| Dp4-R | CAGGGTGCTGCTCGGTGGGTATCTC |
| Neo1 | CAAGATGGATTGCACGCAG |
| Neo4 | CATCCTGATCGACAAGAC |
| Tis1-F | AGGGAGACGGGCAGGAAGCG |
| Tis1-R | AAGGCGGGGCAGCTCTGGAG |

**Table 3.6.** List of primers used for molecular cloning

| **Primer name** | **Primer sequence (5' to 3')** |
|---|---|
| Myt1-R1-KpnI | TTAGGTACCGCACAAGCACATGCACATAGAA |
| Myt1-R1-NheI | TTCGCTAGCCACCGTTCGTAAGGACTTGTCAG |
| Myt1-R2-KpnI | TTAGGTACCTCTGGAACAAGGGATCAAGG |
| Myt1-R2-NheI | TTCGCTAGCCCACCCAGGGTATGAGCAG |
| Myt1-R10-KpnI | TTAGGTACCTGCCTTTGTTTACAGTCCTACC |
| Myt1-R10-NheI | TTCGCTAGCCACCTGGGATCATAGGGTTT |

| | |
|---|---|
| Myt1-R11-KpnI | TTAGGTACCGTCCACTGCTTGCTCGTTT |
| Myt1-R11-NheI | TTCGCTAGCAAGCCCAATCTGGTCACTTC |
| Myt1-R12-KpnI | TTAGGTACCGGCCTGTTGTGTCCAAGTTC |
| Myt1-R12-NheI | TTCGCTAGCTTGAACAGTGAAGGAGGAGATG |
| Plp1-R1-KpnI | TTAGGTACCTACTGAGGGCTGCCTGAGAT |
| Plp1-R1-NheI | TTAGCTAGCCCGAGGGGGAATGTCTATTT |
| Plp1-R2-KpnI | TTAGGTACCCAGGCTAGGTGTACCATTCCA |
| Plp1-R2-NheI | TTAGCTAGCGCTTTGCCCACTCCAGAAA |
| Plp1-R6-KpnI | TTAGGTACCAAGAAGGATGCAGAGGGACTG |
| Plp1-R6-NheI | TTAGCTAGCCCCAGTAAACTCCCAGACACAA |
| Plp1-R8-KpnI | TTAGGTACCAGCTGCTTGCCAGTTTGTGA |
| Plp1-R8-NheI | TTAGCTAGCAGCCAGACGTGCAATGAGAG |

**Table 3.7.** List of antibodies used for IF and ChIP

| **Antibody** | **Source** | **Dilution** | **Use** | **Catalog #** |
|---|---|---|---|---|
| DLX2 | Dr. D. Eisenstat | 1:200 (IF) | Primary antibody and ChIP | N/A |
| Alexa Fluor 488 | Invitrogen | 1:200 | Secondary antibody | A21206, A11055 |
| Alexa Fluor 594 | Invitrogen | 1:200 | Secondary | A11058, A21207 |
| Myt1 | Sigma-Aldrich | 1:50 (IF) | Primary antibody and ChIP | HPA006303 |
| Rabbit IgG | Abcam | N/A | ChIP | ab37415 |
| PLP (Figure 5.7) | Abcam | 1:200 | IF | ab28486 |
| PLP (Figure 5.8) | ThermoFisher | 1:1000 | IF | MA1-80034 |

# Chapter 4: DLX2 regulation of *Myt1:* results

## 4.1 The *Myt1* promoter-proximal region contains multiple candidate homeodomain protein binding sites

DLX2 recognises and binds to candidate homeodomain TAAT/ATTA motifs in target regulatory regions. The 4 kb region upstream of the *Myt1* transcriptional start site was obtained from NCBI GenBank and manually searched for candidate homeodomain binding motifs. The promoter region contains 20 candidate sites. For the purposes of downstream experiments, the upstream region was further subdivided into smaller subregions containing 1-3 binding sites each. Figure 4.1 shows a schematic of the *Myt1* promoter-proximal region and locations of putative binding sites (blue circles). The table below also shows the location of each region relative to the transcriptional start site. Note there is some overlap between regions 12 and 13 for the purposes of primer design. To facilitate interpretation of my ChIP data, I also overlaid the promoter region with a publically available ChIP-seq dataset for several histone posttranslational modifications in E14.5 mouse brain (UCSC Genome Browser) showing locations of H3K27ac, H3K4Me2, and H3K4Me1 (which mark active and transcriptionally primed chromatin regions) and H3K27me3 (a mark of repressive chromatin) enrichment relative to putative DLX2 binding sites. The way this information was used is described in more detail in section 4.2.

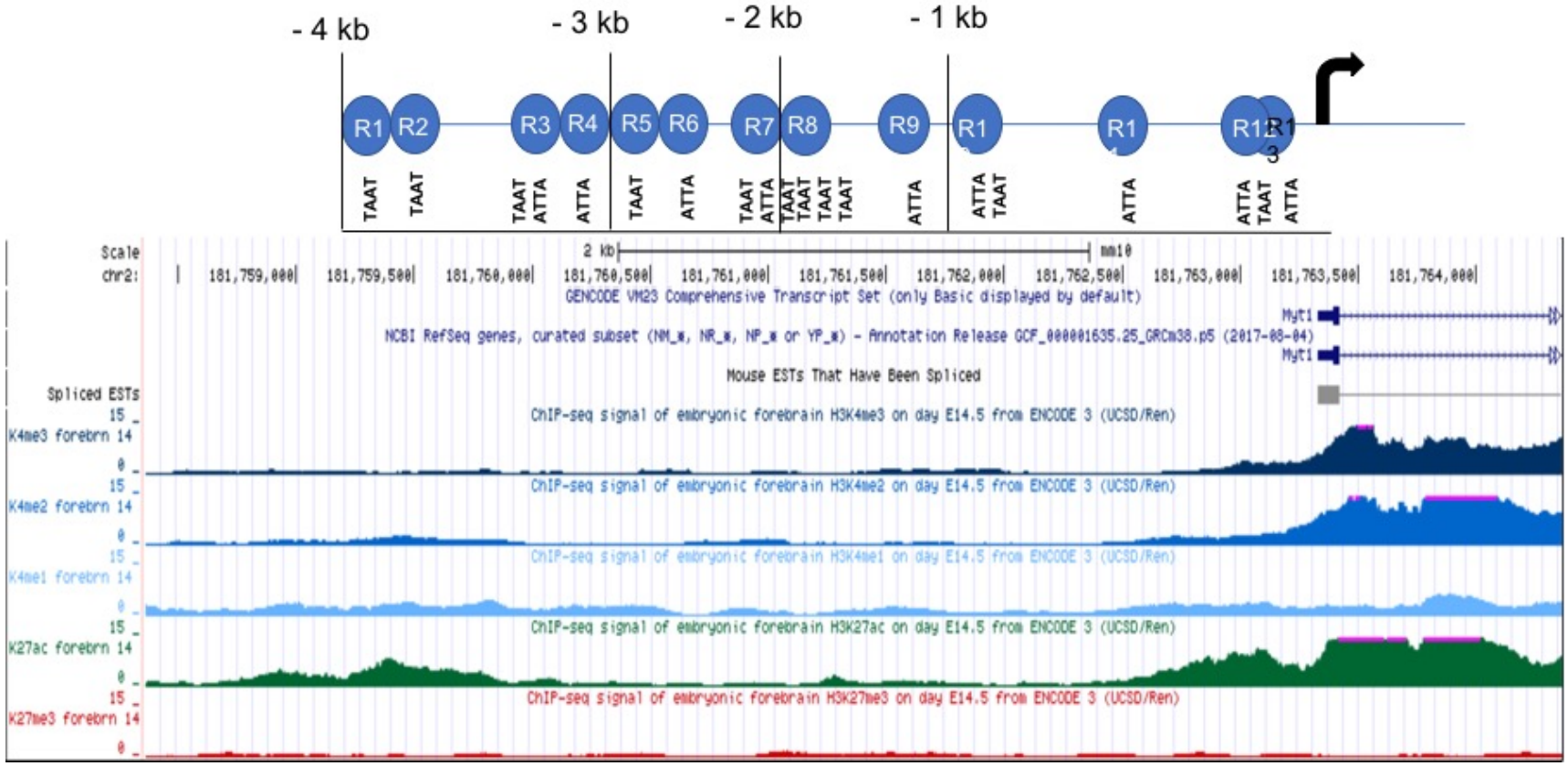
- 4 kb
- 3 kb
- 2 kb
- 1 kb
R1
R2
R3
R4
R5
R6
R7
R8
R9
R1
R1
R12
R13
TAAT
TAAT
TAAT
ATTA
ATTA
TAAT
ATTA
TAAT
ATTA
TAAT
TAAT
TAAT
ATTA
ATTA
TAAT
ATTA
ATTA
TAAT
ATTA
Scale
chr2:
2 kb
mm10
181,759,000
181,759,500
181,760,000
181,760,500
181,761,000
181,761,500
181,762,000
181,762,500
181,763,000
181,763,500
181,764,000
GENCODE VM23 Comprehensive Transcript Set (only Basic displayed by default)
Myt1
NCBI RefSeq genes, curated subset (NM_*, NR_*, NP_* or YP_*) - Annotation Release GCF_000001635.25_GRCm38.p5 (2017-08-04)
Myt1
Mouse ESTs That Have Been Spliced
Spliced ESTs
15
K4me3 forebrn 14
0
ChIP-seq signal of embryonic forebrain H3K4me3 on day E14.5 from ENCODE 3 (UCSD/Ren)
15
K4me2 forebrn 14
0
ChIP-seq signal of embryonic forebrain H3K4me2 on day E14.5 from ENCODE 3 (UCSD/Ren)
15
K4me1 forebrn 14
0
ChIP-seq signal of embryonic forebrain H3K4me1 on day E14.5 from ENCODE 3 (UCSD/Ren)
15
K27ac forebrn 14
0
ChIP-seq signal of embryonic forebrain H3K27ac on day E14.5 from ENCODE 3 (UCSD/Ren)
15
K27me3 forebrn 14
0
ChIP-seq signal of embryonic forebrain H3K27me3 on day E14.5 from ENCODE 3 (UCSD/Ren)

*Figure 4.1 The Myt1 promoter-proximal region contains multiple candidate homeodomain binding sites*

The 4 kb region upstream of the *Myt1* transcriptional start site contains 20 putative homeodomain binding sites (TAAT/ATTA motifs). The figure shows a schematic of the promoter-proximal region, the locations of regions containing putative binding sites (blue circles), and levels of chromatin marks associated with active or primed (H3K4me1, light blue; H3K4me2, dark blue; H3k4me3, indigo; and H3K27ac, green) and repressed (H3k27me3, red) chromatin in E14.5 mouse forebrain.

**Table 4.1** Nucleotide positions of regions containing homeodomain binding sites in the *Myt1* promoter-proximal region.

| **Region** | **Nucleotide position relative to TSS** |
|---|---|
| 1 | -3995 to -3866 |
| 2 | -3607 to -3455 |
| 3 | -3245 to -3136 |
| 4 | -3080 to -2951 |
| 5 | -2818 to -2641 |
| 6 | -2372 to -2201 |
| 7 | -2140 to - 1978 |

| | |
|---|---|
| 8 | -1813 to - 1585 |
| 9 | -1183 to -963 |
| 10 | -920 to -753 |
| 11 | -640 to -471 |
| 12 | -394 to -205 |
| 13 | -249 to -44 |

## 4.2 DLX2 occupies the *Myt1* promoter in E13.5 mouse forebrain *in vivo*

To determine if DLX2 occupied any of these candidate binding regions *in* vivo, chromatin immunoprecipitation (ChIP) was performed with a polyclonal DLX2 antibody on wild-type E13.5 ganglionic eminences. This time point was chosen because it falls in the middle of the peak period of DLX2 expression in forebrain (E12.5-E14.5). As a negative control, chromatin from E13.5 hindbrain was used as this tissue does not express any *Dlx* genes. Protein-DNA interactions were crosslinked with formaldehyde and chromatin was sheared, then immunoprecipitated with a DLX2 antibody. Control samples for each tissue were also prepared without antibody. Following ChIP, PCR was carried out on immunoprecipitated chromatin using primer sets designed to amplify all candidate binding site containing regions in the *Myt1* promoter. Promoter regions 1, 2, 10, 11, and 12 were found to be enriched in E13.5 GE chromatin immunoprecipitated with a DLX2 antibody (Figure 4.2, A-E, red boxed areas). These five regions were chosen to carry forward for further experiments based on this result and the fact that they also fell within regions of open chromatin (having higher levels of H3K27ac and

H3K4 methylation compared to other regions, Figure 4.1) whereas the other regions did not, and had what I considered a negative or ambiguous ChIP result. Although we hypothesize that DLX2 represses *Myt1* and this would be expected to be associated with repressive chromatin marks, I reasoned that first TF binding, except for pioneer TFs, requires accessible chromatin (Slattery, Zhou et al. 2014) and so areas of open chromatin were most likely to contain true sites where DLX2 might bind at this time point to effect transcriptional repression later. The other regions either did not show occupancy or a similar intensity of amplification was also seen in no-antibody and/or hindbrain chromatin samples (see Figure 4.2, F, for representative examples), and were therefore excluded from further experiments because I considered the enrichment in these cases to be nonspecific.

A biologically (i.e. using chromatin prepared from a different litter) and technically separate ChIP experiment was also performed followed by quantitative, rather than endpoint, PCR (DLX2 qCHIP; Figure 4.3). This revealed that several regions of the *Myt1* promoter were markedly enriched in the chromatin immunoprecipitated with DLX2 antibody relative to chromatin immunoprecipitated with a nonspecific, species-matched IgG antibody, particularly regions 7 and 9. This result is preliminary as only one biological replicate was performed; two more replicates are needed for a statistical analysis. However, it does support occupancy of the *Myt1* promoter by DLX2 *in vivo*. The discrepancy between qChIP and qualitative ChIP results regarding which regions seem to be occupied may reflect technical variability between the two experiments in terms of factors such as average chromatin fragment size, since many of the regions are quite close together (see Figure 4.1 and accompanying table). For the end-point PCR ChIP, it could also simply be the case that if more PCR product was loaded on the gel,

enrichment would have been detected also for regions such as region 7 that showed enrichment using qPCR, which is much more sensitive.

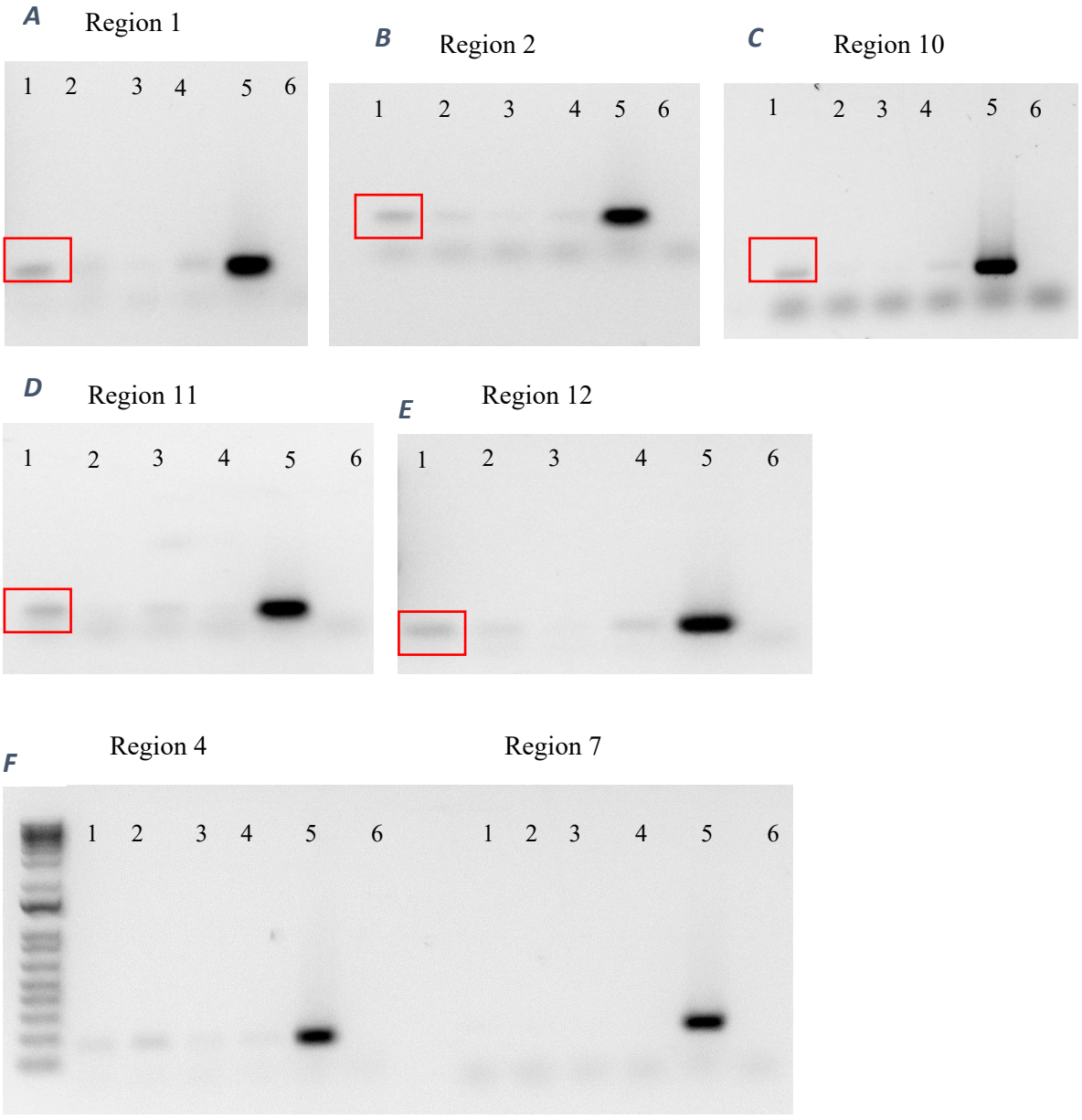

*Figure 4.2 DLX2 occupies the Myt1 promoter in E13.5 forebrain.*

A-E: Regions 1, 2, 10, 11, and 12 show amplification in the GE + DLX2 ab samples that appears specific or more intense than in other lanes, supporting that DLX2 occupies these promoter regions *in vivo.*

F: Two representative examples of ChIP results that were considered negative. For region 4, enrichment appears more intense in the -Ab forebrain chromatin and faint bands can be seen in all lanes, so I assumed it represented non-specific binding. For region 7, no enrichment can be seen.

*Lanes*: 1. E13.5 GE chromatin + DLX2 antibody; 2. E13.5 GE chromatin - antibody; 3. E13.5 hindbrain chromatin + DLX2 antibody; 4. E13.5 hindbrain chromatin - antibody; 5. Genomic DNA; 6. Water

Experiment was performed in one biological and one technical replicate.

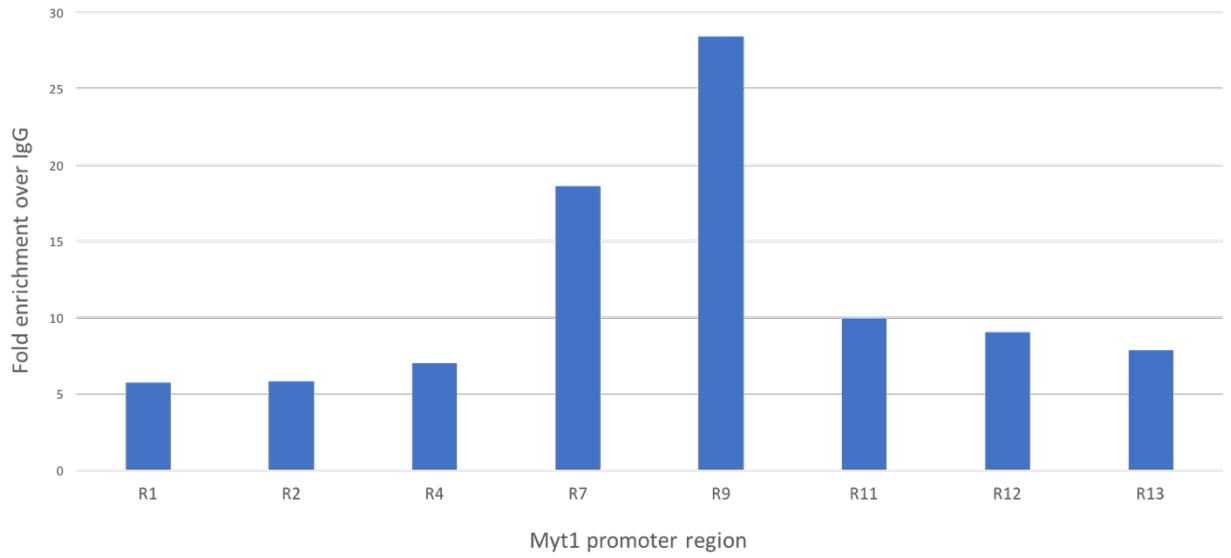


*Figure 4.3 DLX2 qChIP shows that DLX2 occupies Myt1 promoter regions in vivo*

ChIP was performed as described above except hindbrain chromatin was not used as a negative control; a control E13.5 chromatin sample instead received an equivalent amount of rabbit IgG. 15 µg of chromatin was used in the immunoprecipitation. qPCR was performed using primers for all *Myt1* promoter regions and the fold enrichment over the IgG sample of each region in the chromatin immunoprecipitated with DLX2 antibody was calculated. Several regions, such as R7 and R9, show notable enrichment over IgG. This suggests that DLX2 occupies these regions *in vivo.* Note: This graph represents the results of a separate ChIP experiment (using chromatin from a separate litter as well as a technically separate experiment) than what is shown in Figure 4.2. This experiment was performed in one biological replicate and one technical replicate.

## 4.4 DLX2 does not directly bind Myt1 promoter regions *in vitro*

Occupancy detected using ChIP could be direct or indirect (Slattery, Zhou et al. 2014); DLX2 could be bound to the *Myt1* promoter via interaction with another protein. Furthermore, ChIP cannot precisely distinguish exactly which binding sites DLX2 might be occupying, because many of the binding sites are closer together than the chromatin fragment size used in ChIP, so this experiment cannot provide region-level resolution. To address this and determine if DLX2 directly binds any ChIP-positive candidate regulatory regions of the *Myt1* promoter, electrophoretic mobility shift assays were performed using radiolabelled probes corresponding to ChIP-positive regions of the *Myt1* promoter (regions 1, 2, 10, 11, and 12). All regions failed to show binding of DLX2 to any region *in vitro* (Figure 4.4). Two representative examples are shown in Figure 4.4. For R1, the shift appears non-specific as it does not appreciably change in intensity in the presence of excess unlabelled probe (lane 3) or DLX2 antibody (lane 4). For R10, no shifted band is observed.

One possibility I considered for the negative EMSA results shown in Figure 4.4 was that the oligonucleotide probes I used did not contain sufficient sequence surrounding the homeodomain binding motif(s) to allow for binding site recognition by DLX2. Sequence context of TF binding sites, which includes the flanking sequence, is known to be important for TF-binding site recognition (Dror, Rohs et al. 2016, Inukai, Kock et al. 2017, Yella, Bhimsaria et al. 2018). Therefore, I repeated EMSA for promoter regions 1, 2, and 10 using probes that corresponded to the entire promoter region, not just a short portion including the binding site(s) (Figure 4.5). I subcloned each region into pGL3 basic, isolated them by double digestion followed by gel

purification, and radiolabelled them using [γ-32P]-dGTP. Probes for *Myt1* promoter regions prepared in this manner also failed to show direct binding, as shown in Figure 4.5. Note that the marks on the film may represent protein-DNA complexes that are stuck in the wells as they do not appear in the probe-only lanes. It is possible if this experiment was repeated with a titration of protein or probe amounts to address this issue, a mobility shift would be observed. In addition, regions 11 and 12 still need to be tested for direct binding using this approach.

| | | | | | | | | | | | | | | |
|---|---|---|---|---|---|---|---|---|---|---|---|---|---|---|
| rDLX2 | + | + | | + | - | | | + | + | | + | - | | |
| Labelled probe | + | + | | + | + | | | + | + | | + | + | | |
| Unlabelled probe | - | - | | + | - | | | - | - | | + | - | | |
| DLX2 antibody | - | - | | - | + | | | - | - | | - | + | | |

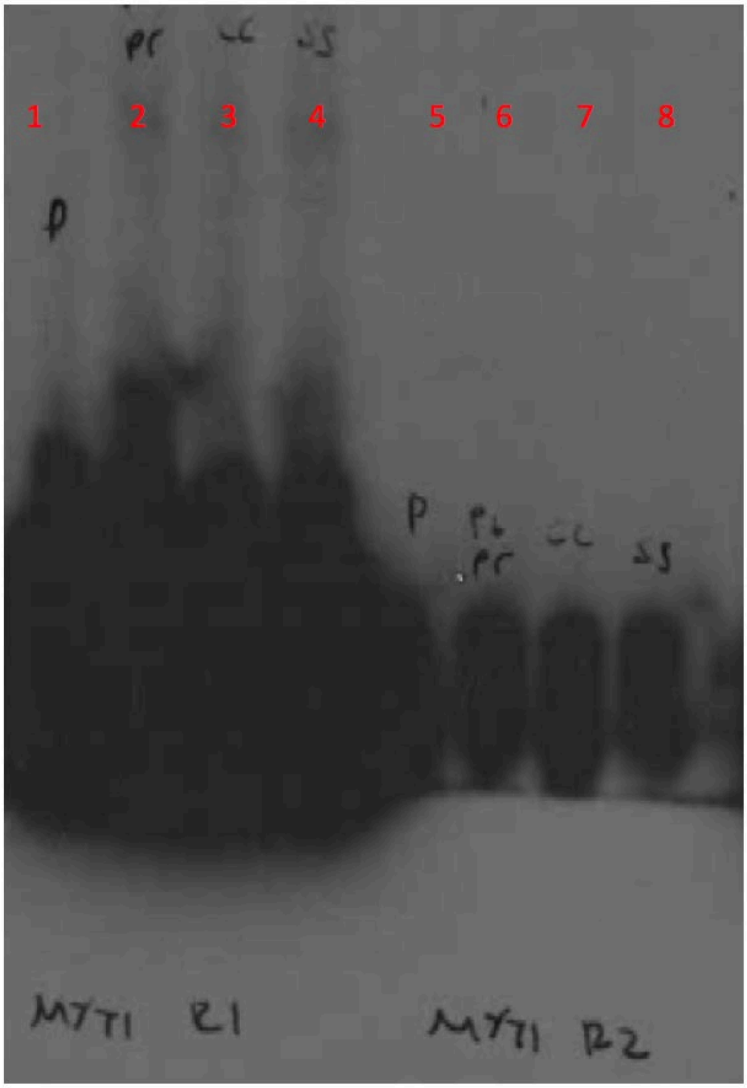

*Figure 4.4 EMSA with short oligonucleotide probes shows that DLX2 does not directly bind Myt1 promoter regions in vitro*

Short (20-30 bp) oligonucleotides containing the TAAT/ATTA motif and a small amount of the flanking sequence of each region were ordered and 5' labelled with [γ-32P]-dATP. EMSA was carried out as described in Chapter 3. Two representative examples of the results are shown. No mobility shift was observed when probes were incubated with recombinant DLX2 (lanes 2, 6) nor was there a supershift when probes were incubated with recombinant DLX2 and DLX2 antibody (lanes 4,8) suggesting DLX2 does not directly bind *Myt1* promoter regions.

Lanes: 1, 5: Free probe; 2, 6: rDLX2; 3, 7: Cold competition; 4, 8: Supershift.

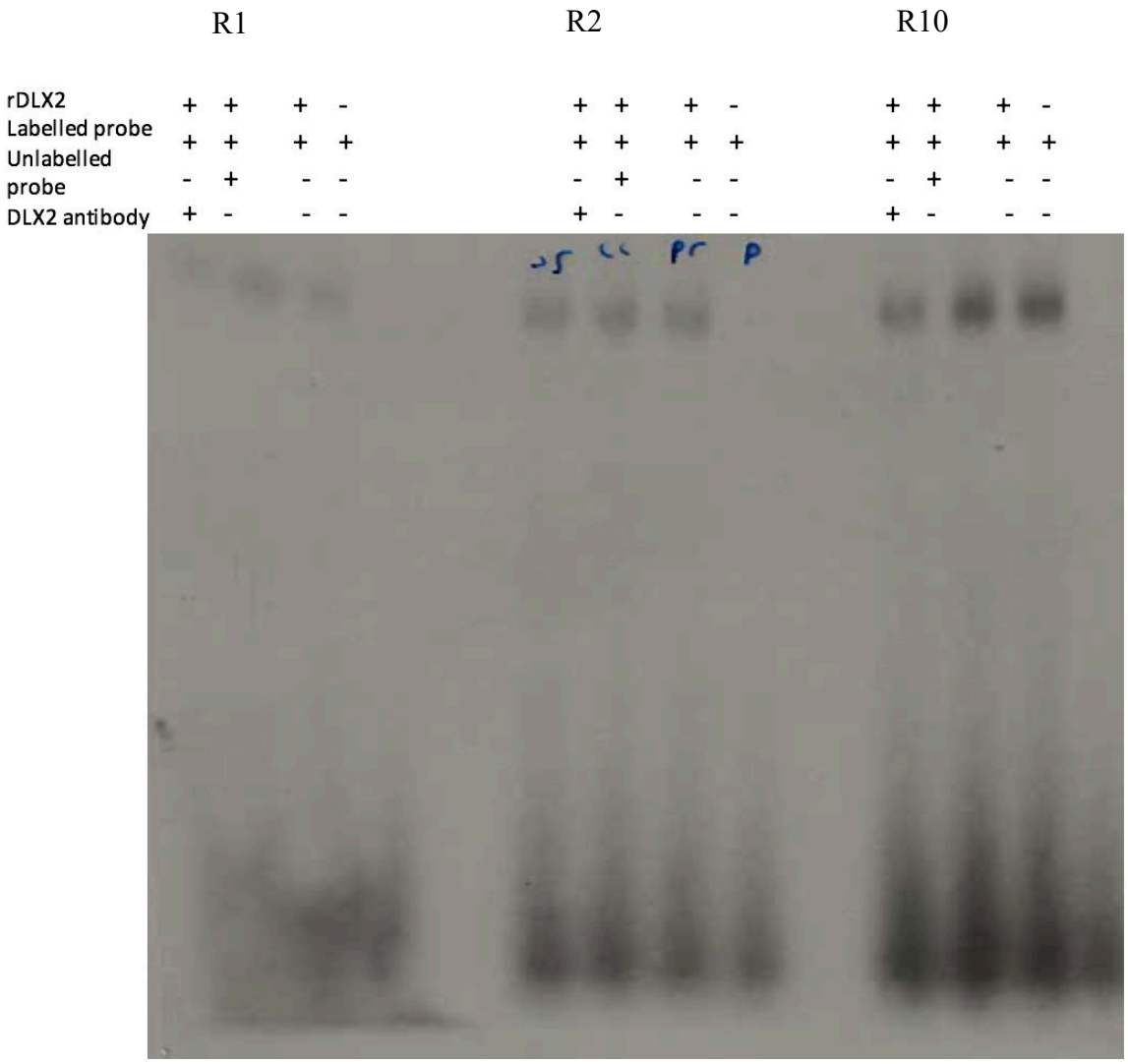


*Figure 4.5 EMSA with whole promoter regions shows that DLX2 does not directly bind Myt1 promoter regions 1, 2, or 10 in vitro*

Following the negative EMSA results shown in Figure 4.4, I prepared longer probes containing more of the flanking region around the DLX2 binding motifs for regions 1 (left), 2 (middle), and 10 (right), as described in section 4.3. These longer regions also failed to show direct binding by recombinant DLX2 as indicated by the lack of mobility shift of probes incubated with recombinant DLX2 compared to free probe.

## 4.6 *Myt1* transcripts are not significantly upregulated in the *Dlx1/2* DKO forebrain *in vivo*

To determine if *Myt1* expression is upregulated in the forebrain in the absence of *Dlx1/Dlx2* gene function, qRT-PCR was performed on RNA harvested from E13.5 *Dlx1/2* DKO and WT GE. This revealed that *Myt1* transcript levels are not significantly upregulated in the DKO forebrain at E13.5 (P=0.052, N=3 biological replicates). However, a strong trend towards upregulation was observed, and given the borderline P-value that was calculated, it is possible that if we acquired additional biological replicates, we would obtain a statistically significant result. This result may also reflect spatial factors in that *Myt1* is broadly expressed in the CNS germinal zones but DLX2 would only be participating in its regulation in a small proportion of forebrain cells.

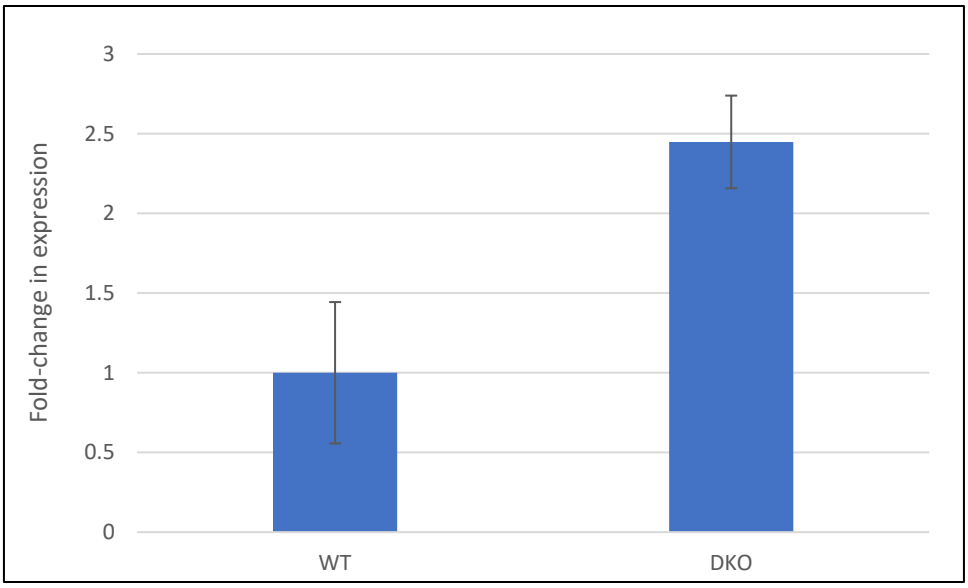


*Figure 4.6. Myt1 expression is not significantly upregulated in the Dlx1/2 DKO forebrain at E13.5*

To determine if *Myt1* expression is upregulated in the forebrain in the absence of *Dlx1/Dlx2* gene function, qRT-PCR was performed on RNA harvested from E13.5 *Dlx1/2* DKO and WT GE. Although *Myt1* transcripts were not significantly upregulated in the DKO forebrain at E13.5 (P=0.052; N=3 biological replicates (litters)), additional experiments are planned. Error bars represent the standard error of the mean normalized change in expression (ddCT). All gene signals were normalised to *Gadph* expression levels. Fold-change was calculated relative to WT expression levels. Experiments were performed in 3 biological replicates and 3 technical replicates. Statistical significance was calculated using Student's unpaired t-test.

# Chapter 5: DLX2 regulation of *Plp1:* results

## 5.1 The *Plp1* promoter-proximal region contains multiple candidate homeodomain protein binding sites

Similar to other homeodomain proteins, DLX2 recognises and binds to TAAT/ATTA motifs in its target regulatory regions. The 4kb region upstream of the *Plp1* transcriptional start site was obtained from NCBI GenBank and manually searched for candidate homeodomain binding motifs. The promoter-proximal region was found to contain 22 candidate binding sites (Figure 5.1). For the purposes of downstream experiments, the upstream region was further subdivided into smaller subregions each containing 1-3 binding sites each. Figure 5.1 shows a schematic diagram of the *Plp1* promoter region and locations of putative binding sites. The promoter region was also overlaid with publically available ChIP-seq data showing the locations of enrichment of histone modifications associated with active (H3K4Me1, H3K27ac) and repressed (H3K27me3) chromatin in E14.5 mouse brain. This information was included primarily to facilitate the interpretation of ambiguous ChIP results later (see section 5.2). We reasoned that binding sites falling within regions of active chromatin would be more likely to represent true binding sites.

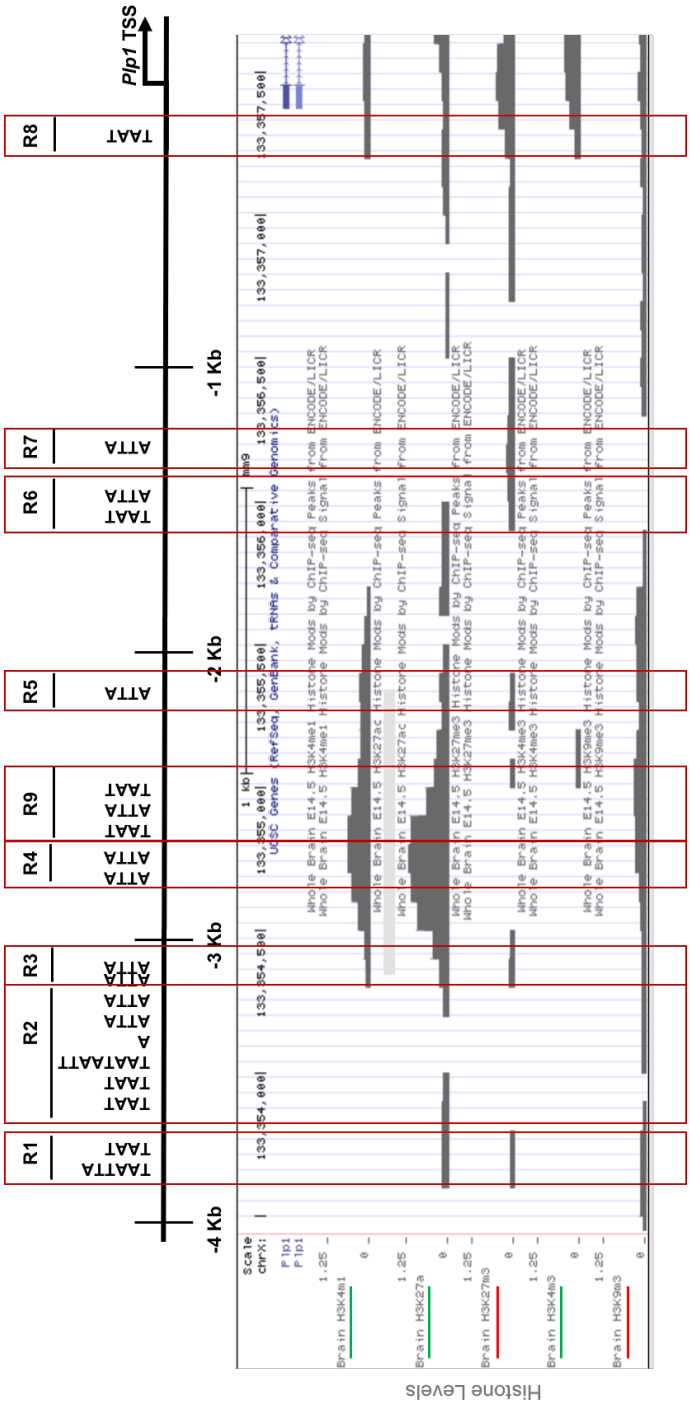
Plp1 TSS
-4 Kb
-3 Kb
-2 Kb
-1 Kb
R1
TAATTA
TAAT
R2
TAAT
TAAT
TAATAATT
A
ATTA
ATTA
R3
ATTA
ATTA
R4
ATTA
ATTA
R9
TAAT
ATTA
TAAT
R5
ATTA
R6
TAAT
ATTA
R7
ATTA
R8
TAAT
Histone Levels

*Figure 5.1. The Plp1 promoter-proximal region contains multiple candidate homeodomain protein binding sites.* The 4 kb region upstream of the *Plp1* transcriptional start site was obtained from NCBI GenBank and manually searched for candidate homeodomain binding motifs (TAAT/ATTA sites). The promoter region was found to contain 22 candidate sites. For the purposes of downstream experiments, the upstream region was further subdivided into smaller subregions containing 1-3 putative binding sites each (red boxed areas). The promoter region is also overlaid with a publically available ChIP-seq dataset for several histone posttranslational modifications in E14.5 mouse brain (UCSC Genome Browser) showing locations of H3K27ac and H3K4me1 (which mark open/active chromatin regions) and H3K27me3 (a mark of repressive chromatin) enrichment relative to putative DLX2 binding sites.
R9 is not in numerical order relative to the rest of the regions because it was identified later.
Figure: courtesy of Janine Gallego.

## 5.2 DLX2 occupies the *Plp1* promoter *in vivo* in E13.5 mouse forebrain

To determine if DLX2 occupied any of the candidate *Plp1* regulatory regions *in* vivo, chromatin immunoprecipitation (ChIP) was performed with a DLX2 antibody on wild-type E13.5 ganglionic eminences. This time point was chosen because it falls in the middle of the peak period of DLX2 expression in forebrain (E12.5-E14.5). As a negative control, chromatin from E13.5 hindbrain was used as this tissue does not express any *Dlx* genes. Interactions between proteins and DNA were crosslinked with formaldehyde and chromatin was sheared, then immunoprecipitated with a DLX2 antibody. Control samples for each tissue were also prepared without the addition of antibody. Following ChIP, PCR was carried out on immunoprecipitated chromatin using primer sets designed to amplify all candidate binding site containing regions in

the *Plp1* promoter. Promoter regions 1, 2, 3, 6, and 8 were found to be enriched in E13.5 GE chromatin immunoprecipitated with a DLX2 antibody (Figure 5.2, red boxed areas). These regions were chosen to carry forward for further experiments based on this result. The other regions failed to show occupancy (Figure 5.2, region 4) or had a result that seemed nonspecific (Figure 5.2, region 7) and were therefore excluded from downstream experiments.

Region 1

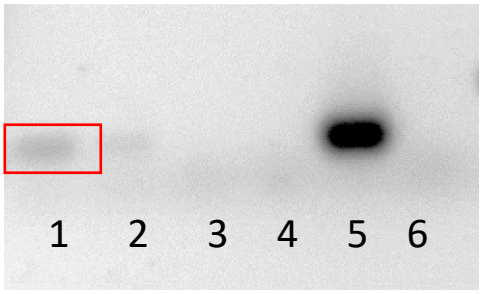


Region 2

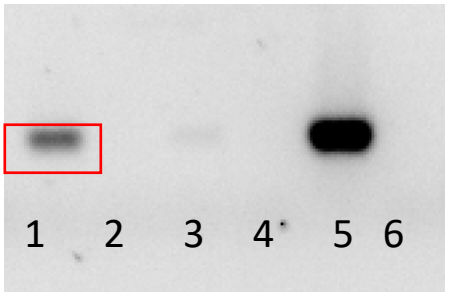


Region 3

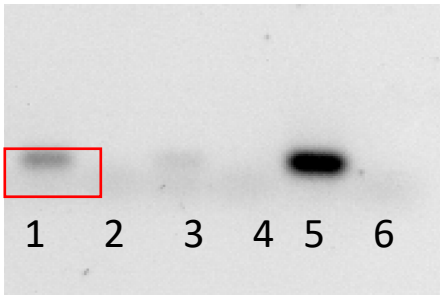


Region 6

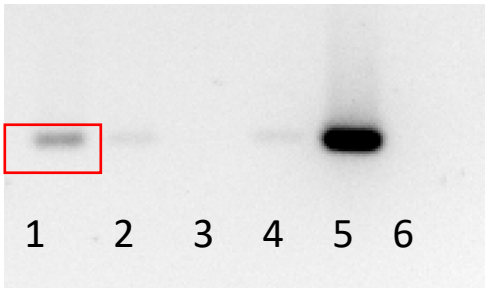


Region 8

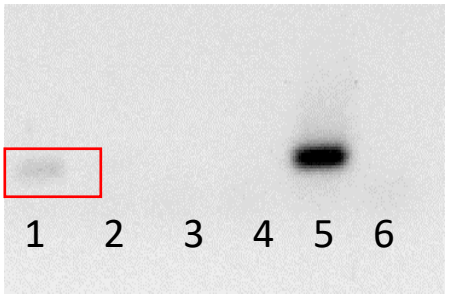


Region 4

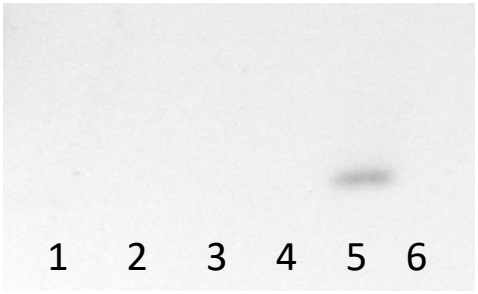


Region 7

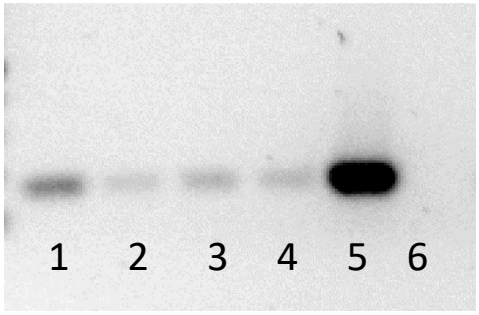

*Figure 5.2 DLX2 occupies Plp1 regulatory elements in E13.5 forebrain in vivo*

**Lanes**: 1. E13.5 GE chromatin + DLX2 antibody; 2 E13.5 GE chromatin - antibody; 3. E13.5 hindbrain chromatin + DLX2 antibody; 4. E13.5 hindbrain chromatin - antibody; 5. Genomic DNA; 6. Water.

**Top**: Regions 1, 2, 3, 6, and 8 show amplification in the GE + DLX2 ab samples that appears specific or more intense than in other lanes, supporting that DLX2 occupies these promoter regions *in vivo.*

**Bottom**: Regions 4 and 7 are included as representative examples of negative results. Region 4 is not enriched in the GE + Ab sample. Region 7 was considered negative (or non-specific) because it appeared enriched in all IP samples (including no-antibody samples).

Experiments were performed in one biological and one technical replicate.

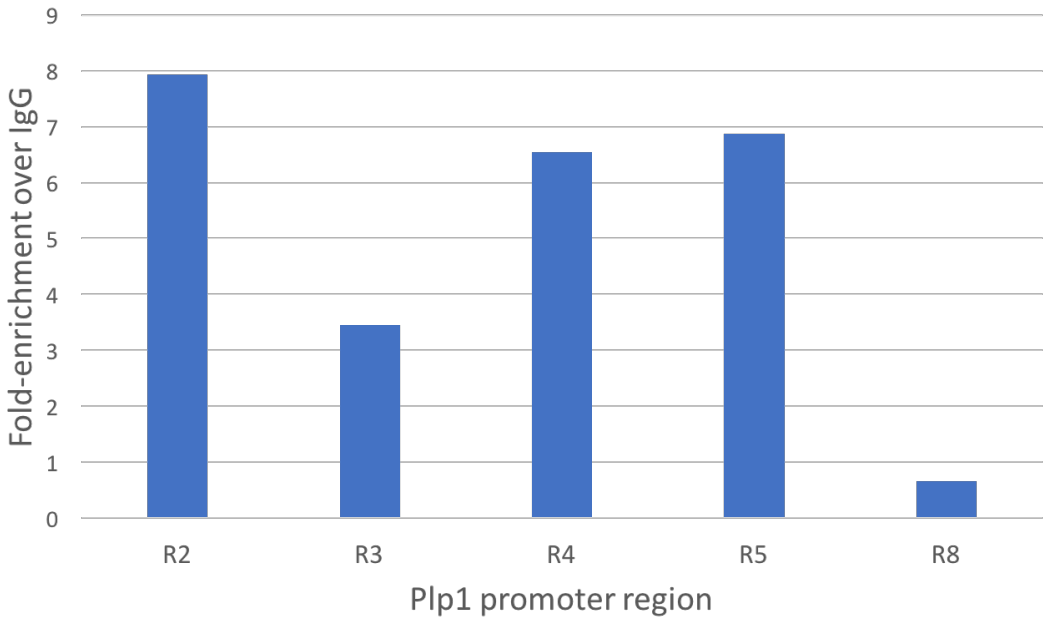


*Figure 5.3 DLX2 qChIP shows that DLX2 occupies Plp1 promoter regions in vivo*

ChIP was performed as described above except hindbrain chromatin was not used; a control E13.5 chromatin sample instead received an equivalent amount of rabbit IgG. 15 µg of chromatin was used in the immunoprecipitation. qPCR was then performed using primers for all *Plp1* promoter regions and the fold enrichment over the IgG sample of each region in the chromatin immunoprecipitated with DLX2 antibody was calculated. Several regions, such as R2, R4, and R5, show notable fold-enrichment over IgG controls. This suggests that DLX2 occupies these regions *in vivo.* Note: This graph represents the results of a separate ChIP experiment (using chromatin from a separate litter as well as a technically separate experiment) than what is shown in Figure 4.2. This experiment was performed in one biological replicate and one technical replicate. Primers for R1, R6, R7, and R9 were not included due to lack of template.

## 5.3 DLX2 directly binds *Plp1* regulatory regions *in vitro*

Occupancy detected using ChIP could be direct or indirect (Slattery, Zhou et al. 2014); DLX2 could be bound to the *Plp1* promoter via interaction with another protein. Furthermore, ChIP cannot precisely distinguish which specific binding sites DLX2 might be occupying, because many of the binding sites are much closer together than the 500 bp chromatin fragment size used in ChIP. To determine if DLX2 directly binds any ChIP-positive candidate regulatory regions of the *Plp1* promoter and narrow down specific regions of binding, electrophoretic mobility shift assays were performed using radiolabelled probes corresponding to ChIP-positive regions of the promoter. Regions were also further subdivided for better binding site resolution. For example, R1.12 contains the first and second homeodomain binding motifs within region 1, and R1.3 contains the third motif. Short (20-30 bp) oligonucleotides containing the TAAT/ATTA motifs and a small amount of the flanking sequence of each subregion were ordered and 5' labelled with [γ-32P]-dATP, incubated with recombinant DLX2, and separated by native polyacrylamide gel electrophoresis on a 4% acrylamide gel. Direct binding of DLX2 to the probe is indicated by the detection of an upwards mobility shift on the gel when probes are incubated with recombinant DLX2 compared to free probe. Controls for this experiment were: labelled probe alone where no rDLX2 was added, supershift control where a specific DLX2 antibody was added to the binding reaction, and cold competition control where an excess of unlabelled probe was added to the binding reaction. In the presence of the DLX2 antibody, there is a greater upward mobility shift (supershift) reflecting the formation of higher molecular weight DNA-protein-antibody complexes, and further demonstrating direct binding of DLX2 to these regions. In the cold competition lanes, the shifted band disappears or is reduced in intensity due to unlabelled probe outcompeting the labelled probe for binding to DLX2; this also shows specificity of binding. In a

few cases, no supershift was observed, but the shifted band disappeared or diminished in intensity instead (Figure 5.3.1 R1.3; Figure 5.3.2 R2.34; Figure 5.3.3 R6.1). This can occur when the antibody competes with the protein for direct binding to the probe, so the lack of a clear supershift does not necessarily mean the protein does not directly bind the probe. This is particularly the case here as recombinant DLX2 was used, so the binding reaction should not contain any other proteins that could bind to the probe and produce a shift. These results indicate that DLX2 directly binds regions 1 (Figure 5.3.1), 2 (Figure 5.3.2), and 6 (Figure 5.3.3) of the *Plp1* promoter *in vitro*.

R3 failed to directly bind DLX2 in EMSA (data not shown) and was not carried forward for further experiments. R8.1 showed a result that was difficult to clearly interpret (Figure 5.3.4) that could not be repeated, but it was carried forward for luciferase assays based on the positive ChIP result and the fact that it fell within a region of open chromatin (Figure 5.1).

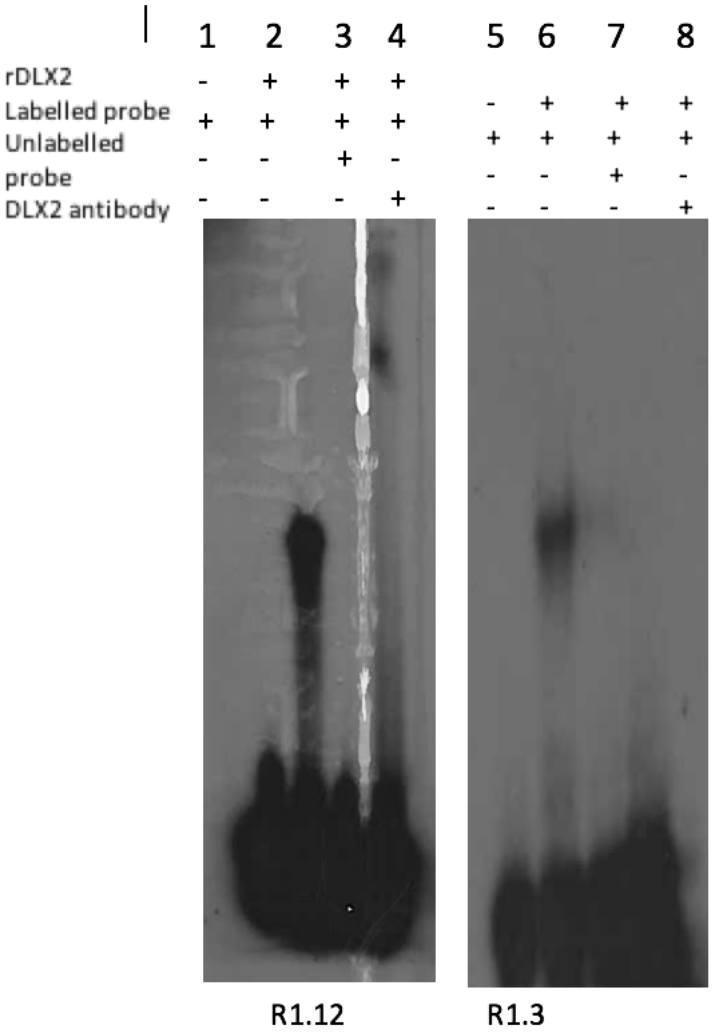


*Figure 5.4.1 DLX2 directly binds Plp1 promoter region 1 in vitro*

Direct binding of DLX2 to regions 1.12 and 1.3 is demonstrated by the presence of a mobility shift on the gel when these probes were incubated with rDLX2 (lanes 1 and 5). Addition of a specific DLX2 antibody to the binding reaction resulted in the appearance of a supershifted band for R1.12 (lane 4) although not R.13 (lane 8). Addition of an excess of unlabelled probe resulted in the disappearance of the mobility shift for both regions (lanes 3 and 7). This result indicates that DLX2 can directly bind *Plp1* promoter regions 1.12 and 1.13 *in vitro*.

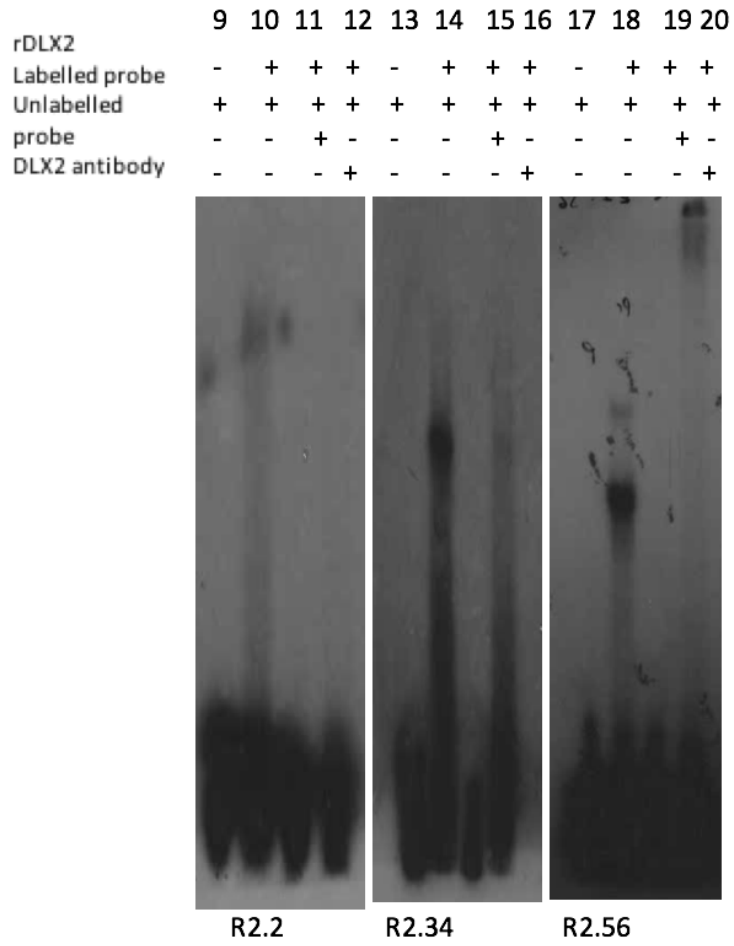


*Figure 5.4.2 DLX2 directly binds Plp1 promoter region 2 in vitro*

Direct binding of DLX2 to regions 2.2, 2.34, and 2.56 is demonstrated by the presence of a mobility shift on the gel when these probes were incubated with rDLX2 (lanes 10, 14, and 18). Addition of a specific DLX2 antibody to the binding reaction resulted in the appearance of a supershifted band for R2.56 (lane 20) although not for R2.2 (lane 12) or R2.34 (lane 16).

Addition of an excess of unlabelled probe resulted in the disappearance of the mobility shift for all regions (lanes 11, 15, and 19). This result indicates that DLX2 can directly bind *Plp1* promoter regions 2.2 2.34, and 2.56 *in vitro.*

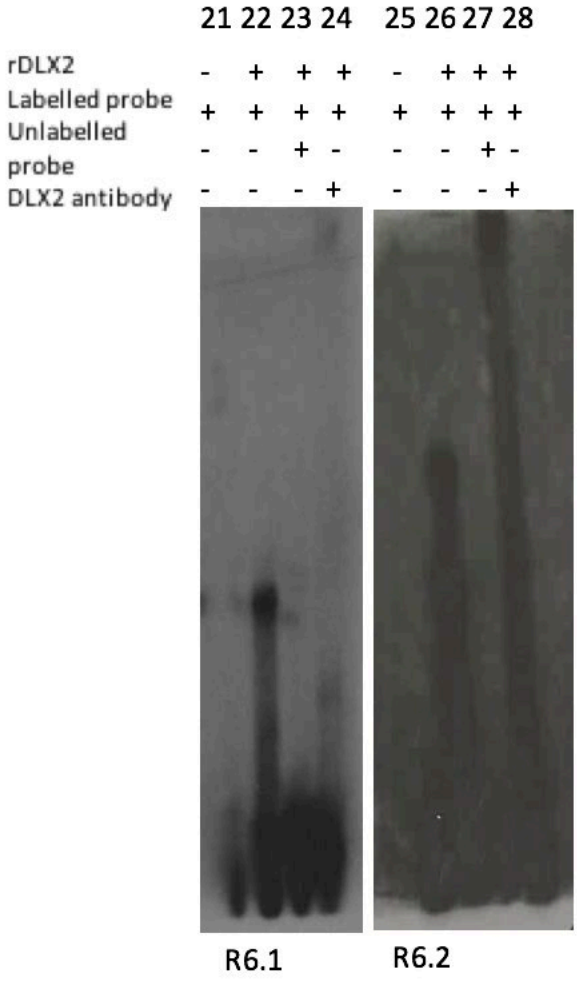


*Figure 5.4.3. DLX2 directly binds Plp1 promoter region 6 in vitro*

Direct binding of DLX2 to regions 6.1 and 6.2 is demonstrated by the presence of a mobility shift on the gel when these probes were incubated with rDLX2 (lanes 22 and 26). Addition of a specific DLX2 antibody to the binding reaction resulted in the appearance of a supershifted band for both regions (lanes 24 and 28). Addition of an excess of unlabelled probe resulted in the

disappearance of the mobility shift for all regions (lanes 23 and 27). This result indicates that DLX2 can directly bind *Plp1* promoter regions 6.1 and 6.2 *in vitro*.


*Figure 5.4.4. DLX2 directly binds Plp1 promoter region 8 in vitro*

Direct binding of DLX2 to region 8.1 is demonstrated by the presence of a mobility shift on the gel when these probes were incubated with rDLX2 (lane 30). Addition of a specific DLX2 antibody to the binding reaction resulted in the appearance of a supershifted band for both regions (lane 32). Addition of an excess of unlabelled probe resulted in the disappearance of the mobility shift for all regions (lane 31). This result indicates that DLX2 can directly bind *Plp1* promoter region 8.1 *in vitro*.

## 5.4 DLX2 binding to *Plp1* regulatory regions may affect reporter gene transcription *in vitro*

Although DLX2 binds PLP promoter regions *in vivo* and *in vitro* (Figures 5.2, 5.3, and 5.4), binding does not necessarily have functional consequences on *Plp1* gene transcription. Luciferase reporter assays were performed to determine if there was a functional effect of DLX2 binding to ChIP identified and EMSA-validated regions. The ChIP- and EMSA-positive *Plp1* regulatory regions (regions 1, 2, 6, and 8) were each subcloned into the pGL3 Basic Firefly luciferase reporter vector, directly upstream of the luciferase gene. pGL3-Plp1 promoter region plasmids and a DLX2 expression vector (pcDNA3-DLX2) were co-transfected into HEK293 cells. As a control for transfection efficiency, cells were also transfected with a vector providing high-level constitutive expression of Renilla luciferase (pRL-SV40). Firefly luciferase results for each well were normalised to Renilla activity. For R1, R2, and R6 there was a slight decrease in reporter expression with DLX2 co-expression (Figure 5.4). This was not significant for R2 (P=0.39, figure 5.4). R8 showed a non-statistically significant upregulation of reporter expression with DLX2 co-expression (P=0.22, Figure 5.4). For R1 and R6 no statistical analysis was performed because one more biological replicate is needed to reach N=3. For R6, one of the original three replicates was excluded because the relative fold-change varied greatly from the other two replicates (32.7 vs 0.54 and 0.99) and I considered this result to be an outlier.

A lack of significant decrease of reporter expression with DLX2 co-transfection is not consistent with the hypothesis that DLX2 represses the *Plp1* promoter. However, a major limitation of this experiment is the use of a vector (pGL3) that does not contain a minimal promoter. Without a baseline level of reporter expression driven by a minimal promoter, it may be difficult to

ascertain whether transcriptional repression is occurring. It is also possible that the full 4 kb promoter-proximal region is needed to see an effect on transcription.

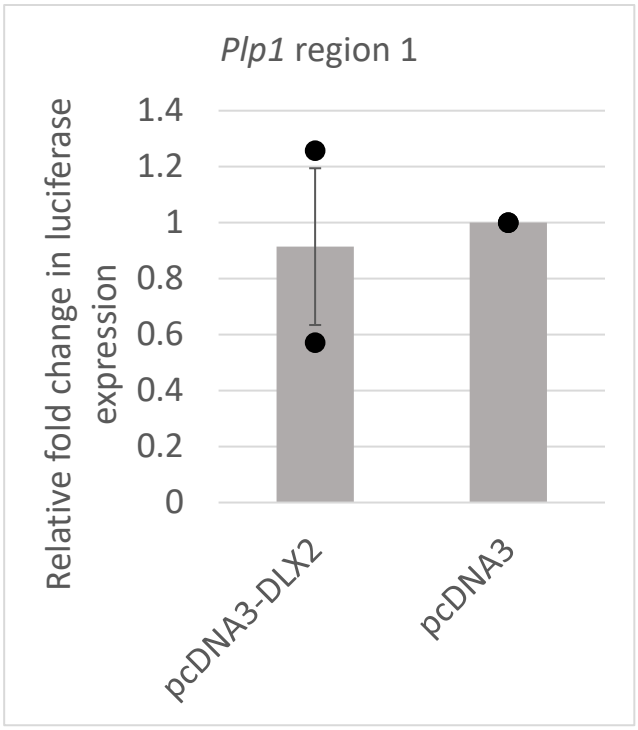
*Plp1* region 1
Relative fold change in luciferase expression
1.4
1.2
1
0.8
0.6
0.4
0.2
0
pcDNA3-DLX2
pcDNA3

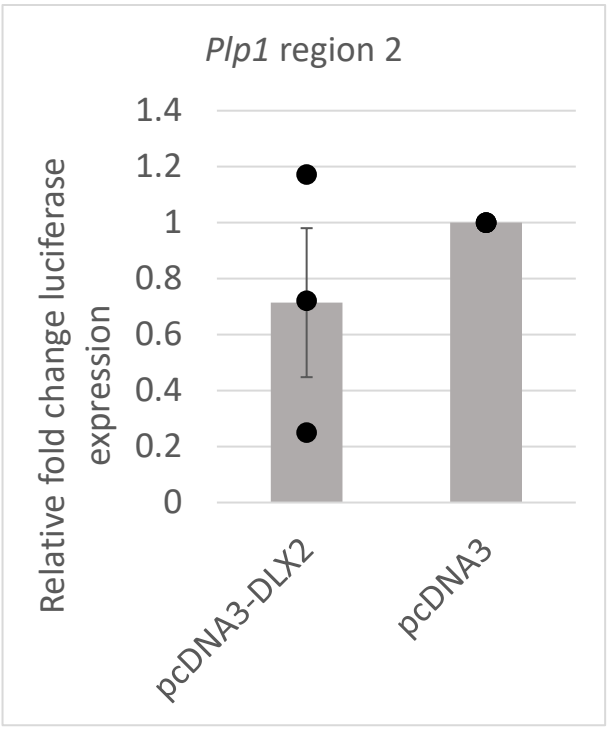
*Plp1* region 2
Relative fold change luciferase expression
1.4
1.2
1
0.8
0.6
0.4
0.2
0
pcDNA3-DLX2
pcDNA3

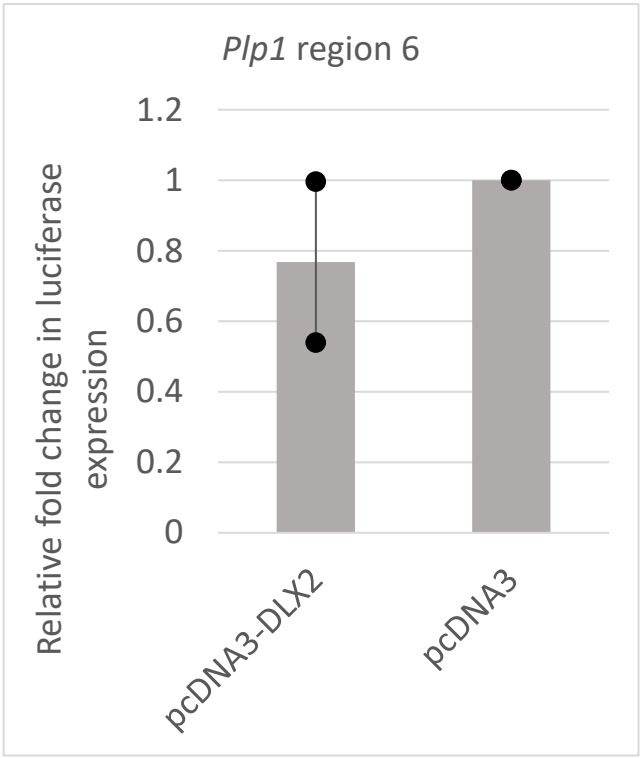
*Plp1* region 6
Relative fold change in luciferase expression
1.2
1
0.8
0.6
0.4
0.2
0
pcDNA3-DLX2
pcDNA3

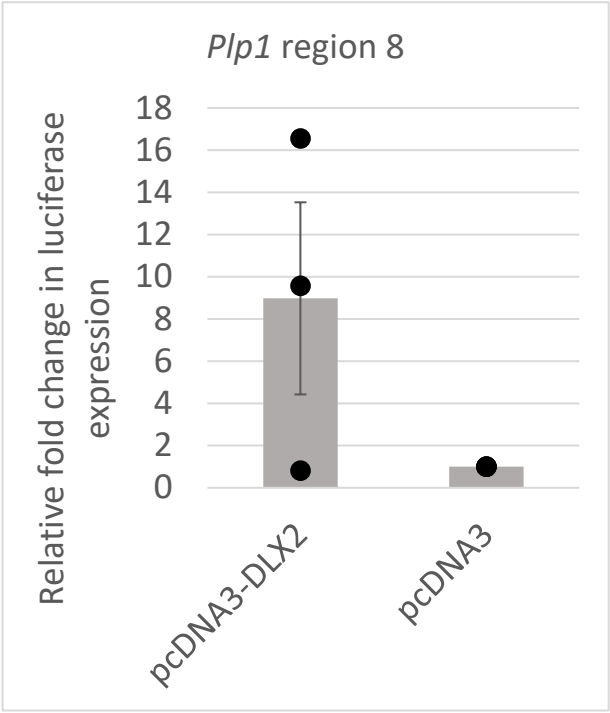
*Plp1* region 8
Relative fold change in luciferase expression
18
16
14
12
10
8
6
4
2
0
pcDNA3-DLX2
pcDNA3

*Figure 5.5: DLX2 binding to Plp1 regulatory regions does not significantly affect reporter gene expression in vitro*

*Plp1* regulatory regions. ChIP- and EMSA-positive *Plp1* regulatory regions were subcloned into the pGL3 Basic Firefly luciferase reporter vector, upstream of the luciferase gene, and co-transfected into HEK293 cells along with a DLX2 expression plasmid (pcDNA3-DLX2). As a control for transfection efficiency, cells were also transfected with a vector providing high-level constitutive expression of Renilla luciferase (pRL-SV40; Promega). Firefly luciferase results for each well were normalised to Renilla activity. Error bars represent the standard error of the mean fold-change in expression. Dots represent individual data points from each biological replicate; bars represent mean fold-change. Fold-change was calculated relative to firefly/renilla ratio in control cells receiving empty pcDNA3. N=2 for R1 and R6, N=3 for R2 and R8. Co-transfection with R2 decreased reporter expression, but this result was not significant (P=0.39, N=3). Co-transfection with R8 increased reporter expression, but this was not significant (P=0.22, N=3). For R1 and R6 no statistical analysis was performed, since one more biological replicate is needed. Experiments were performed in three technical replicates for each plate (i.e. three wells transfected for each condition per plate). Experiments were performed in two biological replicates for R1 and R6, and three biological replicates for R2 and R8. One plate of cells was considered a biological replicate. Statistical significance was calculated using Student's unpaired t-test.

## 5.5 *Plp1* transcripts are not significantly upregulated in the *Dlx1/2* double knockout forebrain *in vivo*

To determine if *Plp1* expression is upregulated in the forebrain in the absence of *Dlx1/Dlx2* gene function, qRT-PCR was performed on RNA harvested from E13.5 *Dlx1/2* DKO and WT GE (Figure 5.5). *Plp1* transcripts were upregulated in the DKO forebrain at E13.5 compared to WT, but this was not significant (P=0.20, N=4). However, the WT data is quite variable with wide errors bars and this would affect the calculation of statistical significance. More litters should be examined to improve variability and address this issue.

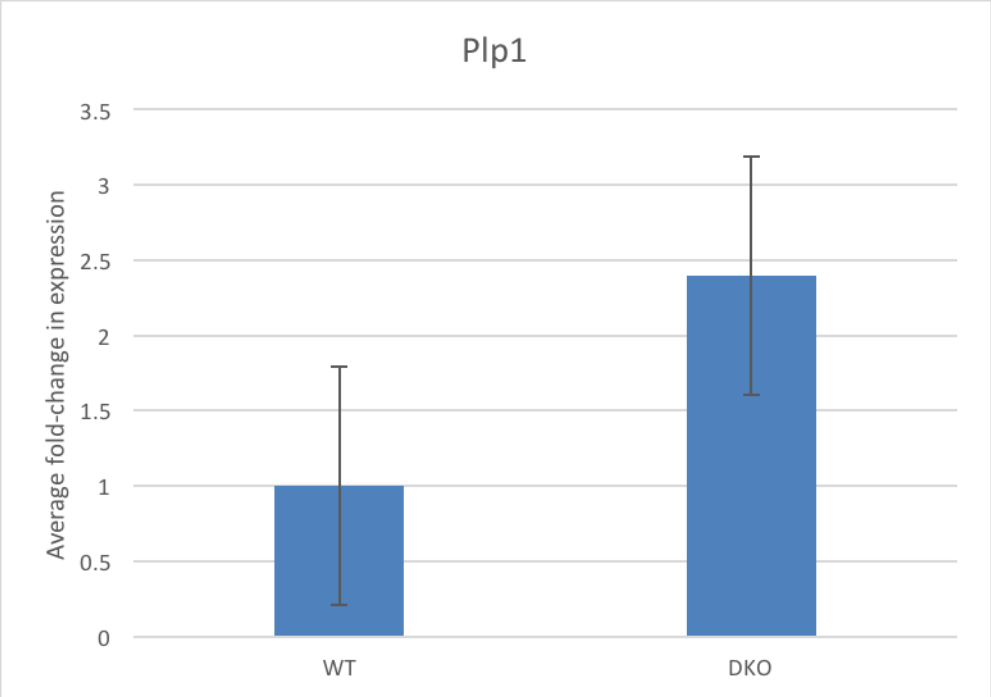

*Figure 5.6 Plp1 transcripts are not significantly increased in the Dlx1/2 double knockout forebrain at E13.5*

To determine if *Plp1* expression is upregulated in the forebrain in the absence of *Dlx1/Dlx2* gene function, qRT-PCR was performed on RNA harvested from E13.5 *Dlx1/2* DKO and WT GE. All gene signals were normalised to *Gapdh* expression levels. Fold-change was calculated relative to expression levels in WT littermates. Error bars represent the standard error of the mean normalised change in expression (ddCT). *Plp1* transcripts were not significantly increased in the DKO forebrain at E13.5 (P=0.20, N=4). Experiments were performed in 4 biological replicates and 3 technical replicates. Statistical significance was calculated using Student's unpaired t-test.

## 5.6 PLP1 expression is increased at E13.5 in the *Dlx1/2* double knockout forebrain

Although not statistically significant, *Plp1* expression was upregulated in the DKO forebrain at E13.5 compared to WT. A redistribution or change in *Plp1*'s expression domain without change in overall levels in the DKO GE could account for the finding of no significant change in transcript levels in the DKO, even if *Dlx1/2* are regulating *Plp* expression. In addition, premature expression of *Plp1* has been reported in the DKO forebrain at E15.5 (Petryniak, Potter et al. 2007). Therefore we decided to examine PLP protein expression in the DKO forebrain. Single immunofluorescence using a PLP antibody was performed on E13.5 WT and DKO and E18.5 WT forebrain sections. At E13.5 PLP was detectable only at a low level in the WT forebrain (Figure 5.7 and Figure 5.8) with levels increasing by E18.5 (Figure 5.7). In contrast, intense staining was observed in the DKO forebrain at E13.5, and the expression domain appeared expanded throughout the DKO GE compared to the WT. E18.5 DKO should be examined to see if the increase in expression persists, and this experiment is planned. To further examine co-

expression of DLX2 and PLP in the WT, double immunofluorescence using DLX2 and PLP antibodies was performed on E13.5 WT forebrain sections (Figure 5.8). Little PLP expression was detected at this time point, and PLP expression was seen only in a few cells that did not appear to co-express DLX2. This result is also consistent with the hypothesis that DLX2 represses PLP during forebrain development. However, to more definitively determine if PLP and DLX2 do not co-localise to the same cells it would also be informative to examine some later time points, such as E15.5, where PLP expression may be more pronounced in the WT.

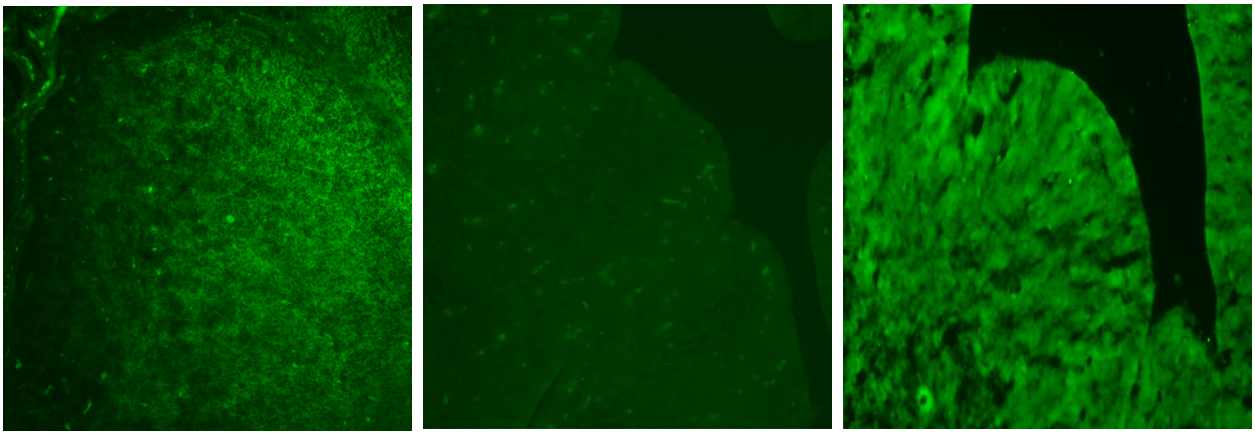

E18.5 WT E13.5 WT E13.5 DKO

*Figure 5.7 PLP expression is increased and expanded in the Dlx1/2 DKO forebrain*

Single immunofluorescence was performed with a PLP1 antibody on forebrain sections obtained from E13.5 DKO, E13.5 WT, and E18.5 WT mice. At E13.5, PLP1 expression is detectable only at a low level in the WT GE, whereas expression is stronger and appears expanded in the DKO GE. This result is consistent with a de-repression of *Plp1* expression in the subpallium in the absence of *Dlx* gene function. Image courtesy: Janine Gallego

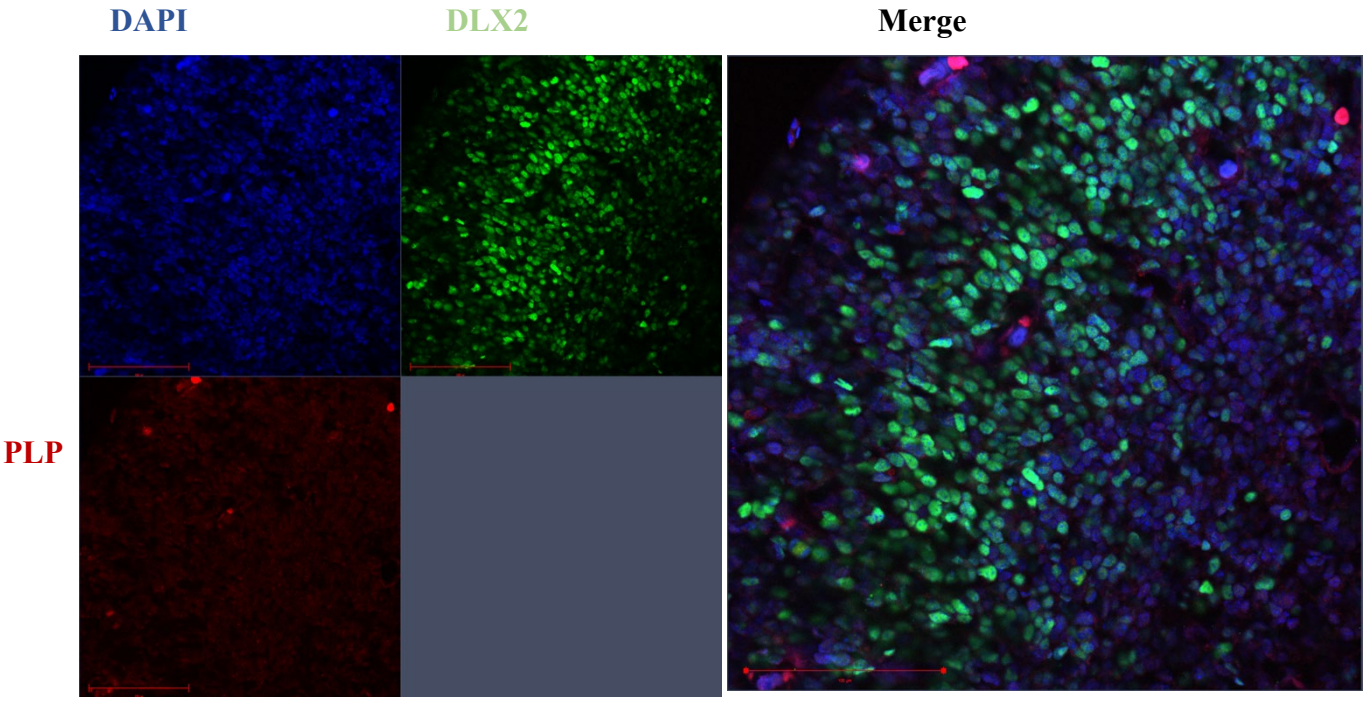


*Figure 5.8 Low PLP protein expression in the WT forebrain at E13.5*

Double immunofluorescence was performed with DLX2 and PLP antibodies on E13.5 WT forebrain sections. In agreement with data presented in Figure 5.7, PLP expression (red) appeared low in the WT at E13.5. Furthermore, the small amount of PLP expression that was visualized appeared localised to different cells than DLX2 expression (green).

Red: PLP. Green: DLX2. Blue: DAPI. Image courtesy: Janine Gallego.

# Chapter 6: MYT1 regulation of *Plp1*: results

## 6.1 The upstream region of *Plp1* contains candidate MYT1 family member binding sites

MYT1 and related family members bind to the consensus sequence AAAGTTT (Bellefroid, Bourguignon et al. 1996, Yee and Victor 1998, Gamsjaeger, O'Connell et al. 2013, Manukyan, Kowalczyk et al. 2018). MYT1 may also bind other motifs such as E-boxes, Rfx/Rbpj binding motifs, and Sox factor binding motifs together with other transcription factors (Vasconcelos, Sessa et al. 2016). To make this experiment more manageable, I decided to restrict my initial analysis to the canonical MYT1 binding site. The sequence from 2kb upstream to the transcriptional start site of mouse *Myt1* was obtained from NCBI GenBank and manually searched for AAAGTTT motifs. The upstream region contains two candidate binding sites, which I designated S1 and S2 (Figure 6.1)

TTTCAGGGAGCAAGTCACTGGACTTCTCAATGCCCTGGTTCAGTGGAGCAAAGAAA
ACTTGTTTGCTTTCTGGCCTTCCAGAATCTGATATGACAGGGGAGAACATGGAGGTA
CTATCCAGATGTTTTGTAGTTCATTGAAGACAGTTGCACAACTAAACTAAGCTGTGA
TCAAGGGGGCCCACGTTTTCTGGTTTACTGCTAGAACTGCATGAAGCACACTGTTTA
CTGGTATACTACAACCCTGCTTTGTTCTTCCTCACAGGCTCCCAAAGCAGGCAGCAG
ACTGCAACCATGAAGGCTCTTGGTGCCCTCTGGAGGAATGTTCAGGCATTGCAGAAG
CCCAGCCAGAATGGAGACTTGTTTTTTGTTCAGCTCACTTAAGAGACCCAATGAAAG
CAGAATCATAGACACAGGTAGGGTGGATGGGGTTTTCTTGGGTCAGGGAAATTCTTG
AAGACTGGAAAAAAAAAGTCCTCTGAGGACTGTAACAGGAGCTTAGAAGAAGGAT
GCAGAGGGACTGTGCAGGCAGACTGTCATGTCAGATAGACAGAGCAACCGCAATGC
ACTAGATCCGAGGGAGCTGGGAACCTTAGGGGACAGGGGAGGGTGTGACATAATCG
CCTGGCTGAGCACCTTTCCTAGCCATTAGCAGAAGAGCATTGCAGAAACAGAAAGA
TCTGCCCCATCAGTGAGGAGAGAGAAAAGGAGGGACAAGAGAAAGAGAACAGAAA
ATCAAATTCAGAGTAAGACAGTGGAGATGATAGAAAGGAGCAAAGAGGCCTCGGG
GAATATGGTAGATAAGTTTGTGTCTGGGAGTTTACTGGGGAATTATTTCCTTCTGAG
TAGCATAAACAGTCCCAGAGATGCTGCTGAGAATGGCTGAGATGCATCTGAGGAGT
CAACCTGAGCGATTCCCCCCACACATAGATCAGCTTTGGCTATTGGCTTTTTGATTTC
CCCACATCAGAATTCCCAAAGTTTAGGGTCAGTTCTTTTTGCCATCGTCCCTCTCCTC
CAGGGCTGTCAATATAAAGAAGACCTACAGCTTCACTTCCATGACAGGCCGAGTCTG

TGTCTGGAGAGCAGACCTAGGAAGGCATGGGTCTTAAGATCCTCAGCAGTCAGTCA
TGGCCTTAGTGTAGGATGCCCTGGGAAGCTCCTACCATACTGTTCCTCATGAGGCAG
GTTCAAGGATCCCTTACCTTTCAAGTTGTACAAGAGCAAAAGATTTGTTTTAGAACC
AGCCTCATACAGTCTACAATTCTGGAGTCCAGAGTTGTAGGTCCTACTCAGTTTTCCT
CCTCTATTGTCTCTTATCTCAAGACAAAAACCACAGGACAAGTTCAGGAGGACATAC
CTTATTTTTTAGAGGTATAGAAATGACAAGTTCCACAACTTTCCTTAGAGCCATTCA
GCAGTAGAATCTTGCTTCTAAATCAAGAGGGTTATGAGTGTGAGGCTTCTGAGGTGA
GAGAGAAGATAGACAAAGAAACCACATAAGCGCTCCTTAAGGTGCACCTGTTTTAG
AAAGGACTAGAAAAGTTTGCCTAGCTAACATCACCTTTTATATTTGGTTCCTTCACA
GACGTCAGAAATCACTCTTACCATTGTAAATGGTTCACAAATACTTCCCCTCTTTTTA
CTGCTTGGCCATATTTTTTCATAGAATCCTCTTTGAGACAAGGACTGTATTTTCTTTC
TCCCCCCCCCCCCCAACTCTGACTGCTGCTTTCCCAAACGCTCCTTCCGTCTCCTTAGC
CTCATCTTCACTCTGATGGGAACACTATTTCCTGGGAAGAGTTTTGACTAGCTGCTTG
CCAGTTTGTGATAATGTCTTGTCTCAGAGTTCATTTTCCTTGAAAATTGCCTACATGG
TCCACTCTGGCCTTTTTGTCCCTTGTGACCTTGGCACAGGTCTTGCCCTCTCCTTTGTA
TCTCTGTTATCCAAATGTACTCTCATTGCACGTCTGGCTTTTTTGAGCCTGGTCACAC
ACAGTCTG

Site 1 (green highlighted): -1025 to -1018; Site 2: -461 to -454. Nucleotide positions are relative to transcriptional start site

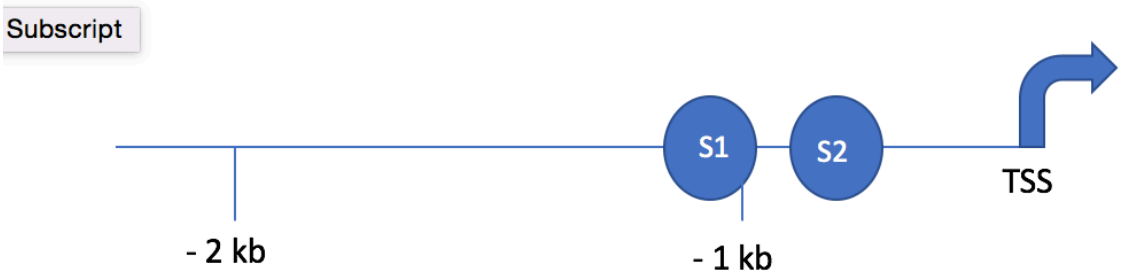


*Figure 6.1 The Plp1 promoter contains two candidate MYT1 binding sites.*

MYT1 and MYT1 family members bind the canonical sequence AAAGTTT. The upstream region of *Plp1* contains two of these candidate binding sites.

## 6.2 MYT1 may occupy the *Plp1* promoter in E14.5 and E18.5 mouse forebrain

To determine if MYT1 occupied either of these potential regulatory regions in the *Plp1* promoter *in vivo,* chromatin immunoprecipitation was performed with a MYT1 antibody on E14.5 ganglionic eminences and E18.5 forebrain dissected from WT CD1 mice. The choice of time point is explained in Chapter 3. Briefly, E14.5 is before the onset of *Plp1* expression (plp isoform) in mouse, and in the qPCR experiments described in Chapter 5, *Plp1* transcript expression was not detectable in WT GE around this time point. Therefore I chose E14.5 as the pre-*Plp1* expression time point for this experiment. Also, as shown in Chapter 5, we found that PLP1 (protein) expression was evident by E18.5 in WT GE, and so I reasoned that by this time point, the *Plp1* promoter should be occupied by other regulatory factors.

Following ChIP, PCR was carried out on immunoprecipitated chromatin using primers designed to flank the putative MYT1 binding sites in the *Plp1* promoter. Because our laboratory has not previously performed a ChIP assay for MYT1, as positive control regions, I also used primer pairs for regions of the *Olig1* and *Hes1* promoters that were reported to be occupied by MYT1 in NS5 cells that had been transduced by HA-tagged MYT1 (Vasconcelos, Sessa et al. 2016). MYT1 specifically occupied the *Hes1* promoter in developing forebrain (Figure 6.2, A), validating the use of this antibody for ChIP. Although S1 and S2 of the *Plp1* promoter appeared enriched in forebrain chromatin immunoprecipitated with the MYT1 antibody (Figure 6.2, C and D) this appeared somewhat nonspecific, especially for S1, and for S2 at E18.5. This result indicates that MYT1 may specifically occupy S2 of the *Plp1* promoter in E14.5 forebrain. E14.5 is well before the onset of myelination, so this result is consistent with the hypothesis that a

function of MYT1 might be to facilitate activation of the *Plp1* promoter later on in oligodendroglial development when high-level expression of *Plp1* is required.

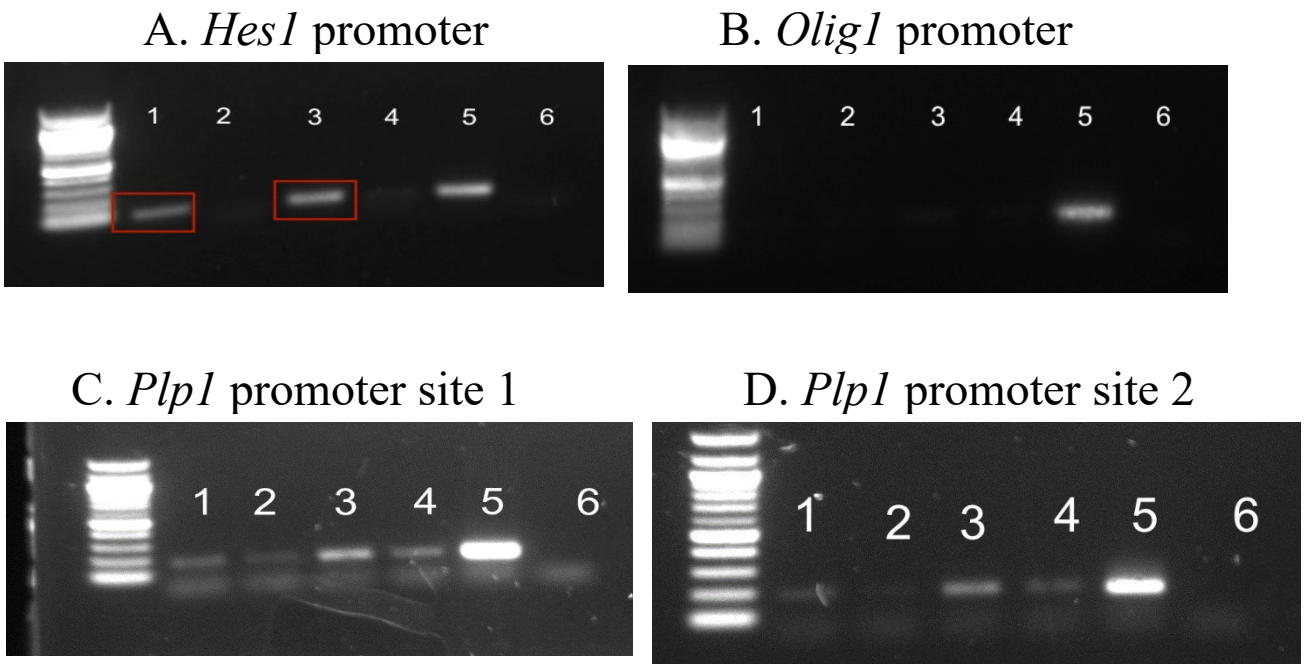


*Figure 6.2 MYT1 may occupy the Plp1 promoter in E14.5 and E18.5 forebrain.*

A. MYT1 was found to specifically occupy the *Hes1* promoter *in vivo* (Lanes 1 and 3). B. MYT1 does not appear to specifically occupy the *Olig1* promoter *in vivo*. C. MYT1 occupies site 1 of the *Plp1* promoter in E14.5 (lane 1) and E18 (lane 3) forebrain, but enrichment in the control samples receiving IgG (lanes 2 and 4) suggest this could represent nonspecific binding to the beads, especially for E18.5 chromatin (lane 4). D. MYT1 occupies site 2 of the *Plp1* promoter in E14.5 (lane 1) and E18.5 (lane 3) forebrain.

Lanes: 1. E14.5 forebrain + MYT1 antibody. 2. E14.5 forebrain + IgG antibody. 3. E18.5 forebrain + MYT1 antibody. 4. E18.5 forebrain + IgG antibody. 5. Genomic DNA. 6. Water. Experiments were performed in one technical and one biological replicate.

# Chapter 7: DLX2 regulation of progenitor cell fate in H3K27M-mutant midline glioma

## 7.1 DLX2 overexpression promotes differentiation and reduces proliferation, invasion, and migration in a mouse model of DIPG

Because DIPG is suggested to have an OPC cell of origin, we asked whether there might be a role for *Dlx* genes in promoting differentiation and altering tumour cell phenotype in this disease. To investigate this in a preliminary manner, we over-expressed murine DLX2 in tumour cells derived from a genetically engineered mouse model of DIPG that was created by using the RCAS/Tv-a system to overexpress PDGF-B, knock in the H3.3K27M mutation, and include p53 mutant expression in Nestin-positive brainstem progenitor cells (hereafter referred to as mDIPG cells). We found that DLX2 over-expression in mDIPG cells resulted in transcriptional changes suggestive of competence to respond to DLX2 regulation including significant upregulation of *Gad1* (P=0.0077) and *Gad2* (P=0.024), and downregulation of *Olig2* (P=0.0023) and *Myt1* (P=0.049) (Figure 7.1). DLX2 over-expression also resulted in reduced migration and invasion *in vitro* (Figure 7.2 A and B), and reduced soft agar colony formation *in vitro* (Figure 7.2, C) and proliferation as assessed via MTT assay (data not shown). Taken together, these results suggested that DLX2 expression might alter differentiation (Figure 7.1) and tumour cell phenotype (Figure 7.2). We therefore pursued the same line of investigation in a human-derived DIPG cell line.

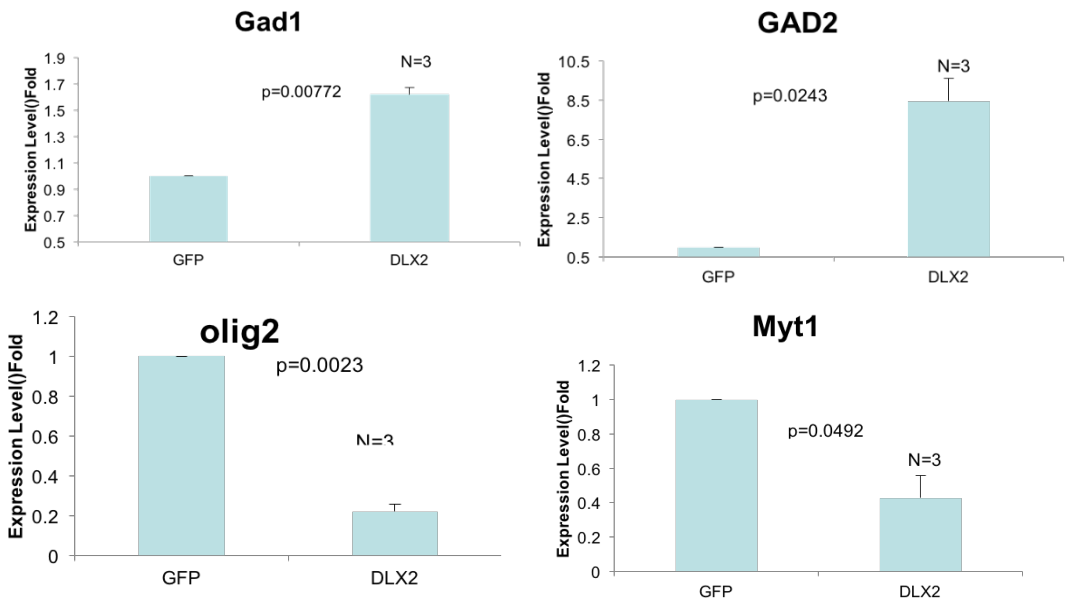


*Figure 7.1 mDIPG cells show a transcriptional response to DLX2 over-expression*

mDIPG cells were transiently transfected with a DLX2 expression vector (DLX2) or an empty control vector (GFP) and harvested two days post-transfection. qPCR was performed for known DLX2 targets (*Gad1*, *Gad2*) and/or oligodendroglial genes (*Olig2, Myt1*). In DLX2-transfected cells, *Gad1* and *Gad2* were significantly upregulated (P=0.0077 and 0.024, respectively) and *Olig2* and *Myt1* were significantly downregulated (P=0.0023 and 0.049, respectively) suggesting mDIPG cells can respond to DLX2 expression. All gene signals were normalised to *Gapdh* expression levels. Experiments were performed in three biological and three technical replicates. Significance was calculated using Student's unpaired t-test.

Figure courtesy: Xiaohua Song

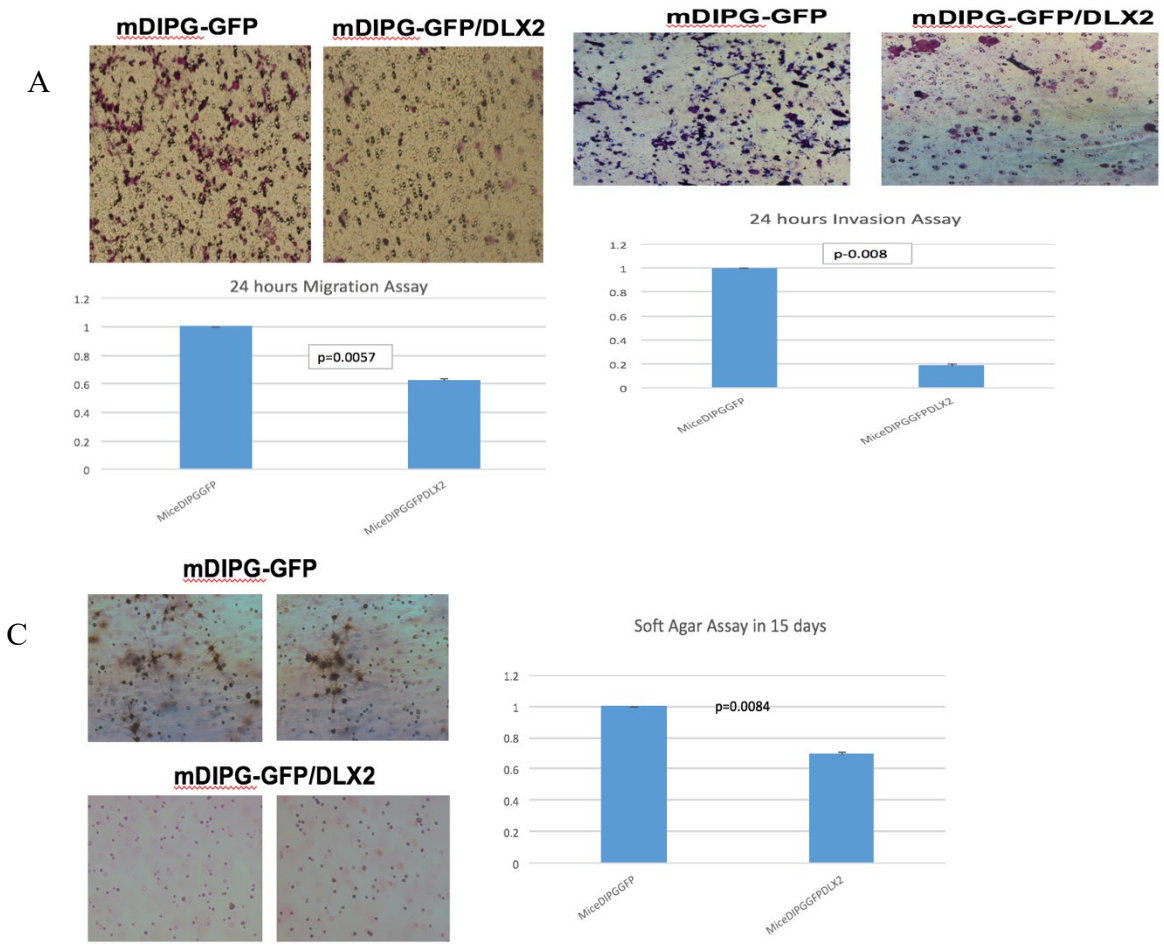


*Figure 7.2 DLX2 overexpression reduces migration, invasion, and soft agar colony formation of mDIPG cells in vitro*

*In vitro* migration, invasion, and soft agar colony formation assays were carried out on mDIPG cells overexpressing DLX2 or control empty vector. DLX2-overexpressing cells showed significantly reduced migration (A; P=0.0057, N=3) and invasion (B; P=0.008, N=3) at 24 hours compared to control cells. DLX2 overexpression also resulted in significantly reduced colony formation on soft agar (C; p=0.0084, N-3). Experiments were performed in three biological and

three technical replicates. Statistical significance was calculated using Student's two sample t-test. Figure courtesy: Xiaohua Song.

## 7.2 Lack of transcriptional response to DLX2 overexpression in SF8628 cells

Following the promising preliminary results regarding the effects of *Dlx2* overexpression on mDIPG differentiation and behaviour *in vitro*, we continued to investigate the role of *Dlx2* in DIPG using patient-derived tumour cell lines. A patient-derived DIPG cell line, SF8628, was obtained and transiently transfected with a GFP-tagged DLX2 expression vector. Control cells received empty vector instead. Two days post-transfection, cells were harvested for RNA and qRT-PCR was performed to measure expression levels of the known DLX2 target genes *Gad1, Gad2, Olig2,* and *Nkx2.2,* as well as *Myt1.* DLX2 is known to activate *Gad1* and *Gad2* expression (Le, Zhou et al. 2017). Unpublished data from our laboratory also indicates DLX2 represses *Olig2* and *Nkx2.2* expression, in addition to the important role of these genes in OPC differentiation. *Myt1* expression was examined because an inverse relationship between *DLX2* and *MYT1* expression was found in one study of histone-mutant pediatric glioblastomas (Schwartzentruber, Korshunov et al. 2012) as well as because of *Myt1*'s role in oligodendroglial lineage development. We predicted that if SF8628 cells could respond to DLX2 expression, we would see upregulation of *Gad1* and *Gad2*, and downregulation of *Olig2, Nkx2.2*, and *Myt1*. However, expression levels of all genes were not significantly different between cells receiving DLX2 or empty vector (Figure 7.3) as indicated by the lack of difference between the mean dCT values of all genes between the two groups. This preliminary result indicates that SF8628 cells do not respond to DLX2 expression, but further experiments with other patient-derived DIPG cell lines are planned.

A

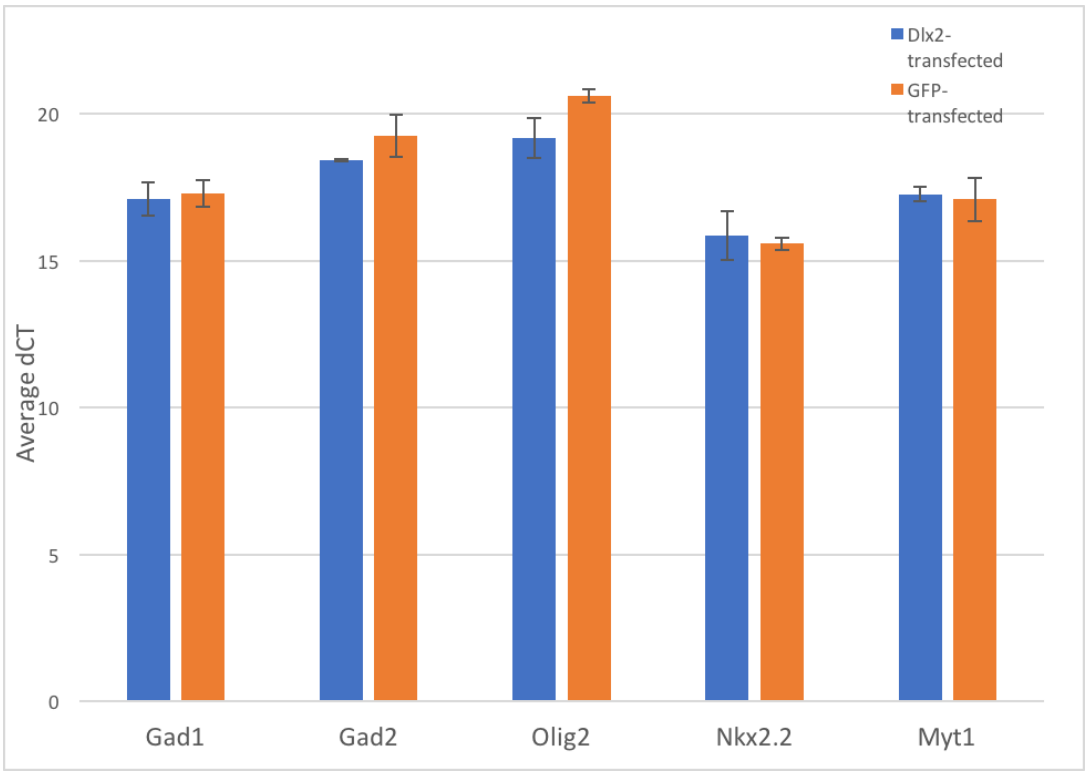
Dlx2-transfected
GFP-transfected
Average dCT
20
15
10
5
0
Gad1
Gad2
Olig2
Nkx2.2
Myt1

B

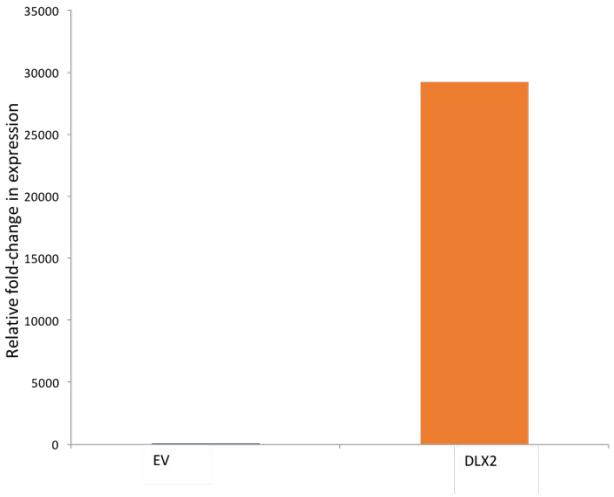
Relative fold-change in expression
35000
30000
25000
20000
15000
10000
5000
0
EV
DLX2

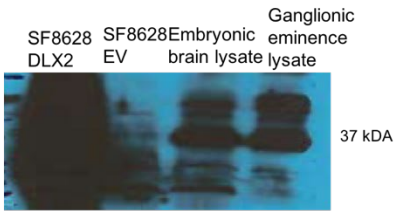
SF8628 DLX2
SF8628 EV
Embryonic brain lysate
Ganglionic eminence lysate
37 kDA

*Figure 7.3 Lack of transcriptional response to DLX2 overexpression in SF8628 cells*

A: A patient-derived DIPG cell line (SF8628) was transiently transfected with a DLX2 expression vector (DLX2-GFP; blue) or empty vector (GFP; orange). 48 hours post-transfection, cells were harvested for RNA and qPCR was used to measure expression levels of known DLX2 target genes (*Gad1, Gad2*) and several genes involved in oligodendroglial lineage development (*Nkx2.2, Olig2, Myt1*). B: *Dlx2* expression was also measured to verify that transfection occurred successfully (B, left), and in a separate experiment, DLX2 protein production in this cell line following transfection was verified by western blot (B, right). Expression levels were normalized to *Gapdh* expression using the dCt method. This experiment was performed in one biological replicate and three technical replicates. Error bars represent the standard error of the mean dCt. Although preliminary, as more biological replicates are needed for statistical analysis, I did not observe the transcriptional response that would be expected in response to DLX2 overexpression: upregulation of *Gad* genes and downregulation of *Olig2*, *Nkx2.2,* and potentially *Myt1*. This suggests that SF8628 DIPG cells may not be able to respond to DLX2 expression. Further experiments are planned.

# Chapter 8: Discussion and Conclusions

**Transcriptional regulation of *Myt1* and *Plp1* by DLX2**

The *Dlx1/2* double knockout mouse displays several abnormalities in forebrain development, including a marked increase in production of oligodendrocyte progenitor cells (OPCs) with an accompanying decrease in interneuron production, as well as accelerated OPC differentiation (Petryniak, Potter et al. 2007). We hypothesized that DLX1/2 repress oligodendroglial fate acquisition and differentiation in GE progenitors that are destined to make GABAergic interneurons by suppressing the expression of multiple genes required for oligodendroglial differentiation. In this project, I investigated whether DLX2 represses expression of myelin transcription factor 1 (*Myt1*) and proteolipid protein 1 (*Plp1*) during forebrain development, and I also began to explore whether MYT1 regulates *Plp1* expression.

## 8.1 Transcriptional regulation of *Myt1* by DLX2

Similar to other homeodomain transcription factors, DLX2 regulates transcription of target genes by binding to sites containing TAAT/ATTA motifs. I assessed every TAAT/ATTA motif within 4kb of the *Myt1* transcriptional start site as a potential DLX2 binding site. Chromatin immunoprecipitation followed by end-point PCR and qPCR on E13.5 forebrain revealed that DLX2 occupies at least five of these potential regulatory regions *in vivo*. This result is consistent with a regulatory role for DLX2 on the *Myt1* promoter. However, electrophoretic mobility shift assays failed to demonstrate direct binding of recombinant DLX2 to any ChIP-positive candidate ATTA/TAAT motif-containing *Myt1* regulatory regions, indicating that recombinant DLX2 might not bind these regions directly. A possibility I considered was that the short oligonucleotide probes I used for EMSA did not contain sufficient sequence surrounding the

homeodomain binding motif to allow for binding site recognition. The flanking sequence surrounding transcription factor binding sites is known to be important in binding site recognition (Dror, Rohs et al. 2016, Inukai, Kock et al. 2017, Yella, Bhimsaria et al. 2018). Therefore, I repeated EMSA for regions 1, 2, 10 using the entire promoter regions. Probes for *Myt1* promoter regions prepared in this manner also failed to show direct binding. Negative results in EMSA via two different methods supports that recombinant DLX2 does not bind *Myt1* promoter regions directly. However, no strong conclusions can be drawn from these experiments because the EMSAs did not include an appropriate positive control region. It is possible that the *Myt1* EMSAs shown in Figures 4.4 and 4.5 failed on a technical level and that is why no binding was detected. To address this limitation and determine whether DLX2 can bind any *Myt1* promoter regions directly, these experiments need to be repeated with a positive control probe that has been previously shown to bind DLX2 directly included in the set of binding reactions run on the gel. This limitation notwithstanding, given the positive ChIP result, it might still be possible that DLX2 only binds the *Myt1* promoter as part of a complex. Moreover, recombinant DLX2 lacks post-translational modifications such as phosphorylation that may be necessary for binding *in vivo*.

Association with other transcription factors is known to modify DLX-DNA binding and transcriptional regulation in some cases. For example, heterodimerization between DLX TFs and the MSX homeodomain proteins has been described, although in this case this interaction blocks DNA binding by DLX proteins and prevents them from acting as transcriptional activators (Zhang, Hu et al. 1997). Transcriptional activity of DLX1 and DLX2 has also been shown to be modulated by association with the long noncoding RNA *Evf2* where association with *Evf2* results

in increased enhancer binding of DLX1/2, with a repressive transcriptional outcome, although the DLX TFs often act as transcriptional activators (Cajigas, Leib et al. 2015). If additional binding partners are required for association with *Myt1* regulatory regions, no promoter interaction would be detected in an EMSA using purified recombinant DLX2. Therefore, an important future direction for this project would be to repeat EMSA using nuclear extracts from E13.5 mouse forebrain as the DLX2 source; this would contain any required binding partners for DLX2 in the developing forebrain (Le, Zhou et al. 2017).

In order to determine if loss of *Dlx1/2* gene function affects *Myt1* expression, I performed qPCR on WT and *Dlx1/2* DKO E13.5 forebrain and compared *Myt1* expression levels between the two tissues. *Myt1* transcript expression was not significantly increased in the DKO. This result also does not support our hypothesis that DLX2 represses *Myt1* during forebrain development. When interpreting this result, it may be worth considering the fact that *Myt1* is rather broadly expressed in the developing CNS whereas our model for cell fate determination by DLX1/2 involves only a small proportion of progenitor cells in the MGE. De-repression of *Myt1* in the absence of DLX1/2 would (potentially) therefore only occur in those cells in the DKO, and not the rest of the subpallium. This difference might not be detectable via qPCR using RNA from the entire GE. In fact, I did see that *Myt1* was upregulated, but not significantly, and this neuroanatomical or spatial factor could be a reason why. There could also be ectopic expression of MYT1 in the DKO outside the MGE; previous work from our lab demonstrated ectopic expression of NKX2.2 in the thalamus in the absence of *Dlx1/Dlx2* gene function (Japoni S et al, in preparation). Therefore, a future direction for this project is double IF for MYT1/DLX2 in WT and DKO E13.5 forebrain, to determine if DLX2 and MYT1 do not co-localise to the same cells, as would

be predicted if DLX2 is suppressing *Myt1* in those MGE progenitors that will go on to generate GABAergic interneurons.

Based upon the data acquired to date, it seems possible that DLX2 may not regulate *Myt1* directly. Recombinant DLX2 failed to bind *Myt1* promoter regions directly in EMSA and *Myt1* expression was not significantly upregulated in the DKO forebrain. However, DLX2 was found to bind the *Myt1* promoter region in two separate ChIP experiments. On this basis it was carried forward for further characterisation as a potential transcriptional target of DLX2. If *Myt1* is not a transcriptional target of DLX2, the positive ChIP result requires an explanation.

One factor to consider is the strategy I used for identifying potential *cis*-regulatory elements. *Myt1* was originally identified as a putative DLX transcriptional target based primarily on the presence of TAAT/ATTA general homeodomain binding motifs in its upstream region. ChIP results in the hands of two independent experimenters (me and S. Zhang) suggests that some of these could represent true DLX binding sites, but it is well-established that regulatory elements are not necessarily involved in regulation of the gene whose promoter they are closest to. In metazoans, *cis*-regulatory elements can be located large distances (on the order of kilobases or megabases upstream or downstream) away from genes that they regulate, and it is not uncommon for there to be multiple genes in between a distal regulatory element and a target gene (Slattery, Zhou et al. 2014). The fact that a potential DLX binding site is located within the promoter-proximal region of a particular gene does not mean that it is involved in regulation of that gene rather than one located somewhere else on the chromosome. It is possible that the DLX2 occupancy near the *Myt1* promoter that I detected in ChIP represents an interaction that is

involved in regulation of a different gene. This would explain why I observed DLX2 binding near the *Myt1* promoter with ChIP, although, based on EMSA and gene expression data, DLX2 does not seem to regulate *Myt1* expression. Another possibility is that DLX2 is binding to the *Myt1* promoter via association with another, as-yet unidentified transcription factor. This would explain the positive ChIP and negative EMSA results.

Interestingly, it was recently reported that in forebrain development the DLX transcription factors show widespread binding/occupancy across the genome with no apparent functional consequences for many binding events. Lindtner et al (2019) performed ChIP-seq for DLX1, DLX2, and DLX5 at E11.5, E13.5, and E16.5 as part of their characterisation of DLX-regulated transcriptional circuits in the developing forebrain. They found that, at lower levels of enrichment, many regions of the genome showed DLX occupancy. However, ChIP-seq for key histone posttranslational modifications (H3K4me1, H3K4me3, H3K27Ac, and H3K27me3) and RNA-seq revealed no change in chromatin state or differential expression of nearby genes for the majority of DLX-bound regulatory elements in the DKO GE at E13.5. Only 6.2% of putative DLX target loci (as identified in ChIP-seq) showed significant changes in histone PTMs in *Dlx1/2* double knockout GE at E13.5. RNA-seq revealed that the expression of the majority of genes near DLX-occupied regulatory elements was also not significantly different in DKO compared to WT GE at E13.5. The authors suggest that the majority of these low-affinity DLX binding events detected in ChIP are not required for normal gene expression or chromatin state at E13.5 and might not be functional (Lindtner, Catta-Preta et al. 2019). It is possible that this is the type of interaction I detected.

An alternative interpretation of the findings reported by Lindtner and colleagues is that DLX TFs regulate target genes mainly by binding distally-located regulatory elements. This seems unlikely because, for genes that did show significant up or downregulation in the *Dlx1/2* DKO, many of these were located nearby putative regulatory elements that showed significant changes in chromatin state in the DKO as well. This paper offers an interesting potential biological explanation for the observation of a positive ChIP result with no apparent effect on target gene expression for the DLX transcription factors, which may be of relevance to my findings. Furthermore, in general, it is well-established that many TF-DNA binding events can be non-functional and the detection of a binding event in ChIP does not signify the detection of a functional interaction (Spitz and Furlong 2012).

## 8.2 Transcriptional regulation of *Plp1* by DLX2

As with *Myt1,* I assessed every TAAT/ATTA motif within 4kb of the *Plp1* transcriptional start site as a potential DLX2 binding site. ChIP-PCR on E13.5 forebrain revealed that DLX2 occupies at least four of these potential regulatory regions *in vivo*. Electrophoretic mobility shift assays using recombinant DLX2 and radiolabelled oligonucleotide probes corresponding to ChIP-positive *Plp1* promoter regions also demonstrated that recombinant DLX2 can directly bind multiple homeodomain binding sites within regions 1, 2, 6, and possibly 8 of the *Plp1* promoter *in vitro*. *In vivo* occupancy and *in vitro* binding of DLX2 to *Plp1* promoter regions is consistent with a regulatory role for DLX2. Next, I conducted luciferase reporter assays using ChIP and EMSA-positive regions of the *Plp1* promoter (regions 1, 2, 6, and 8) to determine if DLX2 binding to any putative *Plp1* regulatory regions had an effect on transcriptional output. If DLX2 represses *Plp1* by binding to any of these regions, a decrease in reporter expression would

be expected with DLX2 co-transfection. However, there was no significant change in reporter expression observed with co-transfection of any of the tested regulatory regions and the DLX2 expression vector. One biological explanation for these results is that an isolated regulatory region inserted into a reporter vector for *in vitro* expression experiments lacks the genomic and chromatin context that it would have *in vivo*, and may not function in the same way to regulate gene expression. Developmental gene regulation generally involves the assembly of multiple regulatory proteins at multiple binding sites within the promoter and other *cis*-regulatory elements. These interactions are often lost in a reporter assay that makes use of only a single regulatory element. Furthermore, combinatorial binding of TFs and combinatorial occupancy of different TF binding sites can have differential effects on gene expression (Reiter, Wienerroither et al. 2017) and the effect on transcription of a single *cis*-regulatory element or TF binding site might not be the same as the effect of the full promoter-proximal region containing many binding sites both for DLXs and other proteins. These factors may explain the discrepancy between the results of the luciferase assays and some of the *in vivo Plp1* expression data in the DKO forebrain. An informative future direction for this project would therefore be to clone the entire 4 kb upstream region of *Plp1* upstream of a reporter gene and assess whether it affects reporter expression when co-expressed with DLX2. Instead of examining individual regions in isolation as I did here, determination of the importance of individual binding sites within each region could be assessed by using site-directed mutagenesis to generate whole promoter constructs in which individual regions or binding sites are deleted or mutated.

An additional consideration is that HEK293 cells were used in this assay primarily due to their low level of endogenous DLX2 and ease of transfection, but HEK293 cells and neural progenitor

cells are likely to differ substantially in terms of what transcriptional cofactors are present. The same transcription factor can have either activating or repressing effects according to the availability of other, cell-type specific transcription factors and cofactors (Spitz and Furlong 2012). For example, the DLX proteins can act as transcriptional activators or repressors; one factor that has been shown to modulate this activity is association in a complex with the chromatin remodeler BRG1 and the long noncoding RNA *Evf-2* (Cajigas, Leib et al. 2015). Differences in cofactor availability between HEK293 cells and neural progenitor cells could explain why *Plp1* regulatory elements did not appear to have any effect on reporter gene expression when co-transfected with DLX2 *in vitro*, although some of the *in vivo* protein expression data suggest DLX1/2 may repress *Plp1* (Figures 5.7 and Figures 5.8). Therefore, an additional possible future direction is to repeat these reporter assays in a cell line that is more representative of neural progenitor cells. A final, major technical limitation of these experiments that must be addressed is that I used a vector (pGL3) that lacks a minimal promoter. Without a minimal baseline level of reporter expression, it might not be meaningful to try and assess repression of expression. This may explain the lack of effect detected and overall high variability of reporter expression in these experiments. Besides the above-discussed considerations about the effects of the full promoter region versus isolated regulatory regions, an essential future direction to determine if DLX2 binding to putative *Plp1* regulatory regions can repress transcription is to repeat the luciferase assays (whether with the full 4kb upstream region or single regulatory elements) using a vector with a minimal promoter that provides a baseline level of reporter gene expression from which repression can be assessed.

In order to determine whether *Plp1* transcript expression was increased in the absence of *Dlx* gene function, I performed qPCR for *Plp1* on E13.5 DKO and WT GE and compared *Plp1* expression levels between the two tissues. *Plp1* expression was upregulated in the DKO forebrain at E13.5, but not significantly. This is in surprising contrast to the IF expression data showing strong expression of PLP protein at E13.5 in the DKO, while PLP protein levels were very low in the WT at this time point (Figure 5.7). IF using a different antibody in the WT also revealed low levels of PLP protein in the WT forebrain at E13.5 (Figure 5.8). It is difficult to reconcile the findings of markedly increased protein expression without an increase in transcript levels in the DKO, as well as the detection of *Plp* transcript in the WT at E13.5 despite the lack of protein expression. One factor that might contribute relates to the existence of two splice isoforms from the *Plp1* primary transcript, *Plp* and *Dm20*. I used qPCR primers that, in theory, were specific to the *Plp* transcript because the forward primer spans the junction between exon 3B and exon 4, and exon 3B is spliced out of the *Dm20* transcript. Predicted specificity for the *Plp* transcript was verified with BLAST. The primers were also validated to ensure that they only give a single melting peak in qPCR. However, in practice, the specificity of splice variant detection with splice variant specific exon-exon junction spanning primers has been shown to sometimes vary considerably according to, among other factors, the relative abundance of the different transcripts (Williams, Koduri et al. 1999, Shulzhenko, Smirnova et al. 2003). Given this, it could be possible that the qPCR primers used did amplify the *Dm20* transcript as well. However, the antibodies used for IF were specific to PLP1. These factors could explain why *Plp* transcript was apparently detected by qPCR in the WT forebrain at E13.5 although there was no PLP protein expression in WT at this time- the product detected by qPCR in the WT may actually have been *Dm20* transcript, which is known to be more highly expressed earlier in

development (LeVine, Wong et al. 1990). DM20 protein would not be detected by the antibodies used, hence the discrepancy between the qPCR and IF results in the WT forebrain.

Another explanation relates to the change in the proportions of different cell types in the DKO forebrain. Some evidence suggests that the *Plp1* promoter shows activity in neuronal and astrocytic progenitors (Michalski, Anderson et al. 2011, Harlow, Saul et al. 2014), at least in the spinal cord, but these cell types do not accumulate PLP protein (Harlow, Saul et al. 2014). The work of Harlow *et al* (2014) did not distinguish between *Plp* and *Dm20* transcript production but was mainly concerned with promoter activity; *Dm20* transcript is known to be produced in non-OPC cell types (Ikenaka, Kagawa et al. 1992). Especially if, as discussed above, our primers may be able to amplify both *Plp* and *Dm20* transcripts, the transcript expression from the *Plp1* promoter observed in the WT by qPCR could represent activity in not just OPCs but also these other cell types. In the DKO MGE, the balance of cell types is shifted towards more OPCs and fewer neuronal progenitors (Petryniak, Potter et al. 2007) whereas the WT MGE will have more neuronal progenitors and fewer OPCs. *Plp1* transcripts (of either isoform) may therefore possibly be found in both cell types, but only the OPCs will accumulate PLP protein as they differentiate (Harlow, Saul et al. 2014). OPC differentiation is also accelerated in the DKO forebrain, such that OPCs express myelin genes and late-stage oligodendroglial markers earlier than in the WT (Petryniak, Potter et al. 2007). Therefore, overall, the transcript levels of *Plp* might not be different between the two, as the increase in *Plp* transcript due to increased OPCs in the DKO will be balanced by a proportional reduction in neuronal progenitors. However, because of the alteration in OPC differentiation rate, PLP protein would be present at much higher levels in the DKO forebrain at E13.5, as we observed.

Another possibility to explain the incongruous qPCR and IF results is that DLX1/2 could be interacting with other factors to regulate splicing of the *Plp1* primary transcript rather than directly regulating its transcription. Given that PLP expression is primarily characteristic of myelinating oligodendrocytes, while DM20 is suggested to play other roles in the developing CNS (Ikenaka, Kagawa et al. 1992, Timsit, Bally-Cuif et al. 1992) regulation of the PLP/DM20 balance through splicing regulation could represent another mechanism by which DLX transcription factors might repress oligodendroglial differentiation. Although a role for the DLX proteins in splicing regulation has not been reported, DLX1 has been shown to interact with long noncoding RNAs (lncRNA) such as *Evf-2* (Feng, Bi et al. 2006, Cajigas, Leib et al. 2015). In this specific case, *Evf-2* functions as a transcriptional coactivator for DLX1 and DLX2 (Feng, Bi et al. 2006, Cajigas, Leib et al. 2015) but lncRNAs can also play a role in regulation of splicing (Yoon, Abdelmohsen et al. 2013). If DLX1/2 specifically repress splicing of the primary *Plp1* transcript to the *Plp* mRNA, this could explain why PLP protein is increased in the DKO while there was no significant difference in transcript levels between WT and DKO. In this situation, the ratio of *Plp* to *Dm20* mRNA should be increased in the DKO but overall levels of both transcripts together might not be significantly different. A significant change in *Plp/Dm20* ratio might not be detected using primers that may be able to amplify both transcripts, as already discussed above. To determine if this is the case, one option is to perform *in situ* hybridisation with probes that are specific for *Plp* and *Dm20*. ISH probes, hybridisation, and washing conditions that allow specific detection of *Plp* and *Dm20* transcripts have been reported (LeVine, Wong et al. 1990) so this experiment should be technically feasible. If DLX1/2 repress splicing of the *Plp* isoform, we should see increased *Plp* transcript and correspondingly decreased *Dm20*

transcript in the DKO forebrain. Also, an IF experiment using an antibody specific for DM20 should reveal decreased DM20 protein in the DKO compared to the WT MGE.

## 8.3 Conclusions and Future Directions

This project provides some evidence that DLX2 directly represses *Plp1* expression during forebrain development. ChIP, EMSA, and IF experiments all provided strong evidence that DLX2 can regulate *Plp1* expression. DLX2 occupied putative regulatory regions in the *Plp1* promoter *in vivo* (Figures 5.2 and 5.3), and directly bound many of these regions *in vitro* (Figures 5.4.1-5.4.4). PLP protein expression was increased and expanded at E13.5 in the DKO GE compared to the WT. These findings are all consistent with a regulatory role for DLX2 on the *Plp1* promoter. However, further investigation into the discrepancy between the qPCR and IF data may be warranted, as discussed above. Given that *Plp* was upregulated in the DKO but this didn't reach statistical significance, it would be worth obtaining more DKO litters for gene expression analysis via qPCR to see if there is a statistically significant upregulation with a larger sample size. In our experience, many DKO litters contain only one DKO pup and so a sample size of 3 litters corresponds to a very small number of DKO mice. Looking at more mice may reveal biologically relevant results in the DKO.

The luciferase assays for *Plp1* promoter regions R1 and R6 also require additional biological replicates to determine if there is any statistically significant change in reporter gene activity when DLX2 is co-transfected with the reporter gene under the control of these regulatory regions compared to control reporter plasmid. However, if not, this would not necessarily mean that *Plp1* is not regulated by DLX2 but that perhaps the entire promoter region is required to see an effect

on reporter expression *in vitro*. Furthermore, this set of experiments must be repeated using a vector that contains a minimal promoter element (such as pGL4), as discussed above.

A final important future direction is to perform double immunofluorescence for DLX2 and PLP in the WT GE at E13.5, E15.5, and E18.5. If DLX2 represses PLP expression in cells fated to become interneurons, then DLX2 and PLP should not co-localize to the same cells in the developing GE. The rationale for looking at both of these time points is that PLP could not be detected at E13.5 in the WT, so a double IF at this point may not be informative regarding co-expression; only a later time point may reveal a lack of co-expression.

Furthermore, the increase in *Plp* positive cells in the DKO was observed at E15.5 by Petryniak and colleagues (2007) so effects of DLX-mediated repression on PLP may begin to show up around this time. For E18.5, this is when PLP expression would be expected to become detectable in the WT (at least with the antibody we used). A potential problem is that DLX2 is not expressed at E18.5 so, again, a DLX2/PLP co-expression IF may not be informative at this time point. One approach would be to instead look at co-expression of later-activated DLX members (DLX5 and DLX6) and PLP at E18.5. Cells that are DLX5/6 positive at this time point would have been DLX2-positive earlier in their development based on what is known about the temporal expression pattern of the DLX genes during development of the subpallium. (Panganiban and Rubenstein 2002).

Based on the data presented here, it cannot be concluded whether *Dlx2* regulates *Myt1* expression in the developing forebrain. DLX2 occupied the *Myt1* promoter *in vivo* (Figure 4.2,

Figure 4.3) which is consistent with a regulatory role. It did not bind *in vitro* (Figure 4.4, Figure 4.5) but, as discussed, this experiment is subject to a substantial technical limitation. The trend towards upregulated expression observed in the DKO is also consistent with a regulatory role. Therefore an important future direction for this project is to repeat EMSA with an appropriate positive control to definitively determine if DLX2 directly binds *Myt1* promoter regions.

## 8.3 Transcriptional regulation of *Plp1* by MYT1

It has been suggested that a function of MYT1 in oligodendroglial development is to place the *Plp1* promoter in a physical conformation that renders it accessible for transcription/activation later on in development (Kim and Hudson 1992). It has been shown via electrophoretic mobility shift assay that MYT1 directly binds *cis*-regulatory elements in the *Plp1* promoter (Kim and Hudson 1992). However, occupancy of the *Plp1* promoter by MYT1 during nervous system development has not been shown *in vivo*. In order to better characterise a possible DLX/MYT1/PLP1 regulatory network, I set out to determine whether MYT1 binds the *Plp1* promoter by performing chromatin immunoprecipitation on chromatin from WT E14.5 and E18.5 forebrain using an MYT1 antibody. My initial results suggest that MYT1 may occupy the *Plp1* promoter *in vivo*.

I was also able to demonstrate that MYT1 binds the *Hes1* promoter *in vivo*, which has only been previously shown in cultured mouse neural stem cells (NS5 cells) transduced with HA-tagged MYT1 (Vasconcelos, Sessa et al. 2016). In this study, it was proposed that *Myt1* promotes neuronal differentiation by repressing transcription of Notch pathway effectors, including *Hes1*.

The confirmation that MYT1 occupies the *Hes1* promoter in the developing brain is a novel finding that supports the hypothesis that MYT1 could regulate *Plp1* during neural development.

### 8.3.1 Conclusions and future directions

Binding of MYT1 to the *Plp1* promoter at multiple developmental time points is consistent with the hypothesis that MYT1 could be involved in positive regulation of *Plp1* expression. However, further experiments are needed to determine if MYT1 binding has any functional consequences for *Plp1* promoter expression. Future directions for this part of the project in addition to EMSA and luciferase reporter gene assays *in vitro*, include assessing whether loss of *Myt1* has any effect on *Plp1* expression by knocking down *Myt1* expression using siRNAs in primary cultures of the embryonic forebrain or in cell lines with endogenous expression of MYT1. If MYT1 acts as a transcriptional activator for *Plp1, Plp1* expression should be decreased in the *Myt1* knockdowns. Another experiment might be to use a dominant negative *Myt1* construct that lacks the ability to bind the *Plp1* promoter (e.g. lacking one or more of the zinc fingers).

## 8.4 Role of DLX2 in differentiation of DIPG

I investigated whether DLX2 overexpression might promote differentiation in DIPG by transiently transfecting a patient-derived DIPG cell line (SF8628 cells) with *Dlx2* and measuring expression levels of some known DLX target genes and genes involved in oligodendroglial differentiation. We predicted that, if SF8628 cells were competent to respond to DLX2 expression, we would see an upregulation of the known DLX2 targets *Gad1* and *Gad2*, and downregulation of oligodendroglial genes like *Nkx2.2* and *Olig2*, in cells that were transfected with DLX2 compared to control cells transfected with empty vector (GFP). However, expression

levels of all these gene were not significantly different in the two conditions. One explanation is that SF8628 cells may not be competent to respond to DLX transcriptional cues, but additional biological and technical factors could be considered here. An important technical limitation of this project concerns the method used to overexpress DLX2 in SF8628 cells. DLX2 overexpression was achieved by transfecting cells with a fusion expression construct consisting of DLX2 cDNA fused to a GFP tag. It is possible that the GFP tag affects the subcellular localisation of the fusion protein. If the fusion transcription factor cannot localise to the nucleus, this would explain the lack of response seen in SF8628 cells to DLX2 overexpression. To rule this out, transfection should be repeated and correct localisation of the fusion protein to the nucleus should be verified by confocal microscopy. An alternative option would be cellular fractionation followed by western blotting for DLX2 on the cytoplasmic and nuclear fractions, to determine if the majority of DLX2 is found in the nuclear fraction. Furthermore, it is also possible that the tag affects interaction of the fusion protein with DNA, even if nuclear localisation is not affected. One way to investigate this would be via *in vitro* translation of the DLX2-GFP fusion protein followed by EMSA using probes for known, EMSA-validated DLX2 binding sites, such as the *Nrp2* promoter (Le, Du et al. 2007), to determine if the fusion protein can still interact with homeodomain binding sites. These will be important considerations for planned future experiments using other DIPG cell lines. Alternatively, we might consider the use of an expression vector that does not have a tag.

I conducted a separate, preliminary transfection experiment and verified that transfected cells overexpressed DLX2 via Western blot (Figure 7.3). However, I didn't verify successful DLX2 protein overexpression in the same experiment as used for gene expression study. It is therefore

possible that DLX2 protein overexpression was not achieved in the cells that were harvested for the gene expression analysis shown in Figure 7.3. qPCR for *Dlx2* was performed on these cells to verify that transfection was successful. However, presence of the expression construct does not necessarily translate into successful expression of DLX2 protein in these cells. Therefore, this experiment should be repeated, but with a portion of the cell lysate reserved for western blotting to verify that DLX2 protein expression occurred in the transfected cells. Lack of DLX2 protein expression after transfection could explain the lack of observed response.

Besides these technical limitations, some biological factors could be responsible. One study found that DLX2 was one of the most significant genes expressed at very low levels in H3K27M-harbouring pediatric glioblastomas compared to tumours with no or an alternate histone mutation (G34R/V) (Schwartzentruber, Korshunov et al. 2012). This is a key result that led us to initiate this project. Rather than necessarily playing a driving role in the biology of this disease, low DLX2 expression might just be reflective of non-forebrain origin of this tumour. In support of this, a single cell RNA-seq analysis of six H3K27M DIPGs as well as other subtypes found the forebrain-specific transcription factor FOXG1 was the only gene that was significantly downregulated in H3K27M DIPGs compared to others. Besides this, the broad gene expression signature was one of many genes being abnormally upregulated, as might be expected from the loss of Polycomb repression that results from H3K27M mutations (Filbin, Tirosh et al. 2018). Additionally, some evidence indicates that DIPG could arise from a precursor cell located in the pons (Monje, Mitra et al. 2011) which, as a hindbrain structure, does not express any DLX members during its development, at least in the mouse.

Another explanation for the lack of response observed in the patient-derived cell line compared to the GEMM-derived cell line is that a patient-derived cell line might be expected to exhibit more cell type heterogeneity. Solid tumours do not just consist of tumour cells but also other components such as the tumour stroma, immune cells, and, in the case of diffusely infiltrating tumours like DIPG, non-malignant tissue (the mouse model lacks this diffusely infiltrating nature). Tumour cells themselves are also heterogeneous as different cells within the tumour accumulate different mutations over the course of the disease (Dagogo-Jack and Shaw 2018). This heterogeneity might be reflected in a cell line derived from a patient. Because of this, not all the cells in the culture might respond in the same way to DLX2- only a subset of them might show the predicted response, maybe not enough to be detectable with qPCR on the whole cell population. This could account for the lack of response I observed compared to the experiment using a GEMM-derived cell line, which may be more homogeneous.

### 8.4.1. Conclusions and future directions

Due to the above-noted technical limitations, it cannot yet be definitively concluded whether SF8628 cells can respond to DLX over-expression. As such, an essential future direction as we move forward with this project is to validate that our over-expression construct localizes and functions in the same manner as the wild-type DLX2 protein. Besides this, it should be noted that although many DIPGs exhibit an OPC-like gene expression signature, a subset of these tumours do not have an oligodendroglial phenotype and might have a different developmental origin (Misuraca, Cordero et al. 2015). If SF8628 is one of these "OPC-low" cell lines, then that could also account for the lack of response we observed with DLX2 overexpression. Therefore, an

important future direction for this project is to obtain other patient-derived DIPG cell lines and repeat these experiments.

# Literature Cited


Anderson, S., D. Eisenstat, L. Shi and J. Rubenstein (1997). "Interneuron migration from basal forebrain to neocortex: dependence on Dlx genes." Science **278**(5337): 474-476.

Anderson, S. A., O. Marin, C. Horn, K. Jennings and J. L. Rubenstein (2001). "Distinct cortical migrations from the medial and lateral ganglionic eminences." Development **128**(3): 353-363.

Anderson, S. A., M. Qiu, A. Bulfone, D. D. Eisenstat, J. Meneses, R. Pedersen and J. L. Rubenstein (1997). "Mutations of the homeobox genes Dlx-1 and Dlx-2 disrupt the striatal subventricular zone and differentiation of late born striatal neurons." Neuron **19**(1): 27-37.

Armstrong, R. C., J. G. Kim and L. D. Hudson (1995). "Expression of myelin transcription factor I (MyTI), a “zinc-finger” DNA-binding protein, in developing oligodendrocytes." Glia **14**(4): 303-321.

Barres, B., I. Hart, H. Coles, J. Burne, J. Voyvodic, W. Richardson and M. Raff (1992). "Cell death and control of cell survival in the oligodendrocyte lineage." Cell **70**(1): 31-46.

Beattie, R. and S. Hippenmeyer (2017). "Mechanisms of radial glia progenitor cell lineage progression." FEBS letters **591**(24): 3993-4008.

Bellefroid, E. J., C. Bourguignon, T. Hollemann, Q. Ma, D. J. Anderson, C. Kintner and T. Pieler (1996). "X-MyT1, a Xenopus C2HC-Type Zinc Finger Protein with a Regulatory Function in Neuronal Differentiation." Cell **87**(7): 1191-1202.

Bulfone, A., F. Wang, R. Hevner, S. Anderson, T. Cutforth, S. Chen, J. Meneses, R. Pedersen, R. Axel and J. L. Rubenstein (1998). "An olfactory sensory map develops in the absence of normal projection neurons or GABAergic interneurons." Neuron **21**(6): 1273-1282.

Bürglin, T. R. and M. Affolter (2016). "Homeodomain proteins: an update." Chromosoma **125**(3): 497-521.

Cajigas, I., D. E. Leib, J. Cochrane, H. Luo, K. R. Swyter, S. Chen, B. S. Clark, J. Thompson, J. R. Yates and R. E. Kingston (2015). "Evf2 lncRNA/BRG1/DLX1 interactions reveal RNA-dependent inhibition of chromatin remodeling." Development **142**(15): 2641-2652.

Chan, K.-M., D. Fang, H. Gan, R. Hashizume, C. Yu, M. Schroeder, N. Gupta, S. Mueller, C. D. James and R. Jenkins (2013). "The histone H3. 3K27M mutation in pediatric glioma reprograms H3K27 methylation and gene expression." Genes & development **27**(9): 985-990.

Comet, I., E. M. Riising, B. Leblanc and K. Helin (2016). "Maintaining cell identity: PRC2-mediated regulation of transcription and cancer." Nature Reviews Cancer **16**(12): 803.

Cordero, F. J., Z. Huang, C. Grenier, X. He, G. Hu, R. E. McLendon, S. K. Murphy, R. Hashizume and O. J. Becher (2017). "Histone H3. 3K27M represses p16 to accelerate gliomagenesis in a murine model of DIPG." Molecular Cancer Research **15**(9): 1243-1254.

Dagogo-Jack, I. and A. T. Shaw (2018). "Tumour heterogeneity and resistance to cancer therapies." Nature reviews Clinical oncology **15**(2): 81.

Dickinson, P. J., M. Fanarraga, I. Griffiths, J. Barrie, E. Kyriakides and P. Montague (1996). "Oligodendrocyte progenitors in the embryonic spinal cord express DM-20." Neuropathology and applied neurobiology **22**(3): 188-198.

Dror, I., R. Rohs and Y. Mandel-Gutfreund (2016). "How motif environment influences transcription factor search dynamics: Finding a needle in a haystack." BioEssays **38**(7): 605-612.

Elbaz, B., J. D. Aaker, S. Isaac, A. Kolarzyk, P. Brugarolas, A. Eden and B. Popko (2018). "Phosphorylation state of ZFP24 controls oligodendrocyte differentiation." Cell reports **23**(8): 2254-2263.

Elbaz, B. and B. Popko (2019). "Molecular control of oligodendrocyte development." Trends in neurosciences.

Emery, B., D. Agalliu, J. D. Cahoy, T. A. Watkins, J. C. Dugas, S. B. Mulinyawe, A. Ibrahim, K. L. Ligon, D. H. Rowitch and B. A. Barres (2009). "Myelin gene regulatory factor is a critical transcriptional regulator required for CNS myelination." Cell **138**(1): 172-185.

Eng, L. F., F.-C. Chao, B. Gerstl, D. R. Pratt and M. Tavaststjerna (1968). "Maturation of human white matter myelin. Fractionation of the myelin membrane proteins." Biochemistry **7**(12): 4455-4465.

Feng, J., C. Bi, B. S. Clark, R. Mady, P. Shah and J. D. Kohtz (2006). "The Evf-2 noncoding RNA is transcribed from the Dlx-5/6 ultraconserved region and functions as a Dlx-2 transcriptional coactivator." Genes & development **20**(11): 1470-1484.

Filbin, M. G., I. Tirosh, V. Hovestadt, M. L. Shaw, L. E. Escalante, N. D. Mathewson, C. Neftel, N. Frank, K. Pelton and C. M. Hebert (2018). "Developmental and oncogenic programs in H3K27M gliomas dissected by single-cell RNA-seq." Science **360**(6386): 331-335.

Gamsjaeger, R., M. R. O'Connell, L. Cubeddu, N. E. Shepherd, J. A. Lowry, A. H. Kwan, M. Vandevenne, M. K. Swanton, J. M. Matthews and J. P. Mackay (2013). "A structural analysis of DNA binding by myelin transcription factor 1 double zinc fingers." Journal of Biological Chemistry **288**(49): 35180-35191.

Gao, P., M. P. Postiglione, T. G. Krieger, L. Hernandez, C. Wang, Z. Han, C. Streicher, E. Papusheva, R. Insolera and K. Chugh (2014). "Deterministic progenitor behavior and unitary production of neurons in the neocortex." Cell **159**(4): 775-788.

Gilmore, E. C. and K. Herrup (1997). "Cortical development: layers of complexity." Current Biology **7**(4): R231-R234.

Goldman, S. A. and N. J. Kuypers (2015). "How to make an oligodendrocyte." Development **142**(23): 3983-3995.

Götz, M. and W. B. Huttner (2005). "Developmental cell biology: The cell biology of neurogenesis." Nature reviews Molecular cell biology **6**(10): 777.

Harlow, D. E., K. E. Saul, C. M. Culp, E. M. Vesely and W. B. Macklin (2014). "Expression of proteolipid protein gene in spinal cord stem cells and early oligodendrocyte progenitor cells is dispensable for normal cell migration and myelination." Journal of Neuroscience **34**(4): 1333-1343.

Hart, I., W. D. Richardson, C.-H. Heldin, B. Westermark and M. C. Raff (1989). "PDGF receptors on cells of the oligodendrocyte-type-2 astrocyte (O-2A) cell lineage." Development **105**(3): 595-603.

He, W., C. Ingraham, L. Rising, S. Goderie and S. Temple (2001). "Multipotent stem cells from the mouse basal forebrain contribute GABAergic neurons and oligodendrocytes to the cerebral cortex during embryogenesis." Journal of Neuroscience **21**(22): 8854-8862.

Hebert, J. M. and G. Fishell (2008). "The genetics of early telencephalon patterning: some assembly required." Nat Rev Neurosci **9**(9): 678-685.

Hornig, J., F. Fröb, M. R. Vogl, I. Hermans-Borgmeyer, E. R. Tamm and M. Wegner (2013). "The transcription factors Sox10 and Myrf define an essential regulatory network module in differentiating oligodendrocytes." PLoS Genet **9**(10): e1003907.

Hudson, L. D., E. Romm, J. A. Berndt and J. A. Nielsen (2011). "A tool for examining the role of the zinc finger myelin transcription factor 1 (Myt1) in neural development: Myt1 knock-in mice." Transgenic research **20**(4): 951-961.

Ikenaka, K., T. Kagawa and K. Mikoshiba (1992). "Selective expression of DM-20, an alternatively spliced myelin proteolipid protein gene product, in developing nervous system and in nonglial cells." Journal of neurochemistry **58**(6): 2248-2253.

Inukai, S., K. H. Kock and M. L. Bulyk (2017). "Transcription factor–DNA binding: beyond binding site motifs." Current opinion in genetics & development **43**: 110-119.

Itoh, M., C.-H. Kim, G. Palardy, T. Oda, Y.-J. Jiang, D. Maust, S.-Y. Yeo, K. Lorick, G. J. Wright and L. Ariza-McNaughton (2003). "Mind bomb is a ubiquitin ligase that is essential for efficient activation of Notch signaling by Delta." Developmental cell **4**(1): 67-82.

Kessaris, N., M. Fogarty, P. Iannarelli, M. Grist, M. Wegner and W. D. Richardson (2006). "Competing waves of oligodendrocytes in the forebrain and postnatal elimination of an embryonic lineage." Nat Neurosci **9**(2): 173-179.

Kessaris, N., N. Pringle and W. D. Richardson (2001). "Ventral neurogenesis and the neuron-glial switch." Neuron **31**(5): 677-680.

Kim, J. and L. Hudson (1992). "Novel member of the zinc finger superfamily: A C2-HC finger that recognizes a glia-specific gene." Molecular and Cellular Biology **12**(12): 5632-5639.

Kim, J. G., R. C. Armstrong, D. v. Agoston, A. Robinsky, C. Wiese, J. Nagle and L. D. Hudson (1997). "Myelin transcription factor 1 (Myt1) of the oligodendrocyte lineage, along with a closely related CCHC zinc finger, is expressed in developing neurons in the mammalian central nervous system." Journal of neuroscience research **50**(2): 272-290.

Klugmann, M., M. H. Schwab, A. Pühlhofer, A. Schneider, F. Zimmermann, I. R. Griffiths and K.-A. Nave (1997). "Assembly of CNS myelin in the absence of proteolipid protein." Neuron **18**(1): 59-70.

Koenning, M., S. Jackson, C. M. Hay, C. Faux, T. J. Kilpatrick, M. Willingham and B. Emery (2012). "Myelin gene regulatory factor is required for maintenance of myelin and mature oligodendrocyte identity in the adult CNS." Journal of Neuroscience **32**(36): 12528-12542.

Kumamoto, T. and C. Hanashima (2017). "Evolutionary conservation and conversion of Foxg1 function in brain development." Development, growth & differentiation **59**(4): 258-269.

Küspert, M., A. Hammer, M. R. Bösl and M. Wegner (2011). "Olig2 regulates Sox10 expression in oligodendrocyte precursors through an evolutionary conserved distal enhancer." Nucleic acids research **39**(4): 1280-1293.

Le, T. N., G. Du, M. Fonseca, Q. P. Zhou, J. T. Wigle and D. D. Eisenstat (2007). "Dlx homeobox genes promote cortical interneuron migration from the basal forebrain by direct repression of the semaphorin receptor neuropilin-2." J Biol Chem **282**(26): 19071-19081.

Le, T. N., Q. P. Zhou, I. Cobos, S. Zhang, J. Zagozewski, S. Japoni, J. Vriend, T. Parkinson, G. Du, J. L. Rubenstein and D. D. Eisenstat (2017). "GABAergic Interneuron Differentiation in the Basal Forebrain Is Mediated through Direct Regulation of Glutamic Acid Decarboxylase Isoforms by Dlx Homeobox Transcription Factors." J Neurosci **37**(36): 8816-8829.

Lee, S.-K., B. Lee, E. C. Ruiz and S. L. Pfaff (2005). "Olig2 and Ngn2 function in opposition to modulate gene expression in motor neuron progenitor cells." Genes & development **19**(2): 282-294.

LeVine, S., D. Wong and W. Macklin (1990). "Developmental expression of proteolipid protein and DM20 mRNAs and proteins in the rat brain." Developmental neuroscience **12**(4-5): 235-250.

Li, H., Y. Lu, H. K. Smith and W. D. Richardson (2007). "Olig1 and Sox10 interact synergistically to drive myelin basic protein transcription in oligodendrocytes." Journal of Neuroscience **27**(52): 14375-14382.

Lim, L., D. Mi, A. Llorca and O. Marin (2018). "Development and Functional Diversification of Cortical Interneurons." Neuron **100**(2): 294-313.

Lindtner, S., R. Catta-Preta, H. Tian, L. Su-Feher, J. D. Price, D. E. Dickel, V. Greiner, S. N. Silberberg, G. L. McKinsey, M. T. McManus, L. A. Pennacchio, A. Visel, A. S. Nord and J. L. R. Rubenstein (2019). "Genomic Resolution of DLX-Orchestrated Transcriptional Circuits Driving Development of Forebrain GABAergic Neurons." Cell Rep **28**(8): 2048-2063 e2048.

Liu, J. K., I. Ghattas, S. Liu, S. Chen and J. L. Rubenstein (1997). "Dlx genes encode DNA-binding proteins that are expressed in an overlapping and sequential pattern during basal ganglia differentiation." Developmental dynamics: an official publication of the American Association of Anatomists **210**(4): 498-512.

Livak, K. J. and T. D. Schmittgen (2001). "Analysis of relative gene expression data using real-time quantitative PCR and the 2− ΔΔCT method." methods **25**(4): 402-408.

Lopez-Anido, C., G. Sun, M. Koenning, R. Srinivasan, H. A. Hung, B. Emery, S. Keles and J. Svaren (2015). "Differential Sox10 genomic occupancy in myelinating glia." Glia **63**(11): 1897-1914.

Lu, Q. R., T. Sun, Z. Zhu, N. Ma, M. Garcia, C. D. Stiles and D. H. Rowitch (2002). "Common developmental requirement for Olig function indicates a motor neuron/oligodendrocyte connection." Cell **109**(1): 75-86.

Lu, Q. R., D.-i. Yuk, J. A. Alberta, Z. Zhu, I. Pawlitzky, J. Chan, A. P. McMahon, C. D. Stiles and D. H. Rowitch (2000). "Sonic hedgehog–regulated oligodendrocyte lineage genes encoding bHLH proteins in the mammalian central nervous system." Neuron **25**(2): 317-329.

Manukyan, A., I. Kowalczyk, T. A. Melhuish, A. Lemiesz and D. Wotton (2018). "Analysis of transcriptional activity by the Myt1 and Myt1l transcription factors." Journal of Cellular Biochemistry **119**(6): 4644-4655.

Marın, O., S. A. Anderson and J. L. Rubenstein (2000). "Origin and molecular specification of striatal interneurons." Journal of Neuroscience **20**(16): 6063-6076.

Marín, O. and J. L. Rubenstein (2001). "A long, remarkable journey: tangential migration in the telencephalon." Nature Reviews Neuroscience **2**(11): 780.

Marques, S., D. van Bruggen, D. P. Vanichkina, E. M. Floriddia, H. Munguba, L. Väremo, S. Giacomello, A. M. Falcão, M. Meijer and Å. K. Björklund (2018). "Transcriptional convergence of oligodendrocyte lineage progenitors during development." Developmental cell **46**(4): 504-517. e507.

Matsushita, F., T. Kameyama, Y. Kadokawa and T. Marunouchi (2014). "Spatiotemporal expression pattern of Myt/NZF family zinc finger transcription factors during mouse nervous system development." Developmental Dynamics **243**(4): 588-600.

McGuinness, T., M. H. Porteus, S. Smiga, A. Bulfone, C. Kingsley, M. Qiu, J. K. Liu, J. E. Long, D. Xu and J. L. Rubenstein (1996). "Sequence, organization, and transcription of the Dlx-1 and Dlx-2 locus." Genomics **35**(3): 473-485.

Meijer, D. H., M. F. Kane, S. Mehta, H. Liu, E. Harrington, C. M. Taylor, C. D. Stiles and D. H. Rowitch (2012). "Separated at birth? The functional and molecular divergence of OLIG1 and OLIG2." Nature Reviews Neuroscience **13**(12): 819.

Michalski, J.-P., C. Anderson, A. Beauvais, Y. De Repentigny and R. Kothary (2011). "The proteolipid protein promoter drives expression outside of the oligodendrocyte lineage during embryonic and early postnatal development." PLoS One **6**(5): e19772.

Miller, F. D. and A. S. Gauthier (2007). "Timing is everything: making neurons versus glia in the developing cortex." Neuron **54**(3): 357-369.

Misuraca, K. L., F. J. Cordero and O. J. Becher (2015). "Pre-clinical models of diffuse intrinsic pontine glioma." Frontiers in oncology **5**: 172.

Monje, M., S. S. Mitra, M. E. Freret, T. B. Raveh, J. Kim, M. Masek, J. L. Attema, G. Li, T. Haddix and M. S. Edwards (2011). "Hedgehog-responsive candidate cell of origin for diffuse intrinsic pontine glioma." Proceedings of the National Academy of Sciences **108**(11): 4453-4458.

Nave, K.-A., C. Lai, F. E. Bloom and R. J. Milner (1987). "Splice site selection in the proteolipid protein (PLP) gene transcript and primary structure of the DM-20 protein of central nervous system myelin." Proceedings of the National Academy of Sciences **84**(16): 5665-5669.

Nielsen, J. A., J. A. Berndt, L. D. Hudson and R. C. Armstrong (2004). "Myelin transcription factor 1 (Myt1) modulates the proliferation and differentiation of oligodendrocyte lineage cells." Molecular and Cellular Neuroscience **25**(1): 111-123.

Noble, M., K. Murray, P. Stroobant, M. D. Waterfield and P. Riddle (1988). "Platelet-derived growth factor promotes division and motility and inhibits premature differentiation of the oligodendrocyte/type-2 astrocyte progenitor ceil." Nature **333**(6173): 560-562.

Panganiban, G. and J. L. Rubenstein (2002). "Developmental functions of the Distal-less/Dlx homeobox genes." Development **129**(19): 4371-4386.

Paridaen, J. T. and W. B. Huttner (2014). "Neurogenesis during development of the vertebrate central nervous system." EMBO reports **15**(4): 351-364.

Park, H.-C. and B. Appel (2003). "Delta-Notch signaling regulates oligodendrocyte specification." Development **130**(16): 3747-3755.

Petryniak, M. A., G. B. Potter, D. H. Rowitch and J. L. Rubenstein (2007). "Dlx1 and Dlx2 control neuronal versus oligodendroglial cell fate acquisition in the developing forebrain." Neuron **55**(3): 417-433.

Qi, Y., J. Cai, Y. Wu, R. Wu, J. Lee, H. Fu, M. Rao, L. Sussel, J. Rubenstein and M. Qiu (2001). "Control of oligodendrocyte differentiation by the Nkx2. 2 homeodomain transcription factor." Development **128**(14): 2723-2733.

Qiu, M., A. Bulfone, I. Ghattas, J. J. Meneses, L. Christensen, P. T. Sharpe, R. Presley, R. A. Pedersen and J. L. Rubenstein (1997). "Role of the Dlx homeobox genes in proximodistal patterning of the branchial arches: mutations of Dlx-1, Dlx-2, and Dlx-1 and-2 alter

morphogenesis of proximal skeletal and soft tissue structures derived from the first and second arches." Developmental biology **185**(2): 165-184.

Reiter, F., S. Wienerroither and A. Stark (2017). "Combinatorial function of transcription factors and cofactors." Current opinion in genetics & development **43**: 73-81.

Richardson, W. D., N. Pringle, M. J. Mosley, B. Westermark and M. Dubois-Dalcg (1988). "A role for platelet-derived growth factor in normal gliogenesis in the central nervous system." Cell **53**(2): 309-319.

Romm, E., J. A. Nielsen, J. G. Kim and L. D. Hudson (2005). "Myt1 family recruits histone deacetylase to regulate neural transcription." Journal of neurochemistry **93**(6): 1444-1453.

Rowitch, D. H. (2004). "Glial specification in the vertebrate neural tube." Nature Reviews Neuroscience **5**(5): 409-419.

Rowitch, D. H. and A. R. Kriegstein (2010). "Developmental genetics of vertebrate glial–cell specification." Nature **468**(7321): 214-222.

Rubenstein, J. L., K. Shimamura, S. Martinez and L. Puelles (1998). "Regionalization of the prosencephalic neural plate." Annual review of neuroscience **21**(1): 445-477.

Schwartzentruber, J., A. Korshunov, X.-Y. Liu, D. T. Jones, E. Pfaff, K. Jacob, D. Sturm, A. M. Fontebasso, D.-A. K. Quang and M. Tönjes (2012). "Driver mutations in histone H3. 3 and chromatin remodelling genes in paediatric glioblastoma." Nature **482**(7384): 226.

Shimamura, K. and J. Rubenstein (1997). "Inductive interactions direct early regionalization of the mouse forebrain." Development **124**(14): 2709-2718.

Shulzhenko, N., A. S. Smirnova, A. Morgun and M. Gerbase-DeLima (2003). "Specificity of alternative splice form detection using RT-PCR with a primer spanning the exon junction." Biotechniques **34**(6): 1244-1249.

Slattery, M., T. Zhou, L. Yang, A. C. D. Machado, R. Gordân and R. Rohs (2014). "Absence of a simple code: how transcription factors read the genome." Trends in biochemical sciences **39**(9): 381-399.

Snaidero, N. and M. Simons (2014). Myelination at a glance, The Company of Biologists Ltd.

Somayajulu, M., D. A. Bessert, M. Hüttemann, J. Sohi, J. Kamholz and R. P. Skoff (2018). "Insertion of proteolipid protein into mitochondria but not DM20 regulates metabolism of cells." Neuroscience letters **678**: 90-98.

Spitz, F. and E. E. Furlong (2012). "Transcription factors: from enhancer binding to developmental control." Nat Rev Genet **13**(9): 613-626.

Timsit, S., L. Bally-Cuif, D. Colman and B. Zalc (1992). "DM-20 mRNA is expressed during the embryonic development of the nervous system of the mouse." Journal of neurochemistry **58**(3): 1172-1175.

Tremblay, R., S. Lee and B. Rudy (2016). "GABAergic interneurons in the neocortex: from cellular properties to circuits." Neuron **91**(2): 260-292.

Vasconcelos, F. F., A. Sessa, C. Laranjeira, A. A. Raposo, V. Teixeira, D. W. Hagey, D. M. Tomaz, J. Muhr, V. Broccoli and D. S. Castro (2016). "MyT1 counteracts the neural progenitor program to promote vertebrate neurogenesis." Cell reports **17**(2): 469-483.

Wang, S., J. Zhang, A. Zhao, S. Hipkens, M. A. Magnuson and G. Gu (2007). "Loss of Myt1 function partially compromises endocrine islet cell differentiation and pancreatic physiological function in the mouse." Mechanisms of development **124**(11-12): 898-910.

Weider, M., L. J. Starost, K. Groll, M. Küspert, E. Sock, M. Wedel, F. Fröb, C. Schmitt, T. Baroti and A. C. Hartwig (2018). "Nfat/calcineurin signaling promotes oligodendrocyte differentiation and myelination by transcription factor network tuning." Nature communications **9**(1): 1-16.

Weinstein, D. C. and A. Hemmati-Brivanlou (1999). "Neural induction." Annual review of cell and developmental biology **15**(1): 411-433.

Wigle, J. T. and D. D. Eisenstat (2008). "Homeobox genes in vertebrate forebrain development and disease." Clin Genet **73**(3): 212-226.

Williams, D. M., S. Koduri, Z. Li, W. D. Hankins and I. Poola (1999). "Primer design strategies for the targeted amplification of alternatively spliced molecules." Analytical biochemistry **271**(2): 194-197.

Wilson, S. W. and C. Houart (2004). "Early steps in the development of the forebrain." Developmental cell **6**(2): 167-181.

Wonders, C. P. and S. A. Anderson (2006). "The origin and specification of cortical interneurons." Nat Rev Neurosci **7**(9): 687-696.

Yang, X., T. Tomita, M. Wines-Samuelson, V. Beglopoulos, M. G. Tansey, R. Kopan and J. Shen (2006). "Notch1 signaling influences v2 interneuron and motor neuron development in the spinal cord." Developmental neuroscience **28**(1-2): 102-117.

Yee, K. S. and C. Y. Victor (1998). "Isolation and characterization of a novel member of the neural zinc finger factor/myelin transcription factor family with transcriptional repression activity." Journal of Biological Chemistry **273**(9): 5366-5374.

Yella, V. R., D. Bhimsaria, D. Ghoshdastidar, J. A. Rodríguez-Martínez, A. Z. Ansari and M. Bansal (2018). "Flexibility and structure of flanking DNA impact transcription factor affinity for its core motif." Nucleic acids research **46**(22): 11883-11897.

Yoon, J.-H., K. Abdelmohsen and M. Gorospe (2013). "Posttranscriptional gene regulation by long noncoding RNA." Journal of molecular biology **425**(19): 3723-3730.

Zhang, H., G. Hu, H. Wang, P. Sciavolino, N. Iler, M. M. Shen and C. Abate-Shen (1997). "Heterodimerization of Msx and Dlx homeoproteins results in functional antagonism." Molecular and cellular biology **17**(5): 2920-2932.

Zhou, Q. and D. J. Anderson (2002). "The bHLH transcription factors OLIG2 and OLIG1 couple neuronal and glial subtype specification." Cell **109**(1): 61-73.

Zhou, Q., G. Choi and D. J. Anderson (2001). "The bHLH transcription factor Olig2 promotes oligodendrocyte differentiation in collaboration with Nkx2. 2." Neuron **31**(5): 791-807.

Zhou, Q., S. Wang and D. J. Anderson (2000). "Identification of a novel family of oligodendrocyte lineage-specific basic helix–loop–helix transcription factors." Neuron **25**(2): 331-343.